


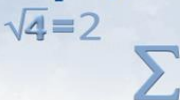
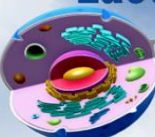


**Year 2024**



# East African Journal of Biophysical and Computational Sciences



**Volume 5 No 2**



**Hawassa University**  
**College of Natural & Computational Sciences**

**ISSN (Online): 2789-3618**

**ISSN (Print): 2789-360X**

## *East African Journal of Biophysical and Computational Sciences (EAJBCS)*

### **Editorial Board members**

#### **Editor-in-Chief**

- Dr. Berhanu Mekibib Faculty of Veterinary Medicine, HU, [berhanumm2002@gmail.com](mailto:berhanumm2002@gmail.com)

#### **Editorial Manager**

- Dr. Zerihun Kinfe Dept. of Mathematics, HU, [zerie96@gmail.com](mailto:zerie96@gmail.com)

#### **Associate Editors**

- Dr. Kiros Gebreargawi Dept. of Mathematic, HU, [kirosg@hu.edu.et](mailto:kirosg@hu.edu.et)
- Dr. Sisay Tadesse Dept. of Chemistry (Physical), HU, [sisaytad@gmail.com](mailto:sisaytad@gmail.com)
- Dr. Tizazu Abza Dept. of Physics, HU, [zabishwork2@gmail.com](mailto:zabishwork2@gmail.com)
- Prof. Desie Sheferaw Faculty of Veterinary Medicine, HU, [mereba480@gmail.com](mailto:mereba480@gmail.com)
- Dr. Abrham Mikru Dept. of Biology, HU, [kedirwoliy@gmail.com](mailto:kedirwoliy@gmail.com)
- Mr. Andualem G/Silase Dept. of Sport Sciences, HU, [livsis@gmail.com](mailto:livsis@gmail.com)
- Mr. Wegene Taleligne Dept. of Geology, HU, [bekele@hu.edu.et](mailto:bekele@hu.edu.et)
- Dr. Dereje Danbe Department of Statistics, CNCS, HU, [dalbrayii@gmail.com](mailto:dalbrayii@gmail.com)
- Dr. Yonnas Shuke Dept. of Statistics, HU, [cherueden@yahoo.com](mailto:cherueden@yahoo.com)
- Dr. Firew Kebede Dept. of Biology, HU, [abigiag@yahoo.com](mailto:abigiag@yahoo.com)
- Dr. Girma Tilahun Dept. of Aquatic Sci., Fisheries & aquaculture, HU, [girmati@yahoo.com](mailto:girmati@yahoo.com)

### **Advisory Board members**

- Prof. Zinabu G/mariam Freshwater Ecology, Biology, CNCS, HU, [luzinabu@gmail.com](mailto:luzinabu@gmail.com)
- Dr. Zeytu Gashaw Department of Statistics, CNCS, HU, [zeytugashaw@yahoo.com](mailto:zeytugashaw@yahoo.com)
- Dr. Yifat Denbarga Faculty of Vet. Medicine, CNCS, HU, [dyifatd@gmail.com](mailto:dyifatd@gmail.com)
- Prof. Abebe Geletu Department of Process Optimization, Technical University of Ilmenau, [abebe.geletu@tu-ilmenau.de](mailto:abebe.geletu@tu-ilmenau.de)
- Prof. Bekele Megersa Faculty of Veterinary Medicine, AAU, [bekelebati@gmail.com](mailto:bekelebati@gmail.com)
- Prof. Abiy Yenesew Dept. of Chemistry, Nairobi University, Kenya, [ayenesew@uonbi.ac.ke](mailto:ayenesew@uonbi.ac.ke)
- Dr. Sintayehu Tesfa Dept. of Physics, Jazan University, Saud Arabia, [sint\\_tesfa@yahoo.com](mailto:sint_tesfa@yahoo.com)
- Prof. Natarajan Pavanagam Dept. of Biology, HU, [drpnatarajan123@gmail.com](mailto:drpnatarajan123@gmail.com)
- Prof. Legesse Kassa Dept. of Statistics, University of South Africa, [debuslk@unisa.ac.za](mailto:debuslk@unisa.ac.za)
- Prof. Endrias Zewdu Faculty of Agri. and Vet. Sciences, Ambo U., [endrias.zewdu@gmail.com](mailto:endrias.zewdu@gmail.com)

### ***Recognition to reviewers***

<b>Name</b>	<b>Affiliation</b>	<b>Email address</b>
Dr. Denekew Bitawu	Bahir Dar University	<a href="mailto:denekewb2020@gmail.com">denekewb2020@gmail.com</a>
Feysal Kemal	Adama Science and Technology University	<a href="mailto:feysal.kemal@gmail.com">feysal.kemal@gmail.com</a>
Dr. Kassaw Beshaw	Wolaita Sodo University	<a href="mailto:beshawkassaw@yahoo.com">beshawkassaw@yahoo.com</a>
Dr. Mihret Dananto	Water Supply and Environmental Engineering, HU	<a href="mailto:mihret@gmail.com">mihret@gmail.com</a>
Dr. Abebe Agonafir	Dept. of Animal Sciences, Debreberhan University	<a href="mailto:dr.abuka@gmail.com">dr.abuka@gmail.com</a>
Prof. Desie Sheferaw	Faculty of Vet. Medicine, HU	<a href="mailto:Mereba480@gmail.com">Mereba480@gmail.com</a>
Dr. Habtamu Tsegaye	Wolkite University	<a href="mailto:hbtmtsgy@gmail.com">hbtmtsgy@gmail.com</a>
Dr. Admasu Tadesse	Department of Mathematics, HU	<a href="mailto:admasut@hu.edu.et">admasut@hu.edu.et</a>
Getachew Teshome	Department of Mathematics, Haramaya University	<a href="mailto:gmgech@gmail.com">gmgech@gmail.com</a>
Yetwale Hailu	Dept. of Mathematics, Debre Markos University	<a href="mailto:yetwalehailu@gmail.com">yetwalehailu@gmail.com</a>

## Table of contents

<b>Mixed Effects Analysis of Height Growth in Ethiopian Children Aged 1-12 Years: A Cohort Study.....</b>	<b>1-12</b>
---	-------------

*Dereje Danbe, Ayele Taye Goshu*

<b>Effect of Land Use Activities on Water Quality and Vegetation Cover Change in Nsooba - Lubigi Wetland System, Kampala City.....</b>	<b>13-28</b>
--	--------------

*Charles Twesigye, Kennedy Igunga, Ritah Nakayinga*

<b>Assessment of Community Knowledge, Attitude and Practices toward Bovine Tuberculosis in Jinka Town, Southern Ethiopia .....</b>	<b>29-40</b>
--	--------------

*Asrat Solomon Kenasew, Said Mohammed Harar, Alemitu Ketema Tamirat, Metadel Molto*

<b>Penalized Intuitionistic Fuzzy Goal Programming Method for Solving Multi-Objective Decision-Making Problems.....</b>	<b>41-57</b>
---	--------------

*Demmelash Mollalign, Berhanu Guta Wordofa, Allen Rangia Mushi*

<b>A Mathematical Model for the Transmission Dynamics of COVID-19 Pandemic Considering Protected and Hospitalized with Optimal Control.....</b>	<b>58-86</b>
---	--------------

*Tinaw Tilahun Asmamaw, Kiros Gebreargawi*





## Mixed Effects Analysis of Height Growth in Ethiopian Children Aged 1-12 Years: A Cohort Study

Dereje Danbe Debeko\*<sup>1</sup> and Ayele Taye Goshu<sup>2</sup>

<sup>1</sup> Department of Statistics, Hawassa University, P.O. Box 05, Hawassa, Ethiopia

<sup>2</sup> Department of statistics, Cotebe Teaching University, Addis Ababa, Ethiopia

### KEYWORDS:

Height growth;  
Mixed effects Models;  
Children;  
Ethiopia

### ABSTRACT

Modelling physical growth is a key component to examine and identify defining characteristics in the growth process. The goal of this study was to model and capture known features of height growth in Ethiopian children aged 1–12 years. Height measurements of 1760 children followed from 1 to 12 years at Young Lives Ethiopia, a younger cohort, used in the study. The mixed effects method was used to estimate the rate of change within and between subjects over time and to identify defining covariates. Adult height and rate of change over time were individual-specific resulting individual-level growth differences. There was a negative relationship between individual-specific adult height and rate of change over time. The decelerated rate of change was observed from childhood to the onset of puberty in both sexes. Boys were taller than girls between the ages of 3 and 7 years. Mother's educational status, access to quality drinking water, age, and sex had a significant effect on height growth. Children who had a decelerated rate of growth change during the childhood period become taller later in life. Adult height could be determined by an individual-specific rate of change over time.

### Research article

### INTRODUCTION

Growth is a continuous and dynamic process influenced by different unknown factors. Modelling this dynamic process to understand, estimate, and capture the defining characteristics such as initial level, rates of change, periods of acceleration and deceleration when the process enters and leaves different developmental phases (Grimm *et al.*, 2011; Howa *et al.*, 2016). A common practice of child growth is to measure the increase in body mass, to control and modify the external conditions that affect

growth gain (Oliveira *et al.*, 2000; Gómez *et al.*, 2008; Aggrey, 2009).

There have been different modeling approaches applied to the growth measurement to identify defining characteristics in growth process. An example is the construction of the curve-fitting models that relate age with height and estimate age at which an individual attain maximum growing by associating features in various growth phases (Laird, 1965; Grossman *et al.*, 1985; Grossman and Koops, 1988; Galeano-Vasco *et al.*, 2014). Studying growth in one phase may have an important influence or

\*Corresponding author:

Email: [dalbrayii@gmail.com](mailto:dalbrayii@gmail.com) +251913927596

<https://dx.doi.org/10.4314/eajbcs.v5i2.15>

association with subsequent phases since individual growth is monitored as a sentinel indicator of overall well-being (Tanner, 1981; Goldstein *et al.*, 2002; Richard *et al.*, 2014).

Many growth modelling approaches are used to obtain descriptions of change in growth processes accounting individual specific effects observed over time, average change, between-individual differences in change and to identify determinants factors (Grimm *et al.*, 2011). However, modelling growth trajectory is difficult process due to the model parameters that could not be possible to elaborate from biological perspectives (Aggrey, 2002; Aggrey, 2009; Galeano-Vasco *et al.*, 2014). Many scholars have been used cross-sectional data to model features in growth process. Despite of cost effectiveness and easy access to data, cross-sectional centiles for example, only offer a cross-sectional coverage, and hence the growth path of an individual monitored longitudinally in time is unknown since these types of modelling do not describe the dynamic aspect of growth process over time (Grajeda *et al.*, 2016).

The mixed effects modeling approaches are among the commonly used methods to capture growth process. This modelling approach is capable of incorporating subject specific rate of change over time and difference across the subjects in the linear predictor expression form (Bates *et al.*, 2015). Mixed effects models have been applied to the longitudinal data in different settings (Devidian and Giltinan, 1995; Pan and Goldstein, 1998; Grimm *et al.*, 2011; Richard *et al.*, 2014; Chirwa *et al.*, 2014). In this approach, mixed effects refer to the population mean of the parameter and random effects that indicate the differences between the mean value of the parameter and the adjusted value for each

subject (Littell *et al.*, 2000; Wang and Zuidhof, 2004). The mixed effects methods quantify variability between and within individuals letting a flexible covariance structure (Pinheiro and Bates, 1995; Aggrey, 2009) to accommodate time dependent and time independent covariates within individual residual terms (Pan and Goldstein, 1998). Many studies have been used the mixed effects models in linear and nonlinear approaches (Pan and Goldstein, 1998; Craig and Schinckel, 2001; Schinckel *et al.*, 2005; Aggrey, 2009; Grimm *et al.*, 2011). However, both modelling approaches have not been applied to the longitudinally collected data from low income countries' settings. Thus, the main objective of the current study was to model height growth in Ethiopian children aged 1-12 years and to identify determinant factors using mixed effects modelling approaches in linear and nonlinear forms.

## MATERIALS AND METHODS

### The study design and source of data

Data on growth measurement gathered over time by Young Lives Ethiopia, a younger cohort, was used in this study. Young Lives is an international collaborative research project supported and coordinated by a team based at Oxford University, UK. The cohort has been studying the lives of children in Ethiopia aiming to reduce childhood poverty. This project built up lives of 3,000 children living in 20 sites across Addis Ababa (the capital) and four other regions (Amhara, Oromia, Former Southern Nations Nationalities and Peoples (SNNPs), and Tigray). The Young Lives Ethiopia cohorts have been aimed to follow children in two age groups: a younger cohort following of 2,000



children who were 0.5 to 1.5 years old and an older cohort following 1,000 children aged 7.5 to 8.4 years at the baseline (first round) in 2002. The rest three rounds of surveys were carried out in 2006, 2009, and 2013, respectively, for both cohorts. Details of the cohort studies have been referred via the official website of the project ([www.younglivesethiopia.org](http://www.younglivesethiopia.org)). Based on the inclusion criteria, a total of 1760 children were included in the study. Height growth measurements observed from each subject in four survey rounds were used as outcome variable (see Figure 1). Age and other socio-economic, demographic and health related covariates were included in the study.

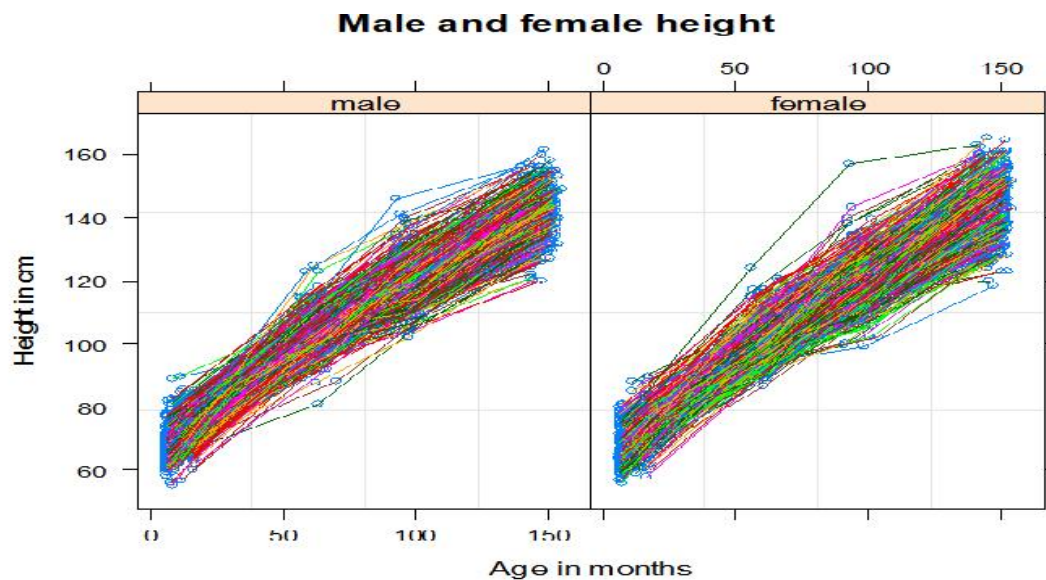
### Statistical Methods

Two modeling approaches were used in the data analysis as described in the next section. The linear mixed effects modeling approach was used to identify determinant factors associated with height growth difference between and

within subjects. The nonlinear mixed effects modeling approach was used to capture growth trajectories and to estimate relationship between rate of change over time and maximum (adult) height.

### Linear Mixed Effects Models

Linear mixed models (LMMs) may be expressed in different but equivalent forms. It is common to express such a model in hierarchical form, or just as a mixed model, including additional random-effect terms and associating variance and covariance components (John and Sanford, 2015). When the levels that we observed represent a random sample from the set of all possible values, the random effects can be incorporated in the model (Bates, 2010). This approach decomposes the outcome of an observations as fixed effect (population mean) and random effect (subject specific change over time), and it account for the correlation structure of variations among subjects.



**Figure 1: Individual height growth measurements plotted on measurement time by sex (male: left and females right).**

## Model description

LMMs used in this study have only two-levels, across and within individual variations. For  $y_{ij}$  is height measurements of  $i^{\text{th}}$  subject taken on  $j^{\text{th}}$  measurement occasion, where  $j = 4; i = 1, 2, \dots, n$ . The extended form of linear model with random components is described as follows:

$$y_{ij} = S_1 x_{1ij} + \dots + S_p x_{pij} + b_{1i} z_{1ij} + \dots + b_{qi} z_{qij} + V_{ij}$$

The matrix form of this model is equivalent and considerably simpler to write as:

$$Y_{ij} = S_0 + X_{ij} S + Z_i b_i + V_{ij},$$

where  $Y_{ij}$  is the  $n_i \times 1$  vector of response observations in the  $i^{\text{th}}$  subject at  $j^{\text{th}}$  measurement occasion,  $X_{ij}$  is the  $n_i \times p$  model matrix of fixed-effect regressors,  $S$  is the  $p \times 1$  vector of fixed-effect coefficients which is invariant across groups,  $Z_i$  is the  $n_i \times q$  matrix of regressors for the random effects of observations in subject  $i$ ,  $b_i$  is the  $q \times 1$  vector of random effects for group  $i$ , potentially different in different groups and  $V_{ij}$  is the  $n_i \times 1$  vector of errors for  $j^{\text{th}}$  measurement in  $i^{\text{th}}$  subject.

## Model assumptions

The linear mixed effects analysis was performed with some assumptions: random effects are different across the subject and normally distributed with mean zero and variance co-

variance structure, covariates are uncorrelated with each other (no multicollinearity), time variant covariates are a subset of the time invariant covariates, error terms are assumed to have a multivariate normal distribution and within subject measurement errors are auto correlated.

Under certain conditions, physical growth does not follow linear pattern over time. Modeling growth spurts using linear form of models could lead us into wrong conclusion and may have weak prediction power. Thus, the nonlinear models are alternative ways of modeling growth spurts. This modelling approach uses mixed or fixed effects form based on the objectives of underlying study.

## Non-Linear Mixed Effects Models

Nonlinear mixed effects models refer to the population mean of the parameter and random effects that indicates the differences between the mean value of the parameter and the adjusted value for each individual growth over time (Wang and Zuidhof, 2004). The nonlinear mixed effects growth curve models used in this study are Logistic and Gompertz which are most commonly used growth curve models due to their mathematical tractability with biologically meaningful parameters.

Logistic Model (Nelder, 1961)

$$y_{ij} = \frac{S_1 + b_{1i}}{1 + (S_2 + b_{2i}) \exp(-(S_3 + b_{3i})t_{ij})} + V_{ij}$$

### Gompertz Model (Winsor, 1932)

$$y_{ij} = (S_1 + b_{1i}) \exp((S_2 + b_{2i}) \exp(-(S_3 + b_{3i})t_{ij})) + v_{ij}$$

where,  $y_{ij}$  is height of  $i^{th}$  subject at  $j^{th}$  measurement occasion,  $t_{ij}$  is age of  $i^{th}$  subject at  $j^{th}$  measurement time,  $S_1$  is asymptotic or maximum height (adult height),  $S_2$  is scaling parameter and  $S_3$  is growth rate (between subjects);  $b_{1i}$  is random effects for  $S_1$ ,  $b_{2i}$  is random effects for  $S_2$ ,  $b_{3i}$  is random effect for  $S_3$  and  $v_{ij}$  is error term.

$$b_{ik} \sim N(0, \Sigma_k), \quad v_{ij} \sim N(0, \tau^2) \text{ for } k = 1, 2, 3,$$

$$\Sigma_k = \begin{bmatrix} \Sigma_{b11} & \Sigma_{b12} & \Sigma_{b13} \\ \Sigma_{b21} & \Sigma_{b22} & \Sigma_{b23} \\ \Sigma_{b31} & \Sigma_{b32} & \Sigma_{b33} \end{bmatrix}$$

Since our sample data is repeated measurements taken on the same subject, the expression for the within-subject variance-covariance matrix can be formed in the following way:

$$R_i = \tau^2 \Gamma_i I_{n_i}, \quad I_{n_i} = \text{An identity matrix } (n_i \times n_i),$$

$\Gamma_i$  = Correlation structures and  $\tau^2$  = Residual variance of the model.

### Methods of parameter estimation

Maximum likelihood estimation method was implemented to estimate underlying model parameters using R-package “lme4” and “nlme”. Statistical test was done at 5% level of significance. Further details of mixed effects model parameter estimation has been described by Lindstrom and Bates (1990), Lindstrom and Bates (1995), Davidian and Giltinan (1995) and, Sedigheh and Debasis (2012).

### Model adequacy checking

The model assumptions were checked using residual plots versus fitted values, QQ and P-P plots. The goodness of fit was tested based on the Bayesian Information Criteria (BIC) and Akaike Information Criteria (AIC). However, some scholars argue that several measures of model fit, even the likelihood ratio chi-square, that often appear to reflect relatively poor fit – when a model fits data very closely – that is, if residual variances are quite small (Browne *et al.*, 2002).

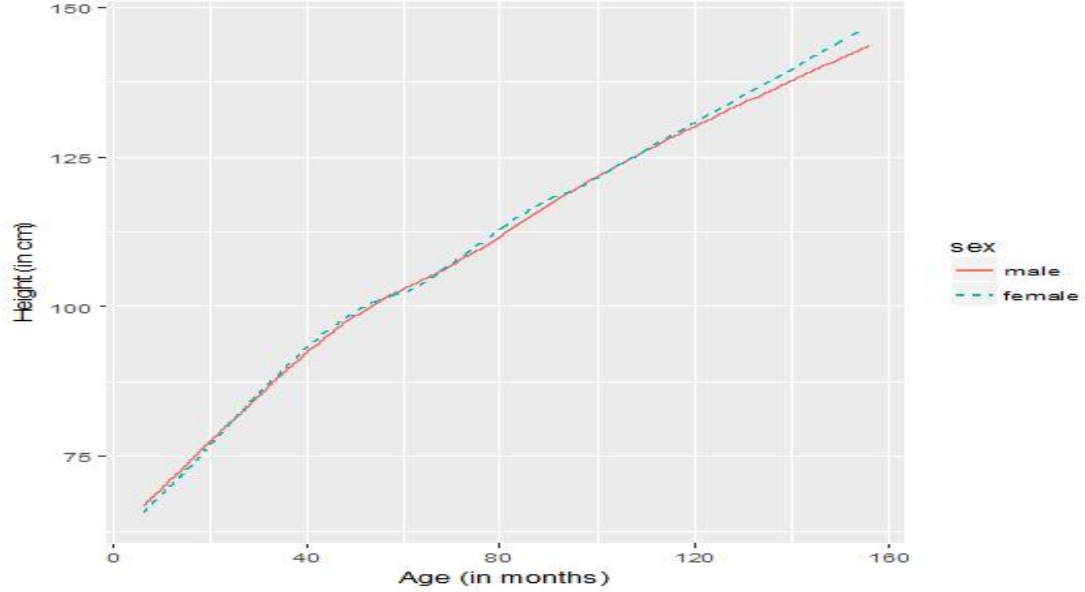
## RESULTS

### Descriptive statistics

Descriptive statistics of height measurements taken on each survey visit presented below in Table 1. More height growth variation was observed in girls than in boys after period I. Growth variation became higher in the fourth period for both sexes

**Table 1: Summary statistics of height in each measurement periods by sex.**

Measurement Period in years	Female					Male				
	N	Min	Max	Mean	Std. D	N	Min	Max	Mean	Std. D
Period I (age 1)	841	56.00	89.50	70.425	5.498	947	55.30	89.50	71.45	5.227
Period II (age 5)	843	86.50	124.00	103.563	5.512	947	80.90	124.90	103.95	5.291
Period III (age 8)	843	99.10	157.00	120.628	6.469	947	102.0	146.00	120.66	6.129
Period IV (age 12)	843	118.2	178.00	142.205	7.880	947	120.0	161.50	139.80	6.628



**Figure 2: Smooth line curve of height growth over measurement time by sex**

Boys and girls had almost the same height between 12-84 months (1-7 years). After 84 months girls become taller than boys (Figure 2). However, the smooth curve plot in Figure 2 doesn't show where the rate of change was accelerated or decelerated. In order to identify where rapid and slow rate of change lies we have used height growth velocity curves presented in Figure 3.

### Height growth Velocity

Height growth velocity was calculated to investigate time of accelerated and decelerated growth periods. To assess these curvatures, the

following velocity formula used (Grajeda *et al.*, 2016):

$$\Delta height(t_{ij}) = \frac{height(t_{i(j-1)}) - height(t_{i(j-1)})}{t_{ij} - t_{i(j-1)}}$$

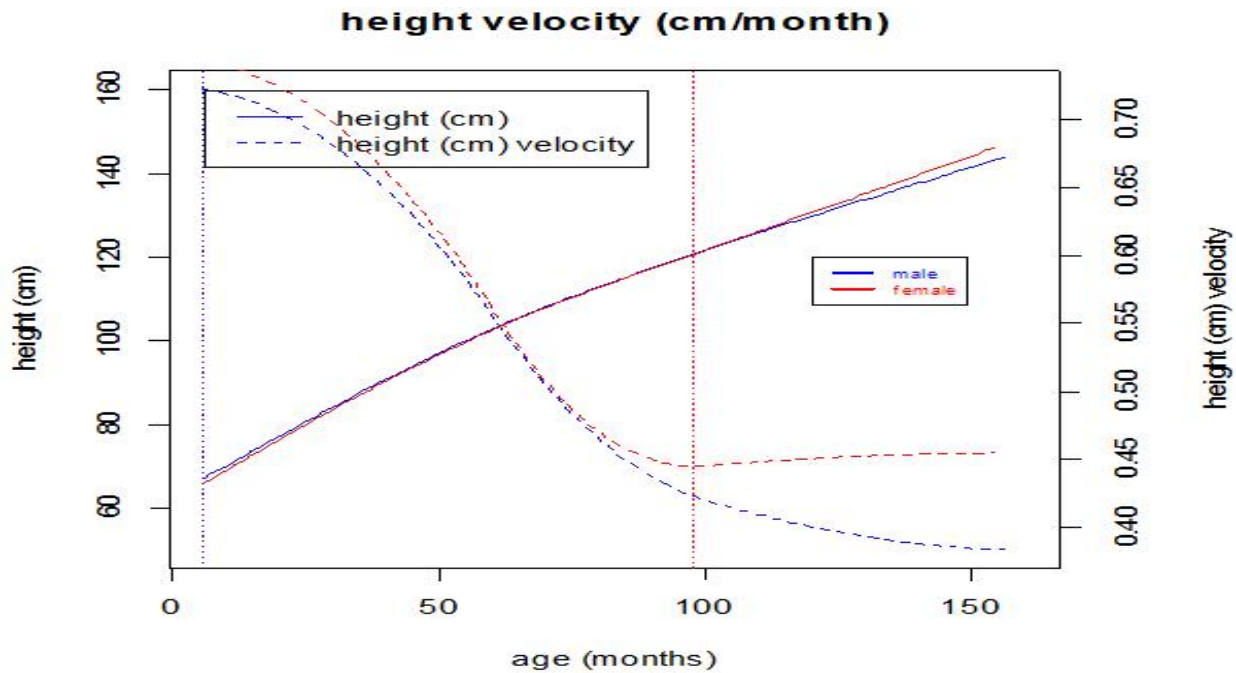
where ,

$\Delta height(t_{ij})$  = height change for  $i^{th}$  individual at  $j^{th}$  measurement period.

Between 60 to 84 months, boys and girls had shown very similar rate of growth change. After 84 months (7 years) rate of change in girls became accelerated than boys. The growth difference in this time could be due to various factors. Thus, we have used linear mixed effects models to identify factors associated with rate of change for both sexes. On the other hand,

nonlinear mixed effects models were used to estimate height at maximum growth and rate of

change over time within and between subjects.



**Figure 3: Smooth line and growth velocity curves by sex**

### Linear fixed and mixed effects models

Table 2 presents the goodness of fit test for the linear models. Linear mixed effects model better fit the data than fixed effects model.

**Table 2: Assessing the goodness of fit of linear models**

Fit statistics	Linear fixed	Linear mixed
AIC	44485.57	43010.67
Log.Lik	-24546.60	-21446.34

The estimated values of the mixed effects model are presented in Table 3. Within an individual growth variation over time was around 0.03 cm. There was a positive relationship between within-individual rate of change (slope) and height at the baseline (random intercept). This points that a child who

was taller at the baseline shown faster growth over time ( $r = 0.728$ ). There was a positive correlation between two consecutive measurements taken on the same subjects at different measurement occasions (AR (1):  $\pi = 0.2$ ) (Table 3).

**Table 3: Estimated values of random effects model**

Random Components	Estimates		Serial correlation Continuous AR(1)
	St. Dev.	Correlation	
(Intercept)	1.893	(Intr)	$\pi = 0.2$
Age in months	0.0299	0.728	
Residual = 4.664			

Access to quality drinking water, mother's educational status and sex had a significant effect on height growth. Children who had access to quality drinking water were 3.8 cm

taller than children who had no access to quality drinking water (Table 4).

**Table 4: Estimated values of different covariates on height growth of children aged 1-12 years based on the linear mixed effects model**

Covariates	Categories		Std.Error	DF	t-value	p-value
(Intercept)	-	66.97115	2.618180	5067	25.57927	0.0000
Age	-	0.49914	0.007732	5067	64.55163	<b>0.0000</b>
Sex	Male (ref.)					
	Female	-1.30927	1.348283	1698	-0.97106	0.3317
Birth order	-	-0.01189	0.042960	1698	-0.27685	0.7819
BCG status	Yes (ref.)					
	No	-0.21590	0.244046	1698	-0.88469	0.3765
Had quality drinking water:	No (ref.)					
	Yes	-3.86616	0.748315	5067	-5.16649	<b>0.0000</b>
Household size	-	0.24943	0.132781	5067	1.87850	0.0604
Had ANC visit	No (ref.)					
	Yes	0.20970	0.225077	5067	0.93170	0.3515
Breast feeding duration	Never fed (ref.)					
	fed for 1-3 months	0.48811	2.516145	1698	0.19399	0.8462
	fed for 4-6 months	2.07767	2.539510	1698	0.81814	0.4134
	fed for > 6 months	1.48964	2.419669	1698	0.61564	0.5382
Mother's age at birth	-	-0.00786	0.019595	1698	-0.40107	0.6884
Father's education:	No education ref.					
	Elementary (1-8)	1.70812	0.210840	5067	8.10153	0.0000
	Other	-1.52816	3.234500	5067	-0.47246	0.6366
Mother's education:	No education ref.					
	Elementary (1-8)	0.83562	0.233946	5067	3.57187	<b>0.0004</b>
	>= High school	1.93923	0.290056	5067	6.68570	<b>0.0000</b>
Region	Addis Ababa ref.					
	Amhara	-1.60553	1.437172	5067	-1.11714	0.2640
	Oromia	-4.24911	1.382365	5067	-3.07380	0.0021
	SNNP	-1.19146	1.384214	5067	-0.86074	0.3894
	Tigray	-2.45187	1.403808	5067	-1.74658	0.0808
Area of residence	Urban ref.					
	Rural	-0.72144	0.436144	5067	-1.65413	0.0982
Interaction effects						
Age*sex	Male (ref.)					
	Female	0.02708	0.007462	5067	3.62902	<b>0.0003</b>
Quality drinking water*region	A.A (No ref.)					
	Amhara	2.17289	0.919798	5067	2.36236	<b>0.0182</b>
	Oromia	6.04705	0.928457	5067	6.51301	<b>0.0000</b>
	SNNP	2.99661	0.911643	5067	3.28704	<b>0.0010</b>
	Tigray	2.14791	0.907350	5067	2.36724	<b>0.0180</b>
Age*Had quality drinking water	(No ref.)					
	Yes	0.03497	0.008313	5067	4.20725	<b>0.0000</b>

Mother's educational status also plays a significant role on height growth of children. Children whose mother had elementary (1-8) and high school plus educational status were 0.84cm and 1.9 cm taller than children whose mother had no formal education, respectively. As age increased by a month, girls' height increased by 0.27 cm compared to boys holding other covariates constant in the model. The interaction effect between age and sex was higher in girls compared to boys. Height in girls increased by 0.035 cm than boys as age increased by one month. On the other hand,

access to quality drinking water had a significant effect on height growth of children (Table 4). Children those who had access to quality drinking was had 0.035 cm increased height compared to children those who had no access to quality drinking water.

### Nonlinear Models

After identifying the best model fit to the data, the average rate of change over time and maximum (adult height) estimated height for both sexes separately.

**Table 5: Goodness of fit test for nonlinear mixed effects models by sex**

Models	Fit statistics	Fixed effects models		Random effects	
		Male	Female	Male	Female
<b>Gompertz</b>	AIC	23759.5	21781.9	4243.28	2902.96
	BIC	23799.2	21798.4	4280.23	2956.96
<b>Logistic</b>	AIC	23784.4	21772.6	4216.93	2921.48

**Table 6: Estimated values and fit statistics based on nonlinear mixed effects growth curve models by sex**

Female										
Nonlinear mixed models	parameter	Fixed estimate		Random components					Fit statistics	
		Estimated	Std.err	$r_{b_1b_3}$	$\hat{\sigma}_1$	$\hat{\sigma}_2$	$\hat{\sigma}_{b_1b_2}$	$r_{b_{sb}}$	AIC	BIC
<b>Gompertz</b>	b1	<b>179.44</b>	2.398	-0.889	10.582	0.049	0.374	0.718	2901.48	2934.96
	b2	1.054	0.0108							
	b3	0.0105	0.0003							
<b>Logistic</b>	b1	<b>166.703</b>	1.716	-0.802	9.750	0.103	0.758	0.752	2922.96	2956.44
	b2	1.623	0.0215							
	b3	0.0156	0.0003							
	b3	0.0087	0.0003							
Male										
<b>Gompertz</b>	b1	<b>171.652</b>	1.3951	-0.879	7.9496	0.039	0.227	0.717	4216.93	4253.88
	b2	0.98945	0.0066							
	b3	0.0111	0.0002							
<b>Logistic</b>	b1	<b>161.340</b>	1.034	-0.802	7.2219	0.047	0.340	0.995	4243.28	4280.23
	b2	1.4912	0.0125							
	b3	0.01618	0.0002							

## Model comparisons

Incorporating an individual-specific rate of change over time in the nonlinear models had dramatically reduced the estimation error and increased the fitting performance of the model. For instance, when adult height, rate of change and scaling (point of growth change) allow to varying across individuals, the fitting performance of the models had improved (Table 6).

Random effects parameters were selected based on their capability to map with theoretical and physical meanings. When adult height and rate of change vary across individual over time, Logistic models better fitted the data for both sexes. The mean adult height was estimated to be 166.7 cm and 171.6 cm in girls and boys, respectively. Adult height and rate of change had inverse relationship for both sexes (for girls  $r_{13} = -0.802$ ; for boys  $r_{13} = -0.879$ ).

## DISCUSSION

This study was aimed to model individual specific growth spurt over time in children aged 1-12 years old. The mixed effects models were applied to the height growth measurements to interpolate growth spurt within and between subjects over time. The effect size of different covariates on height growth was estimated using the linear mixed effects models. Decelerated and accelerated growth periods were identified using growth velocity curves.

The fitting performance of the models increased when adult height and rate of change were allowed to as individual specific. Random effects were partitioned into between ( ) and

within ( ) subject variations. The consistent result by other study (Spyrides *et al.*, 2008) reported that considering random effects in the proposed models increase the precision of estimated parameters since parameters vary from individual to individual that might be demanded using margin of errors in the fixed effects model set-up. However, most of the mixed effects models applied to human physical growth data had no clear identification towards random and fixed effects parameters that should be included in the models. Thus, one of the objects of this study was to identify model that best fits height growth in the defined time points when individual specific effects were taken in to account. In addition, this study was concerned to identify mixed effects parameters that best map on theoretical basis having biologically meaningful interpretations. Of course, here the study was concerned to use some notations suggested by Browne and co-authors (Browne *et al.*, 2002) to identify those parameters and to select best fit to the data. The authors discussed their arguments that many measures of model fit, even the likelihood ratio chi-square, and often appear to reflect relatively poor fit: This suggest a poor fit despite the model closely fitting the data. Therefore, this study had carefully examined and identified that adult height and rate of change over time were individual specific and had random effect on height growth.

The present study found that rapid growth was observed in children between 1 to 3 years followed by decelerated rate of change. Other consistent study reported that children of both sexes grow at approximately the same rate until the adolescent growth spurt (Rogol *et al.*, 2000). Adult height and rate of change had inverse relationship for both sexes. The consistent



findings reported that the adolescents with a later APHV tended to have a higher height later in life (Chen *et al.*, 2022). The interaction effect of age on rate of change in growth was higher in girls compared to boys. This may be due to girls experience adolescence earlier than boys.

## CONCLUSIONS

The logistic mixed effects models best fit and captured height growth pattern for both sexes. Boys were taller than females until onset of puberty. The most decelerated rate of growth was observed in early childhood period for both sexes. Mother's educational status, access to quality drinking water, age and sex could be one of the determinant factors of height growth in children aged 1- 12 years. Rate of change at the base line had no a significant effect on adult height. Child whose growth was accelerated during childhood period attains adult height later in life.

## Competing interest

Authors have no conflict of interest

## Acknowledgement

We, the authors, would like to thank Oxford University and Young Live Ethiopia for the data access.

## References

Aggrey S. E. 2002. Comparison of Three Nonlinear and Spline Regression Models for Describing Chicken Growth Curves. *Poult. Sci.* **81**:1782-1788.

- Aggrey S. E. 2009. Logistic Nonlinear Mixed Effects Models for Estimating Growth Parameters. *Poult. Sci. Asso.* **88**:276-280.
- Agudelo Gómez D. A., Cerón Muñoz M. F. and Restrepo Betancur L. F. 2008. Modeling of growth Functions Applied to Animal Production. *Rev. Colomb. Cienc. Pecu.* **21**:3-8.
- Bates D., Mächler M., Bolker B. and Walker S. 2015. Fitting Linear Mixed-Effects Models Using lme4. *J. Stat. Softw.* **67**(1) 1–48.
- Browne M., MacCallum R. C., Kim C.T., Andersen B. L. and Glaser R. 2002. When Fit Indices and Residuals are Incompatible. *Psychol. Methods* **7**:403–421.
- Chen L., Su B., Zhang Y., Ma T., Liu J., Yang Z., Li Y., Gao D., Chen M., Ma Y., Wang X., Wen B., Jiang J., Dong Y., Song Y., Ma J. 2022. Association between height growth patterns in puberty and stature in late adolescence: A longitudinal analysis in Chinese children and adolescents from 2006 to 2016. *Front Endocrinol (Lausanne)*. **13**:882840.
- Chirwa E. D., Griffiths P. L., Maleta K., Norris S. A, and Cameron N. 2014. Multilevel Modeling of Longitudinal Child Growth Data from Birth to Twenty Cohorts: A Comparison of Growth Models. *Ann. Hum. Biol.* **41** (2): 168-179.
- Craig B. A. and Schinckel A. P. 2001. Nonlinear Mixed Effects Model for Swine Growth. *Prof. Anim. Sci.* **17**(4): 256–260.
- Davidian M. and Giltinan D. M. 1995. Nonlinear Models for Repeated Measurement Data. London: Chapman & Hall. Pp 125.
- Galeano-Vasco L., Cerón-Muñoz M.F. and Narváez-Solarte W.V. 2014. Ability of non-linear mixed models to predict growth in laying hens. *Revista Brasileira De Zootecnia* **43**: 573-578.
- Goldstein H, Browne W, and Rasbash J. 2002. Multilevel modelling of Medical Data. *Stat.Med*; **21**: 3291-3315.
- Goldstein H. and De Stavola B. 2010. Statistical Modelling of Repeated Measurement Data. *Longitudinal and Life Course Studies*; **1**: 170-185.
- Goldstein P. H. 1998. Multi-level Repeated Measures Growth Modelling using Extended Spline Functions. *Stat. Med.* **17**(23):2755– 2770.
- Grajeda L. M., Ivanescu A., Saito M., Crainiceanu C., Jaganath D., Gilman R. H., Crabtree J. E., Kelleher D., Cabrera L., Cama V. and Checkley W. 2016. Modelling Subject Specific Childhood Growth using Linear Mixed Effect Models with Cubic Regression Splines. *Emerg. Themes. Epidemiol.* **13**(1). doi: 10.1186/s12982-015-0038-3.
- Grimm K. J., Ram N. and Hamagami F. 2011. Nonlinear Growth Curves in Developmental Research. *Child Dev.* **82**: 1357–1371.
- Grossman M. and Koops W. J. 1988. Multiphase Analysis of Growth Curves in Chickens. *Poult. Sci.* **67**:33-42.

- Grossman M., Bohren B. B. and Anderson V. L. 1985. Logistic Growth Curve of Chickens: A Comparison of Techniques to Estimate Parameters. *J. Hered.* **76**:397-399.
- John F. and Sanford W. 2015. Mixed-Effects Models in R. An Appendix to An R Companion to Applied Regression, Second Edition.
- Koya P. R. and Goshu A. T. 2013. Generalized Mathematical Model for Biological Growths. *Open Journal of Modelling and Simulation*; **1**: 42-53.
- Laird A. K.; Tyler S. A. and Barton A. D. 1965. Dynamics of normal Growth. *Growth* **29**:233-248.
- Littell R. C, Pendergast J. and Natarajan R. 2000. Modeling Covariance Structure in the Analysis of Repeated Measures Data. *Stat. Med.* **19**:1793-1819.
- Monette Georges, 2012. Mixed Models with R: Longitudinal Data Analysis with Mixed Models. [http://scs.math.yorku.ca/index.php/SPIDA\\_2012](http://scs.math.yorku.ca/index.php/SPIDA_2012).
- Nelder J. A. 1961. The Fitting of a Generalization of the Logistic Curve. *Biometrics* **17** (7): 89- 110.
- Oliveira H. N., Lôbo R. B. and Pereira C. S. 2000. Comparação de modelos não-lineares para descrever o crescimento de fêmeas da raça Guzerá. *Pesquisa Agropecuária Brasileira* **35**:1843-1851.
- Pinheiro J. C. and Bates D. M. 1995. Mixed Effects Models Methods and Classes for S and Splus. Version 1.2, University of Wisconsin-Madison.
- Richard S. A., McCormick B. J., Miller M. A., Caulfield L. E., Checkley W.; MAL-ED Network Investigators. 2014. Modeling environmental influences on child growth in the MAL-ED cohort study: opportunities and challenges. *Clin. Infect. Dis.* **59** (Suppl 4):S255-60. doi: 10.1093/cid/ciu436.
- Richards F. J. 1959. A Flexible Growth Function for Empirical Use. *J. Exp. Bot.* **10**: 290-300.
- Rogol A. D., Clark P. A. and Roemmich J. N. 2000. Growth and pubertal development in children and adolescents: effects of diet and physical activity; *The American Journal of Clinical Nutrition*, **72**, (2); 521S-528S.
- Schinckel A. P, Adeola O. and Einstein M. E. 2005. Evaluation of Alternative Nonlinear Mixed Effects Models of Duck Growth. *Poult. Sci.* **84**:256–264.
- Spyrides M. H., Struchiner C. J., Barbosa M. T. and Kac G. (2008) Effect of predominant breastfeeding duration on infant growth: a prospective study using nonlinear mixed effect models. *J Pediatr (Rio J)*. **84**(3):237-43.
- Tanner J. M. 1981. A History of the Study of Human Growth. Cambridge University Press; WHO: Physical Status: The Use and Interpretation of Anthropometry, Report of a WHO Expert Committee 1995.
- Wang Z. and Zuidhof M. J. 2004. Estimation of Growth Parameters using a Nonlinear Mixed Gompertz Model. *Poult. Sci.* **83**: 847–852.
- Zemel B. S. and Johnston F. E. 1994. Application of the Preece-Baines Growth Model to Cross-sectional Data: Problems of Validity and Interpretation. *Am. J. Hum. Biol.* **6** (5): 563–570.



## Effect of Land Use Activities on Water Quality and Vegetation Cover Change in Nsooba - Lubingi Wetland System, Kampala City

Charles K.Twesigye<sup>1\*</sup>, Kennedy Igunga<sup>1</sup> and Ritah Nakayinga<sup>1</sup>

<sup>1</sup> Department of Biological Sciences, Faculty of Science, Kyambogo University, P.O. Box 1, Kyambogo, Kampala, Uganda

### KEYWORDS:

Agriculture;  
Built environment;  
Public health;  
Pollution;  
Wetland

### ABSTRACT

An assessment of the effect of land use activities on water quality and vegetation cover change in Nsooba - Lubingi Wetland System in Kampala city was conducted between July and October 2020. In order to achieve the set objectives, twelve locations were selected from the Nsooba - Lubingi Catchment. The physico-chemical characteristics of water along the catchment area were determined by standard analytical methods. The average values for Total Dissolved Solids across all the land-use types of wetland, built up areas and agriculture were lower than the National Standard (750 mg/l). A similar pattern of the land-use was observed for the parameters Total phosphorous, Biological oxygen demand, Chemical oxygen demand, Total suspended solids and Total organic carbon, where the observed average values were all below the National Standards of 10 mg/l, 50mg/l, 70mg/l, 50mg/l and 50mg/l, respectively. The Total Nitrogen average value for built-up areas (11.27 mg/l) was higher than the national standard of 10 mg/l while the remaining land use types of wetland (8.05mg/l) and agriculture (5.96mg/l) were below that of the recommended standard. GIS and Remote sensing techniques were used to analyze high-resolution satellite imagery captured during 1998, 2008 and 2018. Wetland coverage declined by approximately 5 hectares (47.2% to 14.58%) from 1998 to 2018. Although most of the measured parameters were below the National standard specified by the Uganda National Environmental Management Authority apart from Total Nitrogen for built-up areas, there is need for close monitoring of the water quality in Nsooba - Lubingi catchment to ensure public health safety. The increased built-up environment in the Nsooba - Lubingi wetland affects ecosystems services of the wetland. The buffer zones for flood control and sewage treatment have been turned into built-up environment. The results from this study suggest a need to protect the Nsooba - Lubingi catchment for its important ecosystems services of flood control and sewage treatment.

### Research article

### INTRODUCTION

The world's growth metrics have been impacted by unchecked expansion in a variety of human undertakings, including industrial,

transportation, agricultural, and urbanization (Gavrilescu *et al.* 2015 and Mishra *et al.*, 2023). Globally, water quality deprivation is one of the main persistent, and greatly observable signs of anthropogenic impacts. Surface water bodies

\*Corresponding author:

Email: [twesigyeck@yahoo.com](mailto:twesigyeck@yahoo.com) +256-782353775

<https://dx.doi.org/10.4314/eajbcs.v5i2.2S>

such as reservoirs, river streams and lakes are enormously vulnerable to primary discharges of solid and liquid waste. Extremely dilute water bodies, specifically in headwater regions are vulnerable to impacts caused by atmospheric deposition (acid rain) (Sasakova *et al.*, 2018).

In developing countries, the changes in land use are directly and indirectly related to pollution challenges that include sewage, insecticides and pesticides, greatly contaminated water quality, principally near intensive agricultural areas and urban industrial centers (Wang *et al.*, 2015). This alters the ecological landscape, severe strain from anthropogenic encroachment as well as consistent land filling activities for reclamation, water drainage for agriculture and livestock farming, human settlements, clay and sand extraction, brick making, harvesting of papyrus, municipal and industrial waste discharges, unsuitable and illegal solid waste disposal (Peters *et al.*, 2015, Kayima *et al.*, 2018). In the natural ecosystem, heavy metal concentrations differ, human activities alter the distributions and natural cycles of metals creating an unbalanced ratio in the metal cycle leading to accumulation (Edokpayi *et al.*, 2018).

Many studies of watershed microbiology focus largely on the detection of indicator microbes such as *E. coli*, *enterococci*, *salmonella* and coliform bacteria and how these might indicate potential risks to human health and environment. Hawumba (2017) indicated that; in Uganda, the leading causes of water quality impairment is high nutrient (phosphorus and nitrogen) discharge to the ground and surface water bodies. The same author further added that, whereas nitrogen is of principal significance in affecting and preventing eutrophication in marine environments,

phosphorous is the restraining nutrient in freshwater (or non-saline) ecosystems. According to Ding *et al.*, (2015), studying the correlation among water quality and land use supports to ascertain primary stresses to water quality which are predetermined for efficient water resource and quality control since they can be used to target key land use regions and to incorporate pertinent methods to curtail contamination discharges.

Similar studies on land use have indicated its substantial impacts on water quality (Twesigye *et al.*, 2011). Deforestation, urbanization and agriculture mostly alter land topography and characteristics, surface runoff volume, upsurge algal production, generate contamination and reduce concentrations of dissolved oxygen in water resources. According to Wang *et al.* (2015), vegetation cover is an indicator that assesses terrestrial environmental surroundings. Minor alterations of vegetation structures of the landscape inhibit ecological processes. The increasing rates of land-use change over natural habitats like wetlands, lakes, rivers have resulted into the conversion of the natural environment for agriculture, sand mining, fishing and urbanization. Any deterioration of the natural vegetation raises the quantity levels of particulate matter in water, and consequently can directly and indirectly affect water quality (Fierro *et al.*, 2017).

According to Sebhatleab (2014), land use change has triggered the decline in both soil physicochemical and biological properties depending on the classification levels across the landscape and soil profile. Constant exposure of top soil can attribute to long-term intensified vegetation deprivation and start a process of land pollution (Marinho *et al.*, 2016). The

correlation between land use activities and its impact on soils involves studying the drivers of the variations in soil structure and help in illustrating good management processes to prevent desertification and attain conservation goals.

Limited studies have been conducted to study the overall interactions between land use and water quality. The consequences of anthropogenic activities on water quality, soils, and vegetation cover are severe and call for sustainable management. This study examines the relationship between land use and water quality to determine the microbial and physico-chemical attributes of the water, soils integrity, as well as the vegetation cover along Nsooba - Lubigi drainage system. This study, therefore, explores the effect of land use activities on water quality, soil and vegetation cover on Nsooba - Lubigi drainage system.

## **MATERIALS AND METHODS**

### **Study Area**

The study area lies within Nsooba - Lubigi drainage system, stretching from Bukoto hills, the origin of Nsooba - Lubigi to Lubigi wetland in Namungona. It is located between 0° 21'N latitude and 32° 35'E longitude, in Kawempe Division, Kampala City.

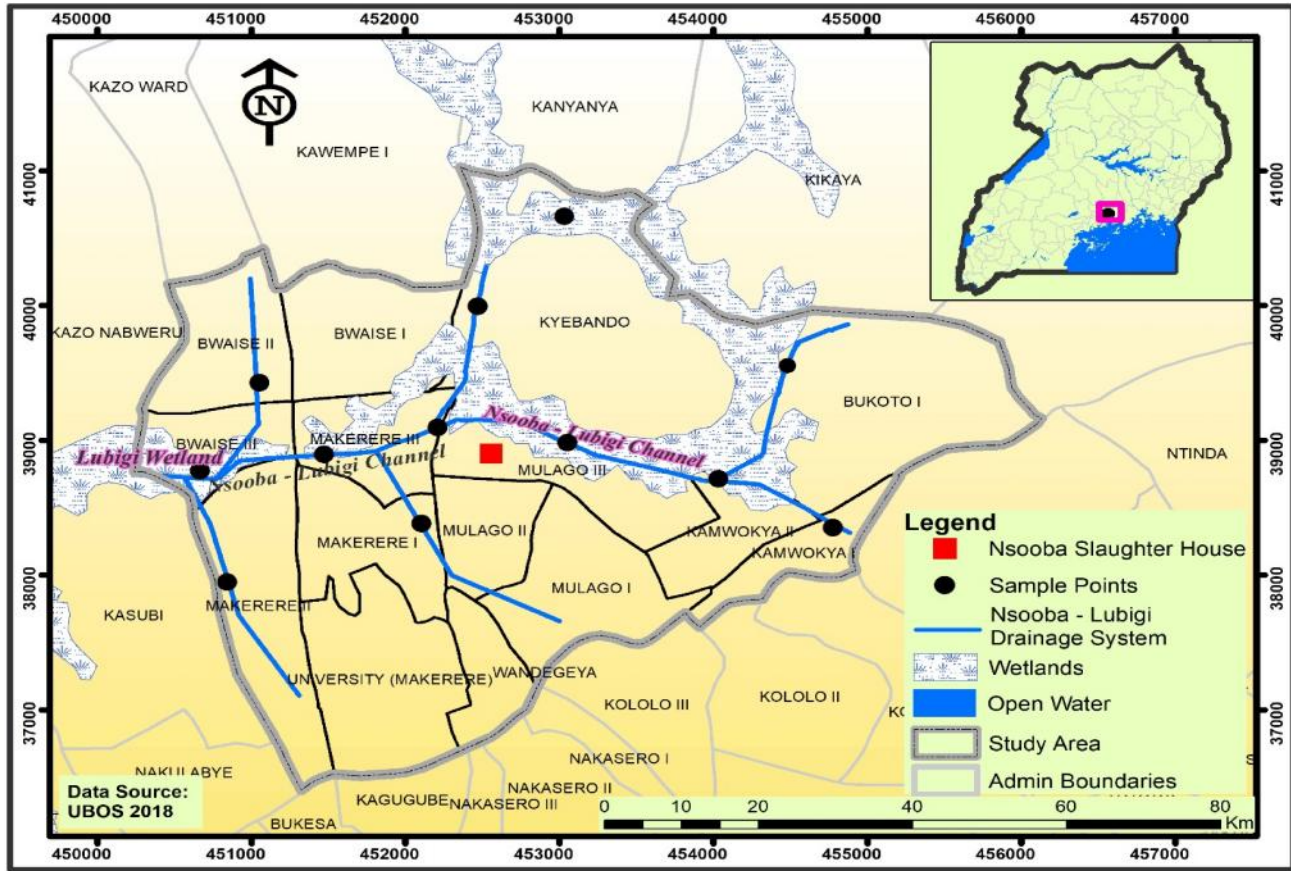
The discharge from the surrounding environment to Nsooba - Lubigi drainage system is about 220,000 m<sup>3</sup>/day and originates from the daily human activities, industrial and municipal effluent, automotive and mechanical discharge, rainwater run-off, surface and sub-

surface water flow from the upstream, as well as the populous slums of Kawaala, Kyebando, Kalerwe, Bwaise, Kanyanya, Nansana and Namungoona (Karabo, 2017). Due to insufficient environmental policies like development of the buffer zone to protect drainage system, Nsooba - Lubigi drainage system has and will continuously receive the initial and direct trickle-down effect of the visually and severely contaminated wastewater from the up-stream storm water draining to the channel as well as the Lubigi Sewage Treatment Plant.

Additionally, Nsooba - Lubigi drainage system has continuously been under serious pressure emanating from human actions and encroachment including unplanned land filling for reclamation, water drainage for agriculture, human settlements and livestock farming, use of agricultural pesticides in management of crops, sand and clay mining, brick making, the harvesting of papyrus for handicrafts, inappropriate solid waste disposal, municipal and industrial effluent disposal and other forms of discharges have led to pollution and contamination of the drainage system thus being a haphazard to the environment and surrounding community.

The area was selected as an ideal site because of the urbanization levels (construction of northern by-road), crowded settlements and the apparent poor sanitation and management of waste water. Further, Nsooba slaughter house also discharges solid and waste water into Lubigi wetland, creating severely contaminated wastewater from the upstream Nsooba - Lubigi water drainage stream and the Lubigi Sewage Treatment Plant.





**Figure 1: Study sites in Nsooba - Lubigi drainage system, Kampala City**

### Data Collection Tools and Methods

#### *Land Use Land Cover Change Activities*

Landsat-5 TM, Landsat-8, and Sentinel 2 images with a spatial resolution of 30m and 10m

**Table 1: Data specifications**

Satellite Data	MM/DD/YY	PATH and Row	Band	Resolution	Source
Landsat 5 (TM)	08/07 <sup>th</sup> /1998	172,059	3,4,5	30m x 30m	USGS
Landsat 7 (ETM+)	09/14 <sup>th</sup> /2008	172,059	3,4,5	30m x 30m	USGS
Landsat 8 (OLI/TIR)	10/07 <sup>th</sup> /2018	172,059	3,4,5	30m x 30m	USGS

A hand held GPS receiver was used for ground verification in evaluating the five land use/cover classes as indicated in Table 2.

for 3 years (2018, 2008, and 1998) were downloaded from an open-source at no cost. These were used for the spatial analysis of land use activities and vegetation cover change in Nsooba - Lubigi.

**Table 2: Land Use Land Cover (LULC) classification by Anderson method**

<b>Land use/cover classes</b>	<b>Description</b>
Agriculture	Subsistence Farming: Mixed farming characterized by crops grown for survival
Small scale farming	Small Scale Farming: Mixed farming, single and multi farming, dry and irrigated farming
Bare Land	Land that is productive and unproductive with no developments activities going on
Wetlands	seasonal and permanent wetlands, swamps, bog
Built-up Areas	Settlements like residentials, commercials, non-residentials, roads

As supervised classification was performed at the study area, each class was calculated while considering the pixel counts and total site (Table 2). Thus, categorizations were made based on area coverage and presented in both hectares and percentage. The five classes included Forestry, Grassland, Wetlands, Settlement, and Small scale farming. Percentages of classes based on these results portrayed land use/land cover events seen in the study area during 1998, 2008, and 2018 respectively.

### ***Sampling Strategy***

Water and soil samples were collected from the field for further analysis. A minimum of 48 water samples and 36 soil samples were gathered from 11 sites along Nsooba - Lubigi drainage system. The sites were selected due to the high anthropogenic activities (urbanization, slaughterhouse, industries and road construction) carried out within the wetland area. A minimum of 4 sampling at each sampling site were collected in Duran. Parameters for analysis included pH, EC, TSS, TN, TP, total coliform and *E. coli*, BOD and COD. These constitute the major parameters in measuring the degree of contamination of a water body (Chapman, 1992; Longe and Omole 2008). All the samples were preserved at 4°C

using a sampling cooler box and transported to the laboratory for analysis. Sampling was done between 08.00 am and 05.00 pm, the time of peak activities at the Nsooba - Lubigi drainage system in July 2020 and October 2020. During sample collection, sampling containers were rinsed twice with sampled water and, labeled and then taken to the Ministry of Water and Environment laboratory in Entebbe, stored in the refrigerator while maintaining a temperature of 4°C prior to analysis.

### ***Water Pollutants***

Water samples were collected between July 2020 and October 2020 in two sets to ensure that the results obtained are more representative. Each set consisted of 24 samples totaling to 48 samples.

### ***Analytical Procedures and Measurement***

In order to assess the effect of land use activities on quality of water and vegetation cover of Nsooba- Lubigi drainage system, physico-chemical properties and nutrients loads from upstream and downstream of the Kalerwe abattoir discharge area were evaluated. The physico-chemical characteristics were determined by the American Public Health

Association (APHA) standard analytical methods of water analysis. HACH standard method was used to determine nutrients concentrations by using a DR 1900 spectrophotometer and a DRB 200 digester as defined in the HACH procedure manual for chemical and physical water quality. Total suspended solids were analyzed using a gravimetric method. The Galen Kamp oven was used for drying at 105°C and a Mettlor Toledo weighing scale was used for weighing.

Chemical Oxygen Demand was determined by a standard HACH procedure using a DR 6000 spectrophotometer and DRB 200 digester as described in the HACH procedure manual. A volume of 2mls of the sample were put in the COD vial and digested at 150 °C for 2hrs. The vials were allowed to cool and COD was read. BOD was analyzed using a BOD<sub>5</sub> day test kit. This was used for digestion and monitoring oxygen changes.

#### ***Determination of pH & Electrical Conductivity***

pH was photometrically analyzed using a thermo scientific Orion star 3 machine whereas Electrical conductivity was analyzed using an Orion star A 222 conductivity meter.

#### ***Determination of Vegetation Cover Change***

This was determined using Landsat8 and sentinel 2. Landsat enabled the acquisition of old satellite images of 2008 and 1998, whereas sentinel facilitated the acquisition of satellite image of 2018.

#### **Data Analysis**

To compare the parameters across land use types, the data were subjected to a non-parametric test known as Kruskal-Wallis *H*-test, because it is more robust and requires smaller samples sizes. The test compares medians among *k* independent groups (*k* > 2) and is formulated based on ranks rather than actual observations (Daniel, 1990). The test is generally robust to departure from normality and homoscedasticity and is less sensitive to outliers. Kruskal-Wallis *H*-test only indicates that more than two groups are significantly different. It cannot show which specific groups of the independent parameters are statistically different from each other. Dunn test was used to determine which land use types were statistically significantly different from each other. Fisher's exact test was used were the data was categorical in nature and therefore difficult to compute the median.

#### ***Image Acquisition***

Re-classification process and change detection analysis of various land-use land-cover classes were performed by three Landsat satellite images of 5 TM, Landsat 7 ETM+ and Landsat 8 OLI/TIR all acquired from path 172 and row 059 as indicated in Table1. The satellite imagery data was downloaded from the United States Geological Survey website (USGS) (<ftp://ftp.glcf.umd.edu/glcf/Landsat/WRS2> and <https://earthexplorer.usgs.gov/>). After downloading, the images were all geo-referenced to the WGS 84 datum with the UTM Zone 36N of the coordinate system. All satellite data were analyzed by assigning per-pixel signatures and segregating the land uses to 5 classes based on different landscape elements.



The delineated classes were: Agriculture, Bare land, Wetland and Built up Areas (Table 2). For each of these, a designated land use/ cover category was assigned training samples by defining polygons within each sites, and signatures files created for the particular land use/ cover categories downloaded from the satellite imagery taken by using pixels enclosed by polygons. The unsupervised classification was performed using the ISO Clustering Classification method which was followed by ground-trothing to guide in the performance of the Maximum Supervised Classification for accuracy assessment. All classification processes were executed using ArcGIS 10.2 as explained in the subsequent paragraphs.

## RESULTS

### Impact of human activity on the water quality

The results for the effect of land use activities on physico-chemical composition of water quality are presented in Table 3 and shows a significant correlation between land use activities and physico-chemical composition of water. According to Table 3, the Kruskal-Wallis test showed p values of less than 0.05 for EC (0.007), TDS (0.022), pH (0.022), TN (0.007), BOD (0.000), TSS (0.003) and TOC (0.010), indicating that they are significantly affected by LUAs. On the contrary, no significant correlation was found between land use activities and TP and COD. The p value was greater than 0.05 with TP recording a p value of 0.317 and COD with 0.203. The results from descriptive statistics indicate that the data from

eight out of the nine physicochemical parameters were positively skewed (skewness > 2.0) signifying the presence of large outliers. These values for the parameters EC, TDS, TP, TN, BOD, COD, TSS and TOC are 2.563, 2.700, 2.731, 2.996, 4.400, 6.808, 2.412 and 2.867 respectively. This implied that the median was preferred to the mean as the measure of central tendency of the data and for comparison to the National Standards. The pH value of 0.966 was negatively skewed, signifying accurate correlation.

According to Table 3, the EC values for wetland (537.5  $\mu\text{S}/\text{cm}$ ), built-up areas (472.5  $\mu\text{S}/\text{cm}$ ) and agriculture (272.50  $\mu\text{S}/\text{cm}$ ) remained below the recommended threshold of 1000  $\mu\text{S}/\text{cm}$ . The average values for TDS across all the land-use types of wetland, built up areas and agriculture (309.00 mg/l, 352.00 mg/l and 155.00 mg/l respectively) were lower than the National Standard (750 mg/l). A similar pattern of land-use types of wetland, built up areas and agriculture was observed for the parameters TP (0.84mg/l, 0.82 mg/l and 0.53 mg/l respectively), BOD (5.75 mg/l, 14.00 mg/l and 8.75 mg/l respectively), COD (41.00 mg/l, 49.50mg/l and 42.00 mg/l respectively), TSS (25.00 mg/l, 42.00 mg/l and 10.00 mg/l respectively) and TOC (16.70 mg/l, 20.50 mg/l and 5.65 mg/l respectively), where the observed average values were all below the National Standards of 10mg/l, 50mg/l, 70mg/l, 50mg/l and 50mg/l respectively. For TN, the average value for built-up areas (11.27 mg/l) was higher than the national standard of 10 mg/l while the remaining land use types of wetland (8.05mg/l) and agriculture (5.96mg/l) were below that of the recommended standard.

**Table 3: Descriptive summary statistics and test for equality of medians for physic- chemical parameters of water quality by land use**

Parameter	Land use Land cover	No. of obs. (n)	Median (homogenous groups <sup>**</sup> )	Kruskal-Wallis test <sup>*</sup>	Overall skewness	National standard for waste water discharge, NEMA
<b>Electrical conductivity (µs/cm)</b>	Wetland	8	537.50 <sup>a</sup>	$H = 9.838$ $p = 0.007$	2.563	1000 (µs/cm)
	Built Up Areas	36	472.50 <sup>a</sup>			
	Agriculture	4	272.50 <sup>b</sup>			
<b>Total dissolved solids (mg/l)</b>	Wetland	8	309.00 <sup>a</sup>	$H = 7.612$ $p = 0.022$	2.700	750 (mg/l)
	Built Up Areas	36	352.00 <sup>a</sup>			
	Agriculture	4	155.00 <sup>b</sup>			
<b>pH</b>	Wetland	8	7.30 <sup>a</sup>	$H = 7.245$ $p = 0.027$	0.966	5.0-8.5
	Built Up Areas	36	7.20 <sup>b</sup>			
	Agriculture	4	7.45 <sup>a</sup>			
<b>Total Phosphorus (TP) (mg/l)</b>	Wetland	8	0.84 <sup>a</sup>	$H = 2.298$ $p = 0.317$	2.731	5 (mg/l)
	Built Up Areas	36	0.82 <sup>a</sup>			
	Agriculture	4	0.53 <sup>a</sup>			
<b>Total Nitrogen (TN) (mg/l)</b>	Wetland	8	8.05 <sup>b</sup>	$H = 9.895$ $p = 0.007$	2.996	10(mg/l)
	Built Up Areas	36	11.27 <sup>a</sup>			
	Agriculture	4	5.96 <sup>b</sup>			
<b>BOD (mg/l)</b>	Wetland	8	5.75 <sup>b</sup>	$H = 16.666$ $p = 0.000$	4.400	50 (mg/l)
	Built Up Areas	36	14.00 <sup>a</sup>			
	Agriculture	4	8.75 <sup>b</sup>			
<b>COD (mg/l)</b>	Wetland	8	41.00 <sup>a</sup>	$H = 3.185$ $p = 0.203$	6.808	70 (mg/l)
	Built Up Areas	36	49.50 <sup>a</sup>			
	Agriculture	4	42.00 <sup>a</sup>			
<b>TSS (mg/l)</b>	Wetland	8	25.00 <sup>a</sup>	$H = 11.896$ $p = 0.003$	2.412	50 (mg/l)
	Built Up Areas	36	42.00 <sup>a</sup>			
	Agriculture	4	10.00 <sup>b</sup>			
<b>TOC (mg/l)</b>	Wetland	8	16.70 <sup>a</sup>	$H = 9.126$ $p = 0.010$	2.867	50 (mg/l)
	Built Up Areas	36	20.50 <sup>a</sup>			
	Agriculture	4	5.65 <sup>b</sup>			

<sup>\*</sup> National Environment (Standards for Discharge of Effluent into Water or Land) Regulations, 2020.

### The effect of land use activities on the vegetation cover in Nsooba - Lubigi drainage system

The results for the effect of land use activities on the vegetation cover for the years 1998, 2008 and 2018 are shown in Table 6..

**Table 4: Land Use Land Cover Change from 1998 to 2018**

Year		1998		2008		2018		Percentage Change (%)
Land Use	Land Cover	Area (Ha)	%	Area (Ha)	%	Area (Ha)	%	
Wetlands		6.93	47.21	4.05	27.59	2.14	14.58	-32.63
Agriculture		2.06	14.03	4.55	31	4.47	30.45	16.42
Bare land		2.13	14.51	1.05	7.15	1.04	7.08	-7.43
Built Up Areas		3.56	24.25	5.03	34.26	7.03	47.89	23.64
Total		14.68	100	14.68	100	14.68	100	0

The vegetation cover change from 1998 to 2018 was investigated for the four land use classes namely; wetlands, agricultural activities, bare land and built-up areas. According to results from table 6 wetlands gradually declined from 47.21% in 1998 to 27.59% in 2008 and 14.58% in 2018. Similarly, results for bare land showed 24.5% in 1998, and drastically dropped to 7.15% in 2008 and with no significant change (7.08) in 2018. Seemingly, there was gradual increase in agriculture and built-up areas by 14.03% in 1998 to 31% in 2018 and slowed growth of 30.45% in 2018; and 24.25% in 1998 to 34.26% in 2008 and 47.89% in 2018. The increase in built-up could have resulted into reduced agricultural activities. The Land use/land cover changes and vegetation cover for the years 1998, 2008 and 2018 are shown in Figure 2. LULC types such as Agriculture and Built-up Areas have shown a notable increase for the last two decades (from 1998-2018).

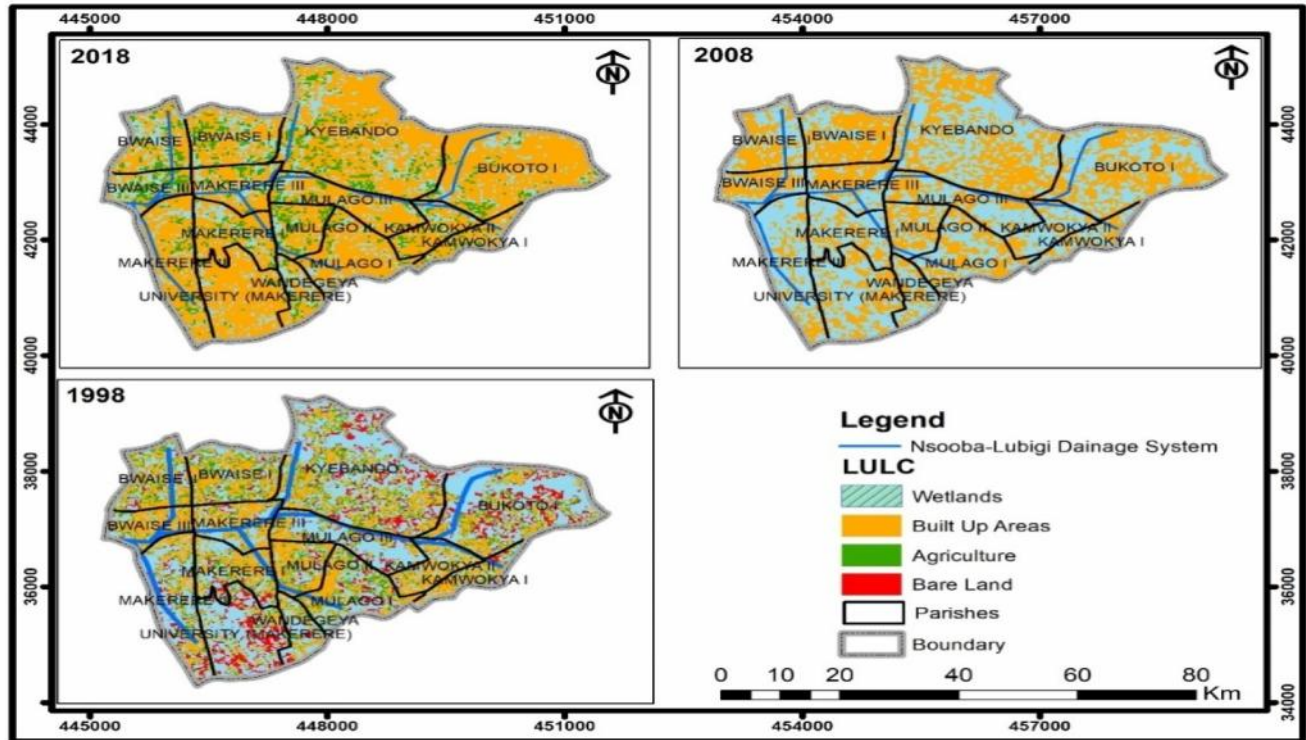
#### **Land use land cover, a, b, c in 1998, 2008, 2018**

Table 4 shows that, the total land area of the study area was 14.68ha with a variation in land

use land cover change of the study area. The dominant land use type was wetlands with an area of 6.93ha (47.21%), followed by built up areas at 3.56ha (24.25%). Both agriculture and bare land showed minimal changes having 2.14ha (15.51%) 2.23ha (14.03%) of the land use land cover respectively.

The analysis indicated that the surrounding environment within Nsooba - Lubigi drainage system in 2008 shows an increase in built up areas 5.03ha (34.26%) and agriculture 4.55ha (31%), these are the major anthropogenic activities that result to contamination of water quality and degradation of the Nsooba - Lubigi wetland. There was a deliberately declined to 4.05ha (27.3%) as well as a significant decline in bare land to 1.05ha (7.15%) resulting from urbanization of the city centre.

It was observed that in 2018 the built up areas consistently increased to 7.03ha (47.89%), followed by 4.5ha (30%) of the total land use and the natural vegetation cover especially wetlands to 2.14ha (14.6%) and bare land at 1.03ha (7.08%) respectively.



**Figure 2: Land use/land cover changes and vegetation cover**

### Land use land cover change

The high levels of built up areas at 23.64% and agriculture to 16.43% of the total percentage land use change between 2018 and 1998 meant intensive pressure is on the natural resources especially the wetlands thereby altering the water quality levels to -32.63% between 2018 and 1998, leading to expansion of urban agriculture along and on marginal lands as well as encroachment into protected Nsooba - Lubigi wetland.

### DISCUSSION

While determining the impact of land use activities on water quality and vegetation cover along the Nsooba - Lubigi drainage system, it was noticed that there are various activities and variations in past land use as compared to the

current land uses and activities. The previous style of land use prevailed on both sides of the Nsooba - Lubigi drainage system in the form of road structures, communication networks, settlements (planned and unplanned), and farmlands. Evidence shows that the land and vegetation cover has deliberately changed compared to the past years. The Nsooba - Lubigi drainage system has been seriously affected by mainly human activities evidenced by the on-going developments of the multi-trillion road construction of the Kampala-Entebbe express way for easy accessibility to the Entebbe international airport which has greatly affected the natural vegetation cover thereby endangering the species diversity within the study area.

The physico-chemical Parameters that were analyzed in water include, Electrical conductivity, Total dissolved solids, pH, Total

nitrogen, Total phosphorous, BOD, COD Total suspended solids and Total organic carbon. These were selected because they bring about severe pollution and eutrophication if not controlled or regulated which subsequently impacts on the receiving ecosystem. Electrical conductivity and Total dissolved solids contribute to an ion influx which consequently increase the saltness of the water. This makes it hard for the water born species to survive. pH, on the other hand increases the alkalinity or acidity of the water hence affecting the aquatic life since they have specific pH in which they survive. Total nitrogen and total phosphorous are nutrients that bring about excessive growth of the algae and the other green plants in the water. This overtime inhibits direct light penetration into the water and also inhibits atmospheric re-oxygenation of the water which consequently leads to suffocation of the fish and other water borne species.

Further, land use activities in the study area range from agriculture which includes animal husbandry, horticulture, floriculture in the Lubigi wetland, road construction, settlement both planned and unplanned. Construction of northern bypass has attracted more development and population increase, this later led to creation of slums in the wetlands for example Bwaise and Kalerwe. National water and sewerage cooperation has also constructed a sewage treatment plant which encroached on the vegetation cover of Lubigi wetland. All these land use activities have led to degradation of the wetland and loss of vegetation cover.

### **The effect of land use activities on the physico-chemical properties of water**

Figure 2 presents the Median (homogenous groups\*\*) of EC, TDS, pH, TP, TN, BOD, COD, TSS and TOC parameter values for the land use activities. Figure 2 revealed that EC and TDS were significantly impacted by land use activities while COD, TTS and TOC were moderately impacted. On the contrary, pH, TP, TN and BOD were minimally impacted by land use activities. Further, wetlands and built-up areas presented the highest significant impact on water quality, specifically EC and TDS, while agriculture presented the lowest impact on water quality and this could have been attributed to the low farming activities carried out in the sampling areas. Despite, the substantial effect of LUAs on the water quality, all the EC, TDS, pH, TP, TN, BOD, COD, TSS and TOC parameter values for wetland, built-up areas and agriculture activities were below the National Standard for wastewater discharge set by National Environmental Management Authority, 2020. This indicates that the results from wetlands, built-up areas and agricultural areas have minimal impact on the water quality.

The agriculture activity recorded the lowest EC compared to built-up areas, which further increased significantly in the wetlands. Similar trends were obtained by Wachu (2018) who presented that EC is highest in urban sites compared to cultivated areas and forested areas. The studies concluded that high EC concentrations in wetlands is due to the increased input of ions from industrial effluents including car garages in Masanafu and slaughterhouse in Kalerwe and domestic wastewater. This conquers with the findings attributed by Ochuka *et al.* (2019); who stated

that anthropogenic activities such as application of agro-chemicals and waste disposal are associated to higher EC in built-up areas.

In regard to TDS, the concentrations from wetlands, built-up areas and agriculture were attributed to different minerals dissolved in water which include potassium, sodium, magnesium, bicarbonates, these can be connected to numerous other compounds which can be water contaminants as well. However, the results of this study differs from recent studies conducted earlier within the drainage system by Hawumba (2017) and Ochuka *et al.* (2019) who stated that increased concentration of TDS results in noxiousness through heightened salinity and change in the ionic composition, influencing water taste, odour, colour and hardness. Water with TDS less than 600 mg/L is considered pleasant; nevertheless, extremely low TDS reduces the flavor of drinking water.

The average values of pH obtained under the three land uses fell within the acceptable range of the national standard (5.0-8.5), signifying that land-use did not impact the water pH. Total phosphorus (TP) had negligible impact on the water quality, since the activities indicated very low quality characteristics in comparison to the national standard. This could have been attributed to the low BOD levels that are recognized to favor phosphorus discharge to the freshwater ecosystem (Shafie *et al.*, 2017). It was observed that Total nitrogen (TN) is moderately higher in all the 3 activities (though below the national standard). Large increases in organic matter from wetland areas and built-up areas (domestic - household wastewater, sewage, detergent waste, etc.) areas might have led to an increase in the factors affecting

moderate concentrations. This is also supported by moderate concentrations in TOC from both the wetland and built-up area activities. This similar trend was also observed in the study conducted by Özdemir *et al.* (2022) who indicated that wastes from agricultural and tourism activities in the field of study could affect nitrogen and its derivatives.

Built-up areas presented the highest TSS and this could be attributed to poor waste management practices through littering and discharge of unhealthy effluent from both domestic and industrial activities. This is in agreement with the studies conducted by Grimm *et al.* (2005) and Shafie *et al.* (2017) who highlighted that bare soil at building sites has frequently resulted in large sediment inputs to the drainage streams through rainfall runoff events. The studies further indicated that the extent of fine particulate was generally higher in drainage streams around residential areas.

Other physico-chemical parameters including BOD, COD TSS and TOC were moderately high though below the National Standard, as observed within the sampling areas. This clearly shows that the high values could be attributed to the undigested materials and animal solid waste released from the Nsooba slaughterhouse. It therefore implies that there is need for huge amount of oxygen to synthesize all of these organic materials into CO<sub>2</sub> and water, which in turn, cause high concentrations of COD and BOD within the study area which could clarify on the linear correlation between solids, COD and BOD. This is in line with Hawumba (2017) who stated that, the subsequent highly concentrated discharge further adversely affects the water quality of Nsooba channel as detected by the increase in COD and microbial overload,

revealing of significant nutrient quantities. The sedimentation of some suspended solids, and the mineralization of the organic loads as the water flows away from the discharge points, should partially describe the reduction in COD linked to what other researchers have studied.

### **The effect of land use activities on the vegetation cover**

From Table 4 it was observed that built-up areas and agriculture are the activities with the lowest stability as they are developing activities in the drainage system. This means that the transitions of wetlands and bare lands types are oriented towards urbanization and developing farming activities. The percentage changes for wetlands, agriculture, bare land and built-up areas between 1998 and 2018 were observed to be -32.63%, 16.42%, -7.43% and 23.64% respectively as shown in table 4.

Further, it was observed that Nsooba - Lubigi drainage system has been subjected to a gradual process of reclamation and presently experiences some of the most dangerous threats and pressures, especially on the wetlands. The sites around the drainage system, including Nsooba channel and Lubigi wetland are observed as major sites for urbanization due to their proximity to the city center and industrial district. The land use land cover (LULC) results showed that Nsooba - Lubigi drainage system was under several anthropogenic uses including industrialization, increased agriculture, road construction among others has increased the rate of loss of vegetation cover. This is agreement with Twesigye *et al.* (2011) who stated that increased development such as urbanization and industrialization, and other anthropogenic practices have led to the decline in vegetation

cover and its loss. Kayima *et al.* (2018) also presented that rapid urbanization coupled with increasing population growth are one of the major driving factors of land use along Nsooba - Lubigi drainage system. This proportionately relates to Ding *et al.* (2015) who elaborated that, in most urbanized areas, land use largely contributes to nitrogen and phosphorus emanating from point source and non-point source pollutants. Ribolzi *et al.* (2011) found that most urban households are the common point source to pollution in waste water contamination, these contain pathogens which harbor low dissolved oxygen conditions in ground water supply leading to high metal concentration in the wetlands and other aquatic plant life.

Urbanization has additionally stretched to water-resistant areas larger volumes of runoff. Impervious rainfall runoff drains all types of pollutants including point and non-point source pollutants into rivers, which intensifies nutrients concentrations into surface waters. The strategic location of Nsooba - Lubigi drainage system means that it offers an exclusive and significant set of amenities to the residents within Bukoto, Kyebando, Bwaise and Kawempe among others. It serves as a buffer through which much of Kawempe division's and part of Kampala industrial and domestic effluents pass before being discharged into River Mayanja which eventually drains into River Kafu. Partially treated sewage from NWSC Lubigi treatment plant is mixed with the untreated wastewater present in the Nsooba Channel before entering the Lubigi wetland.

The current rise in settlements around Nsooba - Lubigi drainage system especially in the areas of Bwaise, Kalerwe, Kyebando and Makerere

among others is largely due to the high demand for affordable accommodation by people who work in the motor vehicle garages, Kalerwe market and other markets around, petrol station fuel attendants and small companies located within Kawempe division. This is in line with Zhang *et al.* (2011), who stated that macroeconomic activities such as industrialization and other businesses, contributing to the growth of GDP often require large areas also contribute to the transition of forest/shrub land/grassland into buildup areas. These results are in agreement with Omagor and Barasa (2018) who reported that the wetland extent was narrowing at a high rate due to settlements. Similar trends in the degradation of wetlands in Kampala city have been reported by Warsame *et al.* (2022) and Karabo (2017). The study by Karabo further reported that the buffer zones/spaces for flood control, sinking sediments, silt, nutrients, pollutants, toxins and sewage treatment have been turned into built-up environment which explains the growing problem of flooding and water quality in the wetland catchments (Karabo, 2017).

A significant number of low income earners find affordable and cheap temporal housing along Nsooba - Lubigi drainage system and wetland. Some of the residents around Masanafu, Sentema, Namungoona and Bulaga settlements depend on harvesting of papyrus materials from Lubigi wetland as a way of making the ends meet. The degraded natural and cultural characteristics of the Nsooba channel and Lubigi wetland show lack of clear channel management policies. The location of Nsooba - Lubigi drainage system makes it suitable for providing exceptional and important ecological services to the residents of Kawempe division and Kampala City at large. Nsooba - Lubigi

drainage system is consequently meant to play an important role in preserving the quality of both water supply and open waters. This signifies that areas made of urbanization, bare land, as well as farming activities are characterized by a significant population size that could be partly contributing to water quality and soil quality deterioration in the area.

## CONCLUSION & RECOMMENDATION

The analytical concentrations of land-use types of wetland, built up areas and agriculture was observed for the parameters EC, TDS, TP, BOD, COD, TSS, TOC, where the observed average values were all below the National Standards of 1000  $\mu\text{s/cm}$ , 750 mg/l, 10mg/l, 50mg/l, 70mg/l, 50mg/l and 50mg/l respectively. For TN, the average value for built-up areas was higher than the national standard of 10 mg/l while the remaining land use types of wetland and agriculture were below that of the recommended standard.

There was a significant decline in land coverage for wetlands and bare land from 1998-2018 attributable to rapid urban development involving infrastructural development, farming activities and rapid population growth. Wetland coverage declined by approximately 5 hectares since 1998 which represents an average decline of 2 hectares per decade. Bare Land was also observed to have declined from 14.5% in 1998 down to 7% by 2018, signifying a rapid decline of about 50% from 1998 to 2008. The percentage changes for wetlands, agriculture, bare land and built-up areas between 1998 and 2018 were observed to be -32.63%, 16.42%, -7.43% and 23.64% respectively.



The Nsooba - Lubigi drainage system, with its natural status is potentially susceptible to land use changes attributed to anthropogenic pressures. The physical and chemical examination of water quality revealed that built up area (Kalerwe) had the highest level of pollution attributed to rapid population growth and human activities including Nsooba slaughter house that discharges untreated effluents to Nsooba channel. The findings of this research can offer scientific orientation for land use management and water pollution regulation as well as guide in the creation of strategies for managing the water and other natural resources. However, other factors associated with water quality, such as the weather, precipitation, and density of population call for further research. From the findings of this study, a degraded land cover pattern in the Nsooba - Lubigi catchment is evident. The study concludes that the people settling around Nsooba - Lubigi Wetland System are victims of the Lubigi wetland system environmental degradation challenges and must be involved in finding solutions to these problems. This calls for the communities in the study area to assume responsibilities in guiding and controlling its development with the help of responsible government institutions like NEMA and research institutions. Our results suggest an urgent need for formation of community based management committees and by-laws to protect the fragile wetland ecosystems in Kampala city which are critical in biodiversity conservation, flood control and waste wastewater treatment.

### Acknowledgement

The authors are grateful to the Uganda Ministry of Water and Environment (MWE) for providing laboratory facilities for water

analysis. Denis Ekakoro is acknowledged for GIS technical support.

### References

- Chapman D. 1992. Water Quality Assessments - A Guide to Use of Biota, Sediments and Water in Environmental Monitoring - Second Edition, 1996 UNESCO/WHO/UNEP. ISBN 0 419 21590 5 (HB) 0 419 21600 6 (PB)
- Daniel T.C. 1990. Measuring the Quality of the Natural Environment: A Psychophysical Approach. *Am. Psychol.* **45**(5) 633 – 637.
- Ding J., Jiang Y., Fu L., Liu Q., Peng Q. and Kang M. 2015. Impacts of Land Use on Surface Water Quality in a Subtropical River Basin: A Case Study of the Dongjiang River Basin, Southeastern China. *Water* **7**(8): 4427-4445
- Edokpayi J.N., Rogawski E.T., Kahler D.M., Hill C. L., Reynolds C., Nyathi E., Smith J.A.J., Odiyo J.O., Samie A., Bessong P. and Dillingham R. 2018. Challenges to Sustainable Safe Drinking Water: A Case Study of Water Quality and Use Across Seasons in Rural Communities in Limpopo Province, South Africa. *Water (Basel)*. **10**(2): doi: 10.3390/w10020159.
- Fierro P., Valdovinos C., Vargas-Chacoff L., Bertrán C. and Arismendi I. 2017. Macro invertebrates and Fishes as Bio indicators of Stream Water Pollution. In: Tutu H. (Ed) *Water Quality* <http://dx.doi.org/10.5772/65084>, pp 428.
- Gavrilescu M., Demnerová K., Aamand J., Agathos S. and Fava F. 2015. Emerging pollutants in the environment: present and future challenges in bio-monitoring, ecological risks and bioremediation. *N Biotechnol.* **32**: 147-156.
- Grimm N. B., Sheibley R. W., Crenshaw C. L., Dahm C. N., Roach W. J. and Zeglin L. H. 2005. N Retention and transformation in urban streams. *J. N. Am. Benthol. Soc.* **24**(3):626 – 642.
- Hawumba J. F. 2017. The Impact of Kalerwe Abattoir Wastewater Effluent on the Water Quality of the Nsooba Channel. *Agri. Res. & Tech: Open Access J* **6**(1): <https://doi.org/10.19080/artoaj.2017.06.555677>
- Karabo Q.C. 2017. Land use and land cover change in Nsooba-lubing wetland system, Central Uganda Masters Dissertation, Makerere University, Kampala, Uganda
- Kayima J. W., Mayo A. and Nobert J. 2018. Ecological Characteristics and Morphological Features of the Lubigi Wetland in Uganda. *Environ. Ecol. Res.* **6**(4): 218–228. <https://doi.org/10.13189/eer.2018.060402>

- Longe E.O. and Omole D.O. 2008. Analysis of pollution status of River Illo, Ota, Nigeria. *Environmentalist* **28**: 451–457.
- Marinho F. P., Mazzochini G. G., Manhães A. P., Weisser W. W. and Ganade G. 2016. Effects of past and present land use on vegetation cover and regeneration in a tropical dryland forest. *J. Arid Environ.* **132**: 26–33.
- Mishra R.K., Mentha S.S., Misra Y. and Dwivedi N. 2023. Emerging pollutants of severe environmental concern in water and wastewater: A comprehensive review on current developments and future research. *Water-Energy Nexus* **6**: 74-95.
- Ochuka M. A., Ikporukpo C. O., Ogendi G. M. and Mijinyawa Y. 2019. Spatial Variability in Physico-Chemical Parameters of Water in Lake Baringo Catchment, Kenya. *Curr. World Environ.* **14**(3): 443–457.
- Omagor A. and Barasa B. 2018. Effects of Human Wetland Encroachment on the Degradation of Lubigi Wetland System, Kampala City, Uganda. *Environ. Ecol. Res.* **6**(6): 562-570.
- Özdemir N., Perktas M. and Döndü M. 2022. Evaluation of Surface Water Quality Parameters by Multivariate Statistical Analyses in Northern Coastal Line of Gökova Bay (Mu la, Turkey) . *ADÜ Z RAAT DERG*, **19**(1): 81 – 91
- Peters N.E., Meybeck M. and Chapman D.V. 2005. 93 : Effects of Human Activities on Water Quality. Water Quality and Biogeochemistry. *Encyclopedia of Hydrological Sciences*. Edited by M. Anderson. John Wiley & Sons, Ltd.
- Ribolzi O., Cuny J., Sengsoulichanh P., Mousque C., Soulleuth B., Pierret A., Huon S. and Sengtaheuanghoung O. 2011. Land Use and Water Quality along a Mekong Tributary in Northern Lao P.D.R. *Environ. Manage.* **47**: 291–302
- Sasakova N., Gregova G., Takacova D., Mojziso J., Papajova I., Venglovsky J. and Kovacova S. 2018. Pollution of Surface and Ground Water by Sources Related to Agricultural Activities. *Front. Sustain. Food Syst.* **2**:42. doi: 10.3389/fsufs.2018.00042
- Sebhatleab M. 2014. Impact of land use and land cover change on soil physical and chemical properties: a case study of Era-Hayelom Tabias, Northern Ethiopia. Land Restoration Training Programme <http://www.unulrt.is/static/fellows/document/Sebhatleab2014.pdf>
- Shafie M. S., Wong A., Harun S. and Fikri A. 2017. The use of aquatic insects as bio-indicator to monitor freshwater stream health of Liwagu River, Sabah, Malaysia. *J. Entomol. Zool. Stud.* **5**(4): 1662-1666.
- Twesigye C. K. Onywere S. M. Getenga Z. M. Mwakalila S. S. and Nakiranda J. K. 2011. The Impact of Land Use Activities on Vegetation Cover and Water Quality in the Lake Victoria Watershed. *The Open Environmental Engineering Journal* **4**: 66-77.
- Wachu C. M. 2018. Effects of Land Use and Seasonality on the Distribution of Mayflies and Water Quality Along Thika River, Kenya. Nairobi: Kenyatta University. MSc. Thesis.
- Wang H., Wang T., Zhang, B., Li F., Toure B., Omosa I. B., Chiramba T., Abdel-Monem M. and Pradhan M. 2014. Water and Wastewater Treatment in Africa - Current Practices and Challenges. *Clean - Soil, Air, Water* **42**(8): 1029–1035.
- Wang J., Wang K., Zhang M. and Zhang C. 2015. Impacts of climate change and human activities on vegetation cover in hilly southern China. *Ecol. Eng.*, **81**: 451–461.
- Warsame A., Luyiga S. and Akiyode O. 2022. Assessing Wetland Degradation in a Growing Urban Area: Case of Nsooba in Kampala, Uganda. *KIU J. Eng. Sci. Technol.* **1**(1): 1 – 6.
- Zhang W. Ren L. L. Yang X. & Jiang S. 2011. The impact of land use and land cover changes on runoff in a semi-arid River basin. *IAHS-AISH Publication*, **350**: 38–44.



## Assessment of Community Knowledge, Attitude and Practices toward Bovine Tuberculosis in Jinka Town, Southern Ethiopia

Asrat Solomon Kenasew<sup>1\*</sup>, Said Mohammed Harar<sup>1</sup>, Alemitu Ketema Tamirat<sup>1</sup>, Metadel Molto<sup>1</sup>

<sup>1</sup>College of Agricultural and Natural Resource, Department of Veterinary Medicine, Jinka University, P.O. Box: 165, Jinka, Ethiopia

### KEYWORDS:

Attitude;  
Bovine Tuberculosis;  
Jinka town;  
Knowledge;  
Practice

### ABSTRACT

Bovine tuberculosis is yet a major public health problem throughout the world, including African countries like Ethiopia. Limited public knowledge about the disease, coupled with negative attitudes and poor health practices, are contributing to this issue. A cross-sectional study was carried out from March 2023 to July 2023 to assess the community knowledge, attitude, and practice on Bovine Tuberculosis in Jinka Town. Questionnaire survey and retrospective data were used as a tool for data collection. Among 382 respondents, 254 (66.5%) knew about Bovine tuberculosis, whereas 128 (33.5%) respondents did not have any idea about the disease. Except sex, other predictors like age, marital status, educational level and occupation were significantly associated with knowledge and preventive practices towards Bovine tuberculosis. Respondents had misconceptions on zoonotic importance of the disease and 95 (24.87%) respondents consume raw milk. Regarding retrospective data result, among 1278 patients examined for Tuberculosis, 316 (24.7%) and 5 (0.39%) were positive for pulmonary and extra pulmonary Tuberculosis in 2020 G.C. During 2021 G.C, among 1066 patients examined for Tuberculosis, 190 (17.8%) and 12 (1.12%) patients were positive for pulmonary and extra pulmonary Tuberculosis respectively. Number of patients for pulmonary and extrapulmonary were increased to 18.25% and 4% respectively in 2022 G.C. Since there were misconceptions among the respondents, awareness creation and detailed investigation on the status of Bovine and human Tuberculosis was recommended.

### Research article

## INTRODUCTION

### Background of the Study

Ethiopia has 70 million cattle, 42.9 million sheep, 52.5 million goats, 2.15 million horses, 10.8 million donkeys, 0.38 million mules and 8.1 million camels (CSA, 2020). Despite this abundant cattle population in the country, the livestock sub-sector is generally less productive, its capacity is small, and its direct contribution

to the national economy is minimal (Shitaye *et al.*, 2007). The poor health condition of its livestock has been one of the responsible factors for the low productivity and hence profitability (Giday and Teklehaymanot, 2013).

Bovine tuberculosis (BTB) remains to be a major public health problem throughout the world, including Ethiopia. The condition is worse in low income countries like Ethiopia, where lower knowledge, attitude, and practice

\*Corresponding author:  
Email: [asratsolomon48@gmail.com](mailto:asratsolomon48@gmail.com) +251-920440837

<https://dx.doi.org/10.4314/eajbcs.v5i2.3S>

(KAP) of the public is poor about the disease (Adugna *et al.*, 2023). Bovine Tuberculosis (TB) is characterized by the formation of tubercles, which are distinct granulomatous lesions in affected organs and tissues that exhibit varying degrees of calcification, necrosis, and encapsulation (Thakur *et al.*, 2020).

This disease is the second main cause of death from an infectious disease world-wide, after the human immunodeficiency virus (HIV). Tuberculosis (TB) is one of the most serious public health issues in the world, infecting billions of people each year and ranking as the second highest cause of death from an infectious disease behind HIV/AIDS. In 2013, about 9 million new TB cases and 1.5 million TB deaths were estimated. About 85 percent of the disease burden is found in Asia and Africa (WHO, 2014). The TB situation has worsened over the last three decades, which can be attributed to the HIV/AIDS pandemic (Getahun *et al.*, 2010).

*Mycobacterium bovis* is not the major source of human tuberculosis, but humans remain susceptible to bovine tuberculosis (Bulto, 2012). Humans can be infected primarily by ingesting the agent by drinking raw milk containing the infective bacilli, secondly, by inhaling infective droplets when there is close contact between the owner and his/her cattle, especially at night since in some cases they share shelters with their animals. In some countries, it is estimated that up to 10% of human tuberculosis are due to bovine tuberculosis (Gebremedhin *et al.*, 2014). Furthermore, *M. bovis* can infect human when raw meat and other products from infected animals (Malama *et al.*, 2013) are consumed or by inhaling infective droplets or direct exposure to infected animals (Verma *et al.*, 2014).

Ethiopia has one of the world's highest rates of human tuberculosis, which is primarily caused by *Mycobacterium tuberculosis*. It is imperative that tuberculosis positive animals must be slaughtered (culled); as soon as the initial group of reactors is removed, rigorous hygienic practices must be put in place to control the spread of infection. This involves thoroughly cleaning and disinfecting all feed troughs with a hot, 5% phenol solution. In general terms, control measures of bovine tuberculosis in the traditional extensive production systems are more difficult and complex (OIE, 2009).

### Statement of Problem

Bovine tuberculosis is a zoonotic disease transmitted from animal to human. It induces a substantial economic impact through high cost of eradication programs and the severe consequences for movements of animals and their products, biodiversity, public health and substantial economic effect (Le Roex *et al.*, 2013, Rodriguez-Campos, *et al.*, 2014). Zoonotic tuberculosis incidence varies across regions and countries, with higher rates observed where there is close contact between people and large cattle populations, particularly when unpasteurized milk and dairy products are frequently consumed (Kock *et al.*, 2021).

Ethiopia is one of the African countries where BTB is considered as an expanding disease in animals. Diagnosis of BTB in Ethiopia is usually carried out on the basis of tuberculin test, meat inspection at the abattoir and rarely on bacteriological techniques (Ameni *et al.*, 2003). But researchers conducted milk borne zoonosis so far in Jinka town revealed that there is still a gap in KAP towards the zoonotic diseases. The KAP towards BTB alone was not studied in

Jinka town and that is why the current research was contemplated in the study area. Therefore, this study was conducted with the objective of assessing the knowledge, attitude and practices towards Bovine tuberculosis in Jinka town of southern, Ethiopia.

## **MATERIALS AND METHODS**

### **Description of the Study Area**

The study was conducted from March 2023 to July 2023 in Jinka town which is the capital city of South Omo Zone. It is located in the hills north of the Tama Plains. Currently, Jinka is the center of Jinka town administration. It has a latitude and Longitude of 5°47'N and 36°34'E Coordinates respectively and an elevation of 1490 meters above sea level. The average annual temperature and precipitation are 21.1°C and 1274 mm, respectively. It is 750 KM south of the main capital city of the country, Addis Ababa. Currently, it is one of the seats for six regional bureaus of Southern Ethiopia. The town has 40,311 cattle, 11,411 Goats, 2868 Sheep, 95,718 poultry, and 1402 equine population (Jinka town Agriculture office, 2023).

### **Study Population**

The study population were individuals who are resident in Jinka town with different Socio-demographic characteristics. This study includes individuals of sex, different age categories, different occupation, different marital status, and those, which were found on different educational levels. Besides this, the target populations were interviewed with specific questions related to knowledge, attitude, and

practice of the community toward Bovine Tuberculosis.

### **Study Design**

A cross-sectional study was carried out from March 2023 to July 2023 to assess the community knowledge, attitude, and practice on Bovine Tuberculosis in Jinka Town. Accordingly, individuals will be selected by simple random sampling.

### **Sample Size Determination**

The study population of the current study was comprised of simple randomly selected students of different educational levels (elementary, high schools, colleges), farmers, a governmental and self-employee that are found in Jinka town and its surroundings. Thus, the formula given by Yamane (1967) for the questionnaire survey was employed to calculate the sample size required for this study.

$$n = \frac{N}{(1 + N * (e)^2)}$$

where n -sample size, N-population size = 20,267 Jinka town Population (Jinka town Finance and economic development office, 2023), e-acceptable sampling error =0.05, 95% confidence level and p= 0.05 were assumed. Hence, the total sample size was calculated to be 392.

### **Method of Data Collection**

#### ***Questionnaire Survey***

A structured questionnaire was prepared to assess the knowledge, attitude, and practice of the community settled on urban and peri-urban areas of the study area. In addition, the socio-

demographic information of each respondent was recorded. Randomly selected individuals who live within the different locality of the study areas (i.e. the study population) were the target group for this study. The questionnaire was administered to the randomly selected individuals by common local language in (Amharic and Ari language) during the interview. There was a brief discussion on the objective of the survey and respondents were asked for their consent before administration of the questionnaire.

### ***Retrospective Data***

Retrospective data (cases of Tuberculosis in 3 consecutive years starting from 2020 to 2022) was collected from Jinka General Hospital in order to compare the prevalence of the disease and the level of the knowledge in the town. It was also important to have data of age-related cases of Tuberculosis.

### **Data management and Analysis**

All collected data were entered into the Microsoft Excel 2010 spreadsheet, coded and

then imported to STATA version-13 statistical software for descriptive statistical analysis. Pearson's chi-square ( $\chi^2$ ) test was used to access knowledge, attitude and practice with their respective age, sex, education level, marital status and occupation towards bovine tuberculosis disease. In all the analysis, confidence level was held at 95% and statistical analysis was considered as significant at  $p < 0.05$

## **RESULTS**

### **Respondents' Socio Demographic Characteristics**

The response rate was 382 (97.45%). 10 (2.55%) respondents didn't respond for the questionnaire during the study period. Among the respondents, 284 (74.3%) and 98 (25.7%) were male and female, respectively. Among the age groups, adults were the dominating group with 292 (76.4%) and youths were 90 (23.6%). Of the total respondents, 268 (70.2%) were married and 114 (29.8%) were unmarried, 50 (13.09%) were illiterate and 232 (86.92%) were considered as educated (Table 1).

**Table 1: Socio demographic characteristics of respondents in Jinka Town (n=382)**

<b>Variables</b>		<b>Frequency</b>	<b>Percentage (%)</b>
<b>Sex</b>	Male	284	74.3
	Female	98	25.7
<b>Age</b>	Youth (15-24 yrs)	90	23.6
	Adult (>25 yrs)	292	76.4
<b>Marital Status</b>	Married	268	70.2
	Unmarried	114	29.8
<b>Educational level</b>	Illiterate	50	13.09
	Primary School	116	30.37
	Secondary School	96	25.13
	Diploma, degree and above	120	31.41

### Knowledge of Respondents on Bovine Tuberculosis

A total of 254 (66.5%) respondents in the study area knew about bovine tuberculosis whereas 128 (33.5%) respondents haven't heard about the disease. Among the informed / knowledgeable respondents, 213 (83.86%) knew that bacteria causes Bovine tuberculosis. About

80% (n=204) respondents clearly mentioned emaciation as a clinical sign of BTB. Among the respondents who knew about BTB (n=254), 208 (81.89%) knew that Bovine tuberculosis is a zoonotic disease where as 46 (18.11%) did not have any idea about its zoonotic nature. Likewise, 147 (57.87%) respondents knew that ingestion of raw milk can transmit Bovine TB from animal to human (Table 2).

**Table 2: Knowledge of respondents regarding Bovine Tuberculosis (n=382)**

Variables		Frequency	Percentage (%)
Know BTB before	Yes	254	66.5
	No	128	33.5
Knowledge on cause of the disease (n=254)	Bacteria	213	83.86
	Parasite	11	4.33
	Shortage of feed	12	4.72
	Religion	18	7.09
	Lethargy	17	6.7
Clinical signs of BTB (n=254)	Coughing	31	12.2
	Lymph node enlargement	2	0.79
	Emaciation	204	80.31
Zoonotic disease (n=254)	Yes	208	81.89
	No	46	18.11
Method of transmission to human (n=254)	Consumption of raw milk	147	57.87
	Consumption of raw meat	62	24.41
	Through cold air	26	10.24
	I do not know	19	7.48

### Relationship Between Knowledge about Bovine Tuberculosis and the Variables

Among 284 male and 98 female respondents, 195 (68.79%) and 59 (60.2%) were knowledgeable on BTB, respectively. The remaining 31.33% males and 39.9% females did not have any idea about the disease. Regarding the age groups, only 40% of the youths knew

about the disease and 74.66% of the adults had good knowledge towards BTB. Based on educational level, 78% of Illiterate respondents had poor knowledge on the disease. Except sex, all independent variables (Age, Marital Status, and Educational Level) considered in this study were significantly associated with the Knowledge of Bovine Tuberculosis ( $P < 0.05$ ) (Table 3).

**Table 3: Relationship between knowledge on Bovine Tuberculosis and the variables**

Variables		Number of respondents	Know About BTB		$\chi^2$	P-value
			Yes (%)	No (%)		
Sex	Male	284	195 (68.67)	89 (31.33)	2.3393	0.126
	Female	98	59 (60.2)	39 (39.8)		
Age	Youth (15-24 yrs)	90	36 (40)	54 (60)	37.0886	0.000
	Adult (>25 yrs)	292	218 (74.66)	74 (25.34)		
Marital Status	Married	268	206 (76.87)	62 (23.13)	43.5410	0.000
	Unmarried	114	48 (42.1)	66 (57.9)		
Educational level	Illiterate	50	11 (22)	39 (78)	66.2325	0.000
	Primary School	116	66 (56.9)	50 (43.1)		
	Secondary School	96	56 (58.33)	40 (41.67)		
	College level & above	120	109 (90.83)	11 (9.17)		

### Attitudes Toward Disease prevention

Among the respondents, 137 (35.86%) considered the disease prevention status in Jinka town as poor and 245 (64.14%) considered it as good. Among the 382 respondents, 233 (82.2%) had positive attitude towards the disease to prevent BTB and the remaining 149 (27.8%) were remained with negative attitude towards BTB.

### Relation Ship Between Educational Level and Preventive Practices

All considered preventive practices such as consumption of milk, boiling of milk, actions taken when animal and human are affected with the disease were significantly associated ( $p < 0.05$ ) with the educational level of the respondents (Table 4).

**Table 4: Relationship Between Educational Level and Preventive Practices toward BTB**

Variables		Educational Level				$\chi^2$	P-value
		Illiterate (50)	Primary school (116)	Secondary school (96)	Diploma and above (120)		
<b>Consumption of raw milk</b>	No (287)	10 (20%)	96 (82.8%)	77 (80.2%)	104 (86.7%)	31.1480	0.000
	Yes (95)	40 (80%)	20 (17.2%)	19 (19.8%)	16 (13.3%)		
<b>Boiling of milk before consumption prevent BTB</b>	Yes (265)	37 (74%)	55 (47.4%)	64 (66.67%)	109 (90.8%)	52.1416	0.000
	No (117)	13 (26%)	61 (52.6%)	32 (33.33%)	11 (9.2%)		
<b>Actions taken if human is affected with TB</b>	Seek doctor (260)	40 (80%)	56 (48.28%)	58 (60.41%)	106 (88.3%)		0.000
	Seek traditional healers (58)	7 (14%)	24 (20.69%)	18 (18.75%)	9 (7.5%)		
	No action (64)	3 (6%)	36 (31.03%)	20 (20.84%)	5 (4.2%)		
<b>Actions taken if animal is affected with BTB</b>	Seek veterinarian (39)	39 (78%)	54 (46.55%)	58 (60.42%)	103 (85.8%)	51.7462	0.000
	Seek traditional healers (8)	8 (16%)	27 (23.28%)	20 (20.83%)	13 (10.8%)		
	No action (4)	3(6%)	35 (30.17%)	18 (18.75%)	4 (3.34%)		



## Retrospective Data Results

Retrospective data on the prevalence of Pulmonary and extrapulmonary Tuberculosis was collected from Jinka General Hospital. The data include a 3-years registered disease report of the hospital from 2020 to 2022. The data was classified in to different age and sex groups. The data revealed higher prevalence of Human tuberculosis and its prevalence was higher in

males. Among 316 people which were positive for pulmonary TB, 163 (51.6%) were males and 153 (48.4%) were females in 2020. In 2021, there were 190 peoples from which 118 (62.1%) were males and 72 (37.9%) were females. This number was increased to 205 peoples in 2022, among which 127 (61.95%) were males and 78 (38.05%) were females. The result also indicated the presence of extrapulmonary TB in Jinka town. Accordingly, there were 5, 12 and 45 peoples positive for this condition during 2020, 2021 and 2022, respectively (table 5).

**Table 5: Retrospective data result based on sex groups**

Year	Total examined for TB	Positive cases		Prevalence (%)	Type of TB	
		Male	Female		Pulmonary	Extra Pulmonary
2020	2045	163 (51.6%)	153 (48.4%)	15.69	316	5
2021	1732	118 (62.1%)	72 (37.9%)	11.66	190	12
2022	2111	127 (61.95%)	78 (38.05)	11.8	205	45

## DISCUSSION

Based on the detailed assessment of KAP towards BTB, 254 (66.5%) respondents in the study area knew about BTB, while the remaining 33.5% respondents did not have any idea about the disease. This finding is higher than the finding of Abebe *et al.* (2020) who revealed KAP towards BTB as 39.39% at Jinka town. This difference might be due to increased provision of awareness to the community by the different stake holders and those NGOs implementing their community services at the study area and the surroundings. Even though, there is still a knowledge gap towards BTB, the higher knowledge might be related with the recommendation of the previous study of Abebe *et al.* (2020) who recommended awareness creation as a part of zoonotic disease prevention.

The current finding is lower than the study conducted in Jarso district West Wollega zone, Oromia Region by Hailu *et al.* (2022) who revealed that 100% participants defined TB as a disease of lung. A study conducted in Gambia by Boshorum *et al.* (2020) also revealed that most participants had heard about tuberculosis. Moreover, study conducted in Gambella by Bati *et al.* (2013) revealed higher KAP than the current finding. Hailu *et al.*, (2021) reported 57.2% respondents were well-informed about TB in Bahir dar, Amhara region Ethiopia. Furthermore, Zeru *et al.* (2014) revealed that 30.8% of the respondents have good awareness about BTB in Mekelle town, Ethiopia. This finding is lower than the findings of the current study (66.5%). The difference of KAP between different regions and countries might be partly related with the difference of awareness level and it might be due to their ecological, socio-

cultural and socio-economic differences. Since the studies were implemented in different levels of urbanization where awareness creation level through media and access to internet might be different.

The current study indicated that, among the knowledgeable respondents (n=254), 208 (81.89%) knew that BTB is a zoonotic disease. This result was higher than the report of Hailu *et al.* (2022) and Zeru *et al.* (2014) who reported 24.4% and 15% respondents, respectively, agreed with the idea that tuberculosis can easily spread from animals to humans and vice versa. Furthermore, Wendmagegn *et al.* (2016) reported that 48% of the respondents in Woldiya knew that BTB is zoonotic. The inconsistency between different studies might be due to differences in the degree of consciousness among the participants in the study areas of concern.

The predictors of the knowledge were sex, age, marital status, and educational level. Males have higher knowledge (68.67%) towards BTB than females (31.33%) but gender /sex was the only factor not associated with the knowledge of BTB ( $p>0.05$ ). There is no difference between sex groups. The current study predicted that knowledge about BTB is higher in older age groups than youths. This is inconsistent with the finding of Hailu *et al.* 2021 who revealed as knowledge about BTB is higher in the age groups between 46 and 60 years. It might be suggested that elders have low level of knowledge due to limited access to training and awareness associated with BTB due to different reasons. The current finding is consistent with the result of Ismiala *et al.* (2015) who reported that age groups greater than 58 years are knowledgeable than the youngsters in Nigeria.

As underlined by Hailu *et al.* (2021), knowledge increases with years of working experience. Similar study by Addo *et al.* (2011) in Ghana supported this finding suggesting that herds men with long practical experiences had a greater knowledge due to past experiences on BTB in their herd. Ngoshe *et al.* (2023) also suggested that despite their lower level of education, older farmers were well-informed on animal diseases compared to younger farmers.

In the current study, marital status is significantly associated ( $p<0.05$ ) with the knowledge towards TB. Among 268 married respondents, 206 (76.87%) were knowledgeable than the unmarried ones (42.1%). This might be due to previous experience and exposure to training. As couples are two, one of them might have awareness and they can share it together. In addition to this, in order to take care of their children, married respondents might be likely to have more access to health centers where awareness creation takes place than unmarried ones.

Regarding education, those who attend college (diploma level) and above have high knowledge and practice on BTB as compared to those who joined primary and no formal education at all. Similar findings were also reported in Ethiopia by Asebe and Gudina (2018), Kerorsa (2019) and recently by Hailu *et al.* (2021). The study conducted in Nigeria by Ismaila *et al.* (2015) revealed similar result. As stated by Asebe and Gudina (2018), providing education plays a pivotal role in adding knowledge. Moreover, Education is an important tool in increasing awareness towards BTB among livestock owners and limited access to education results in low awareness among the community. Furthermore, education was among the factors

associated with better level of precautionary practice for BTB. This finding is consistent with the finding of Hailu *et al.* (2021), who revealed education as a factor which is associated with level of practice for BTB.

Regarding the causes of BTB, among the knowledgeable respondents about BTB (n=254), most of the respondents 213 (83.86%) knew that bacteria cause BTB. This finding is similar to Buregyeya *et al.* (2011) in Ethiopia where 79.9% of the respondents discerned the source of TB. But the current study indicated that yet 7.09%, 4.33% and 4.72% have misconception that religion, parasite and shortage of feed, respectively cause BTB. Onyango *et al.* (2020) also revealed very similar result who stated there was high misunderstanding that cold air and dust cause TB.

Regarding consumption of raw milk, 95 (24.87%) of respondents consume raw milk. This result is lower than the study conducted in South Gondar Zone by Alelign *et al.* (2019) who reported that 69% respondents consume raw or under cooked milk and dairy products. Similarly, Wario *et al.* (2018) showed that 66.2% respondents consume raw milk in Yabello. Moreover, the finding of Tschopp *et al.*, (2013) from Arsi zone, Ethiopia revealed that 55.4% respondents consume raw milk.

The study conducted in Ghana by Addo *et al.* (2011) and by Ngoshe *et al.* (2023) in Far Northern Kwa Zulu-Natal reported that 40% and 51.98% of the study participants consume raw milk respectively. This might be linked with food consumption habit and geographical difference (Hailu *et al.*, 2021). Unlike the current study, most of the studies mentioned were carried out in rural and agro-pastoral areas,

where raw milk consumption is likely to be practiced. According to Ismaila *et al.* (2015), the inconsistency might be due to difference in knowledge on zoonosis and consequence of raw food consumption. Educational level is among the factors significantly associated with raw milk consumption ( $p < 0.05$ ). The prevalence of raw milk consumption was 80%, 17.2%, 19.8% and 13.33% in illiterate, primary, secondary and diploma and above educational levels respectively. This indicates that as educational level of the respondent increases, awareness level on the consequence of raw milk consumption also increases.

Among 120 respondents educated to college level and above, 109 (90.8%) considered boiling milk before consumption as a preventive method of the transmission of BTB from animals to humans. In another side, among 50 respondents who have no formal education, 74% respondents considered boiling milk as preventive method. This result is almost similar to the result of Hailu *et al.*, (2021) who stated that 99% of the respondents knew boiling milk prior to drinking can prevent the transmission of BTB to humans. The current finding is different from that of Hailu *et al.* 2022 and Bihon *et al.* (2021) who indicated that more than 60% respondents disagree that pasteurization of milk before consumption prevents TB. This difference might be due to the difference in the educational level of the respondents in the study areas.

The retrospective data revealed that there was high prevalence of Human tuberculosis in Jinka town and its surroundings. This might be related with low awareness towards the transmission of BTB to human and limitations to follow possible preventive measures including boiling

of milk destined for consumption. This in turn increases the frequency of raw milk consumption in the study area and the surrounding. Furthermore, most TB patients fail to get treatment in the study area as there is no enough health services. Almost 92% people do not come back to clinics for follow up after their first treatment because of panic of what people will say about them (Onyango *et al.*, 2020). Concomitantly, this increases the transmission rate of TB to susceptible ones. The prevalence of TB was higher in males than females. Among the individuals who showed-up to Jinka General hospital for medical support and diagnosed positive for tuberculosis, majority of them were males. The higher prevalence of human TB in male might be related with occupational behavior, wider home range and exposure to TB patients. Occupationally, females remain in the home and have low exposure to sick people and the other risk factors associated with human TB than males.

## CONCLUSION & RECOMMENDATION

This study has identified that relatively there is good level of knowledge and moderate level of attitude and practices towards the prevention and control of the disease and yet there are misconceptions which require additional work to minimize the gap of KAP among the community. This study revealed that there is high prevalence of human tuberculosis as a result of low attitude and practice towards the preventive and control measures of BTB. Moreover, they also have knowledge gap on the impact of consumption of raw milk and possible disease prevention strategy. Analysis of the retrospective data also indicated that, there is high prevalence of human TB in the study area which is believed to be due to the above

problems. It also indicates that the disease can affect all age and sex groups.

Based on the above conclusions, regular community awareness creation work on the possible prevention strategies of the disease, and collaborative engagement of veterinarians and physicians for the control and further investigation of the level of BTB and Human TB in the region are recommended.

## Acknowledgement

The authors are grateful to the Jinka General Hospital for provision of the 3 years retrospective data. Staff members of Jinka University Department of Veterinary medicine are also acknowledged for their direct or indirect support.

## References

- Abebe F., Getachew S., Hailu T. and Fesseha H. 2020. Assessment of community knowledge attitude, and practice on milk borne zoonotic diseases in Jinka, Southern Ethiopia. *Myth or fact. Ann. Public Health Res.* 7: 1096.
- Adugna G., Mahendra P., Ararsa B., Segni A., Abdi G., Behera F. and Mulatu N. 2023. A Study on the Community Knowledge, Attitude and Practice of Bovine Tuberculosis in Ejere Town, Ethiopia. *Int. J. Clin. Exp. Med. Res.* 7(1): 1-10.
- Addo K. K., Mensah G. I. and Nartey N. 2011. Knowledge, Attitudes and Practices (KAP) of herdsmen in Ghana with respect to milk-borne zoonotic diseases and the safe handling of milk. *J. Basic Appl. Sci. Res.* 1(10):1566–1562
- Alelign A., Zewude A., Petros B. and Ameni G. 2019. Tuberculosis at farmer-cattle interface in the rural villages of South Gondar Zone of northwest Ethiopia. *Tuberc Res Treat.* 2019:1–8.
- Ameni G. and Wudie A. 2003. Preliminary study on bovine tuberculosis in Nazareth municipality abattoir of central Ethiopia. *Bull. Anim. Health Prod. Afr.* 51: 125-132.
- Asebe G. and Gudina E. 2018. Community knowledge, attitudes and practices on bovine tuberculosis and associated risk factors in Gambella Regional State

- Lare Woreda, South West Ethiopia. *Veterinaria* **67**(1):27–35.
- Bashorun A. O., Linda C. and Omoleke S. 2020. Knowledge, attitude and practice towards tuberculosis in Gambia: a nation- wide cross-sectional survey. *BMC Public Health* **20** (1):1–13.
- Bati J., Legesse M. and Medhin G. 2013. Community's knowledge, attitudes and practices about tuberculosis in Itang Special District, Gambella Region, South Western Ethiopia. *BMC Public Health* **13** (1): 734,
- Bihon A., Zinabu S., Muktar Y. and Assefa A. 2021. Human and bovine tuberculosis knowledge, attitude and practice (KAP) among cattle owners in Ethiopia. *Heliyon* **7**(3): e06325
- Bulto G. B. 2012. Zoonotic significance of *Mycobacterium bovis* infection. *J. Nat. Hist.* **8**: 86–89.
- Buregyeya E., Kulane A., Colebunders R. et al. 2011. Tuberculosis knowledge, attitudes and health-seeking behavior in rural Uganda. *Int. J. Tuberc. Lung Dis.* **15**(7): 938–42.
- CSA (Central Statistical Authority) 2020. Central statistical agency agricultural sample survey 2020/21. Volume II report on livestock and livestock characteristics (private peasant holdings). Pp. 5,13,16, 20
- Gebremedhin R., Gebremedhin G. and Gobena A. 2014. Assessment of bovine tuberculosis and its risk factors in cattle and humans, at and around Dilla Town, Southern Ethiopia. *J. Anim. Vet. Sci.* **2**: 94.
- Getahun H., Gunneberg C., Granich R. and Nunn P. 2010. HIV Infection Associated tuberculosis. The epidemiology and the response. *Clin. Infect. Dis.* **50**(suppl. 3): S201–S207
- Giday M. and Teklehaymanot T. 2013. Ethnobotanical study of plants used in management of livestock health problems by Afar people of Ada'ar District, Afar Regional State, Ethiopia. *J. Ethnobiol. Ethnomedicine* **9**:8.
- Hailu F. A., Dejene H., Akalu T. Y. and Alemu Y. F. 2021. Knowledge and Practice for Prevention of Bovine Tuberculosis and Its Derivers Among HIV Positive People in Bahir Dar City Public Hospitals, Ethiopia. *HIV AIDS (Auckl)* **13**: 1025–1034.
- Hailu G., Etefa M. and Begna F. 2022. Assessment of Knowledge, Attitudes, and Practices (KAP): Public Health and Economic Burden of Tuberculosis in Jarso District of West Wollega Zone, Oromia, Western Ethiopia. *Biomed Res Int.* 2022:3314725. doi: 10.1155/2022/3314725.
- Ismaila U. G., Rahman H. A. and Saliluddin S. M. 2015. Knowledge on bovine tuberculosis among abattoir workers in Gusau, Zamfara State, Nigeria. *Int. J. Public Health Clin. Sci.* **2**(3):45–58.
- Jinka General Hospital, 2023: Annual Disease Registration Sheet. Un published, Pp 6.
- Jinka town Agriculture office, 2023. Annual socio-economic report. Unpublished, Pp 2.
- Jinka town finance and economy development office, 2023. Annual socio-economic report. Unpublished, Pp 2.
- Kerorsa G. B. 2019. Assessment of public awareness on common zoonotic diseases in Lalo Kile District, Kellem Wollega Zone, Ethiopia. *Int. J. Biomed. Eng. Clin. Sci.* **5** (4): 59–64.
- Kock R., Michel A. L., Yeboah-Manu D., Azhar E. I., Torrelles J. B., Cadmus S. I., Brunton L., et al. 2021. Zoonotic Tuberculosis - The Changing Landscape. *Int. J. Infect. Dis.* **2021** (Suppl 1): S68–S72.
- Le Roex N., Van Helden P. D., Koets A. P. and Hoal E. G. 2013. Bovine TB in Livestock and Wild life: What's in the Genes? *Physiol. Genomics* **45**:631–637.
- Malama S., Muma J. B. and Godfroid J. 2013. A Review of Bovine Tuberculosis at Wild life- Livestock-Human Interface in Zambia. *Infect. Dis. Poverty* **2**: 13.
- Ngoshe Y. B., Etter E., Gomez-Vazquez J. P., Thompson P. N. 2023. Knowledge, Attitudes, and Practices of Communal Livestock Farmers regarding Animal Health and Zoonoses in Far Northern KwaZulu-Natal. South Africa. *Int. J. Environ. Res. Public Health* **20**: 511.
- OIE (Office International des Epizooties) 2009. Bovine Tuberculosis: Terrestrial Manual. *Office of International des Epizootics, Paris, France. Chapter, 2.4.7,1-16.*
- Onyango P. A., Ter Goon D. and Rala N. M. D. 2020. Knowledge, attitudes and health-seeking behaviour among patients with tuberculosis: a cross-sectional study. *Open Public Health J.* **13**:739–47.
- Rodriguez-Campos S., Smith N. H., Boniotti M. B. and Aranaz A. 2014. Over View and Phylogeny of Mycobacterium Tuberculosis Complex Organisms: Implications for Diagnostics and Legislation of Bovine Tuberculosis. *Res. Vet. Sci.* **97**: S5–S19.
- Shitaye J. E., Tsegaye W. and Pavlik. I. 2007. Bovine tuberculosis infection in animal and human populations in Ethiopia: a review. *J. Vet. Med.* **52**: 317.
- Thakur, Monika, Sood N. K. and Kuldip G. 2020. Pathomorphological Study of Atypical Pulmonary Tuberculosis in Cross-Bred Cow - A Case Report. *Indian J. Vet. Pathol.* **44** (3):172–76.
- Tschopp R., Abera B., Sourou S. Y, et al. 2013. Bovine tuberculosis and brucellosis prevalence in cattle from selected milk cooperatives in Arsi zone, Oromia region, Ethiopia. *BMC Vet. Res.* **9**:163.
- Verma A. K., Tiwari R., Upadhayay U. P. and Vishwavidyalay P. C. 2014. Insights into bovine tuberculosis (bTB), various approaches for its

- diagnosis, control and its public health concerns: an update. *Asian J. Anim. Vet. Advances* **9**: 323-344.
- Wario E., Tehetna A. and Zewdie W. 2018. Assessment of community awareness on common zoonotic disease in and around Yabello District of Oromia Regional State, Ethiopia. *Multidiscip Adv. Vet. Sci.* **2**(4):388–394.
- Wendmagegn O., Negese D. and Guadu T. 2016. Bovine tuberculosis and associated factors among adult HIV positive people in Woldya Town, Northeast Ethiopia. *World J. Med. Sci.* **13**(1): 38–48.
- WHO (World Health Organization) 2014. Global tuberculosis report. World health Organization Geneva, Switzerland. Pp.1-147.
- Yamane T. 1967. Statistics, An Introductory Analysis, 2nd Ed., New York: Harper and Row.
- Zeru F., Romha G., Berhe G., Mamo G., Sisay T. and Ameni G. 2014. Prevalence of bovine tuberculosis and assessment of Cattle owners' awareness on its public health implication in and around Mekelle, Northern Ethiopia. *J. Vet. Med. Animal Health.* **6**(6): 159–167.



## Penalized Intuitionistic Fuzzy Goal Programming Method for Solving Multi-Objective Decision-Making Problems

Demmelash Mollalign Moges<sup>1,\*</sup>, Berhanu Guta Wordofa<sup>2</sup>, Allen Rangia Mushi<sup>3</sup>

<sup>1</sup>Department of Mathematics, Hawassa University, Hawassa, Ethiopia

<sup>2</sup>Department of mathematics, Addis Ababa University, Addis Ababa, Ethiopia

<sup>3</sup>Department of mathematics, University of Dares Salaam, Dares Salaam, Tanzania

### KEYWORDS

Multiobjective decision-making;  
Intuitionistic fuzzy decision set;  
Goal programming;  
Interactive penalty function.

### ABSTRACT

Many applicable problems have multi-goals that optimize simultaneously, and decision-makers set imprecise aspiration levels for each goal. Although such types of problems solved by fuzzy optimization are common in the literature, intuitionistic fuzzy optimization techniques are more efficient to handle than fuzzy and classical optimization. This research study focused on establishing a novel method by combining the penalty function method with an interactive goal programming methodology for addressing multi-objective decision-making problems in an intuitionistic fuzzy environment. One of the challenge that exists in the literature of the optimization method under an imprecise decision environment is that it is not guaranteed to generate a Pareto-optimal solution for the introduced problem. Therefore, in order to ensure the Pareto-optimality of the obtained solution, the suggested method has developed a new aggregation operator, an appropriate relaxation of the constraint set, and a well-structured extended Yager membership function. In addition, unlike other methods in the literature, the suggested method gives decision-makers the option to penalize the most unsatisfied objective function at a specific attained solution instead of starting from scratch and working their way through the problem. To illustrate the proposed method, we used a numerical example.

### Research article

### 1. INTRODUCTION

Many real-world decision-making problems such as agricultural cropland alloca-

tion problems by Moges et al. (2023a); Basumatary and Mitra (2022), transportation problems by Tadesse et.al. (2023), water

Corresponding author

Email address: [danieldemelashalem@gmail.com](mailto:danieldemelashalem@gmail.com) +251913845944 <https://dx.doi.org/10.4314/eajbcs.v5i2.4S>



resource allocation problems by [Sharma et.al. \(2007\)](#), production planning decision-making problems by [Khan et.al. \(2021\)](#), etc are defined as multi-objective programming problems (MOPPs). Often, the input data used in these problems does not have exact numerical values because of various uncontrollable circumstances. To solve such types of MOPPs, the most appropriate and straightforward techniques are fuzzy optimization methods, which were introduced by [Bellman and Zadeh \(1970\)](#). Many authors ([Tadesse et.al., 2023](#); [Jameel and Radhi, 2014](#); [Kahraman et.al., 2016](#)) have been more committed to apply fuzzy set tools for various application issues after [Bellman and Zadeh \(1970\)](#) provided a model to tackle fuzzy-multi-objective programming problems (FMOPPs).

The core idea behind the widely used approach for solving FMOPPs in the literature is to transform the original FMOPPs into a crisp single-objective optimization model using aggregation operators and ranking accuracy approaches, and then solve it using classical methods ([Zimmermann, 2001](#); [Kahraman et.al., 2016](#); [Bellman and Zadeh, 1970](#)). Few papers have focused on developing new mathematical models for identifying fuzzy non-dominant solutions to FMOPP in the fuzzy optimization environment. These new models were developed by applying different aggregation operators like max-min operator by [Bellman and Zadeh \(1970\)](#),  $\gamma$ -operator by [Zimmermann \(2001\)](#), bounded min-sum operator by [Cheng et.al. \(2013\)](#), and fuzzy-and operator by [Singh and Yadav \(2015\)](#) to convert the multi-objective functions into single-objective functions. Using the newly introduced concepts, numerous approaches and models have been developed for various theoretical and scientific fields ([Bogdana and Milan, 2009](#); [Kassa and Tsegay, 2018](#); [Tadesse](#)

[et.al., 2023](#)). However, when uncertainty results from vagueness, inaccurate data, or intentional judgments, the modeling capabilities of fuzzy set theory are limited. Decision-makers may also experience some hesitancy as a result of imprecise information, unawareness of customers, seasonal change, etc. These kinds of factors are critical to consider while building realistic, suitable models and solving decision-making problems ([Singh and Yadav, 2015](#); [Razmi et.al, 2016](#); [Moges and Wordofa, 2024](#); [Kumar, 2020](#); [Fathy et.al., 2023](#)).

To overcome these limitations, numerous researchers suggested various fuzzy extensions that expanded the conventional fuzzy set theory concepts. [Atanassov \(1986\)](#) developed a novel concept called an intuitionistic fuzzy (IF) theory which successfully addresses the limitation of fuzzy theory. Since the IF set can offer degrees of acceptance, hesitancy, and rejection, it has been found to be more helpful for handling imprecision in optimization procedures than fuzzy and crisp-based models, ([Mollalign et.al., 2022](#); [Sharma et.al., 2023](#)). [Angelov \(1995\)](#) proposed a new model to determine the MN<sup>1</sup> Pareto-optimal solution based on intuitionistic fuzzy optimization (IFO) which is a direct extension of the fuzzy optimization technique put out by [Bellman and Zadeh \(1970\)](#). Subsequently, numerous scholars such as ([Ghosh and Kumar, 2014](#); [Moges et al., 2023a](#); [Rukmani and Porchelvi, 2018a](#); [Bharati and Singh, 2014](#); [Dey and Roy, 2015](#); [Mollalign et.al., 2022](#); [Moges et.al., 2023b](#); [Bharati et.al., 2014](#)) have been proposed different IFO methods to solve the domain of MOPPs utilizing the benefit of IFS tools.

[Yager \(2009\)](#) highlighted certain drawbacks of [Angelov \(1995\)](#)'s method for determining the optimal choice for decision-makers. He suggested a new approach by con-

---

<sup>1</sup>MN represent Membership-Nonmembership



verting the intuitionistic fuzzy decision environment (IFDE) into a fuzzy decision environment using a convex combination of non-membership and membership functions. By addressing the shortcomings of the Angelov (1995) technique, Dubey et.al. (2012) applied the Yager (2009) strategy to solve the MOPP. Garai et.al. (2015) exposes the shortcomings of the Dubey et.al. (2012) method by demonstrating how certain constraints in their model can impede the pursuit of the optimal solution or render the model impractical. They also suggest a new function by broadening the scope of non-membership and membership functions.

As with fuzzy optimization, a problem in the IFO environment can be formulated as a two-step process to be solved. The first is to convert a multi-objective function into a crisp single-objective optimization model using an appropriate aggregation operator, and then solve this model using suitable optimization technique. The majority of the existing IFO methods in the literature for resolving MOPP are based on the max-min operator, (Moges et al., 2023a; Dubey et.al., 2012; Garai et.al., 2015). However, the max-min operator is not guaranteed to generate the Pareto dominance solution, and there is always no compensation for the resulting solution. The compensatory of the developed aggregation operator has a critical role in the procedure of solving MOPPs and it affects the optimality of the resulting non-dominant solution. As a result, the MN Pareto-solution might not be the result of a model that was developed using the max-min operator approach.

The second limitation is that even if the IFO method generates a MN Pareto-optimal solution under an IFDE, there is not always a guarantee of a Pareto-optimal solution to the given MOPP due to the boundary problem. To overcome this difficulty, many researchers have proposed different approaches to fuzzy decision-making problems. But the two-phase method which used by Lu et.al.

(2015); Dubois and Fortemps (1999); Wu and Guu (2001); Dubey et.al. (2012); Tsegaye et.al. (2021); Jiménez and Bilbao (2009) is the most commonly applied approach for finding a Pareto-optimal solution to MOPPs in fuzzy decision environment. A two-phase method means that in phase one, use the max-min operator technique and then use the mean-operator technique in phase two to improve the previous solution obtained by the max-min operator approach. However, Dubois and Fortemps (1999) indicated that this kind of strategy is not entirely consistent because we need to switch from the max-min operator to the mean-operator at different stages, and they suggested a multiphasons for objective functions provides upper and lower tolerances to avoid decision deadlock. Additionally, Razmi et.al (2016) point out that in situations where a certain level of satisfaction is fully achieved, there might not be a guarantee that a fuzzy efficient solution is Pareto-optimal. In order to generate the Pareto-optimal solution, Jiménez and Bilbao (2009); Razmi et.al (2016) extended the technique by Wu and Guu (2001) and developed a generic strategy based on the goal programming method. On the other-hand, Mollalign et.al. (2022) demonstrate that there is no assurance that the imprecise environment approach put forward by Razmi et.al (2016) will be the only method used to obtain the Pareto-optimal solution of MOPP when using intuitionistic fuzzy hierarchical optimization.

Furthermore, the IFO approach offers upper and lower tolerances to prevent decision stalemate when defining membership/ satisfaction and nonmembership/ dissatisfaction for objective functions. The third limitation in the literature of IFO is that to determine upper and lower tolerance, researchers use the “payoff matrix” approach without consideration of underestimation or overestimation values of the nadir point. Therefore, decision-makers may perceive the solution derived from this approach incorrectly. But the

interactive approach is helpful to a decision-maker since it offers mechanisms for learning about a problem in the IFO. There are a few researchers that concern an interactive method for solving a different domain of MOPPs in an intuitionistic fuzzy decision environment, (Hanine et.al., 2021; Garai et.al., 2016). However, in the existing interactive method, decision-makers do not have the freedom to punish/ penalize the more unsatisfied objective function at each iteration when the current solution does not satisfy the DM, rather than solving the problem from scratch.

By taking into account the aforementioned limitations, the key goal of this research study is to develop a general and powerful novel method for solving the multi-objective linear decision-making problem (MOLDMP) in an IFDE using the combination of penalty function method, the interactive method, and the goal programming. Additionally, the following points are specific and basic contributions of current research-study works:

- i. We formulated an IF membership and nonmembership function by finding the correct ideal and nadir point to set boundary for intuitionistic fuzzy goals (IFGs).
- ii. We proposed an extended Yager-membership function that eliminates the boundary value problem.
- iii. A new IF aggregation operator is developed to convert MOLDMP into a single-objective decision-making problem.
- iv. Using a new IF aggregation operator, we proposed an IFG programming model to find a Pareto-optimal solution for MOLDMP.
- iv. Decision-makers provide an interactive penalty function method to punish un-

satisfactory objective functions at the current solution.

The rest of the paper is presented as follows: the basic concepts and terms related to the paper are presented in Section 2. Section 3 illustrates the mathematical formulation of IF-MOLDMPs and its IFG model. In Section 4, we demonstrated the newly proposed method developed based on goal programming techniques and interactive penalty function method. The general framework or algorithm of the proposed method presented in Section 5 and the numerical examples used to summarize and demonstrate the applicability of the introduced method are discussed in Section 6. The results and discussion of the study are given in Section 7. Finally, the conclusion of the present work and its future scope are given in Section 8.

## 2. PRELIMINARIES

### 2.1. Intuitionistic Fuzzy Set

**Definition 2.1.** (Atanassov, 1986; Fathy et.al., 2023) An **intuitionistic fuzzy set (IFS)**  $\tilde{A}^I$  in a non-empty universal  $X$  is a set of ordered-triplets  $\tilde{A}^I = \{ \langle x, \mu_{\tilde{A}^I}(x), \nu_{\tilde{A}^I}(x) \rangle : x \in X \}$  where,  $\mu_{\tilde{A}^I} : X \rightarrow [0, 1]$  represent the membership function or degree of belongingness and  $\nu_{\tilde{A}^I} : X \rightarrow [0, 1]$  represent non-membership function or degree of non-belongingness of the element  $x \in X$  being in  $\tilde{A}^I$ , so that  $\forall x \in X$ ,  $0 \leq \mu_{\tilde{A}^I}(x) + \nu_{\tilde{A}^I}(x) \leq 1$ . For any IFS  $\tilde{A}^I$  on  $X$ ,  $\pi_{\tilde{A}^I}(x) = 1 - \mu_{\tilde{A}^I}(x) - \nu_{\tilde{A}^I}(x)$  is the degree of indeterminacy of  $x \in \tilde{A}^I$  or  $x \notin \tilde{A}^I$ .

#### 2.1.1. Operations over Intuitionistic Fuzzy Sets

Assume that  $\tilde{A}^I = \{ \langle x, \mu_{\tilde{A}^I}(x), \nu_{\tilde{A}^I}(x) \rangle : x \in X \}$  and  $\tilde{B}^I = \{ \langle x, \mu_{\tilde{B}^I}(x), \nu_{\tilde{B}^I}(x) \rangle : x \in X \}$  are any IFSs on the universal set  $X$ , (Husain et.al., 2012).

1. subset  $\tilde{A}^I \subseteq \tilde{B}^I \iff \mu_{\tilde{A}^I}(x) \leq \mu_{\tilde{B}^I}(x)$  and  $\nu_{\tilde{A}^I}(x) \geq \nu_{\tilde{B}^I}(x), \forall x \in X$ .

2. Equal Set:  $\tilde{A}^I = \tilde{B}^I \iff \mu_{\tilde{A}^I}(x) = \mu_{\tilde{B}^I}(x)$  and  $\nu_{\tilde{A}^I}(x) = \nu_{\tilde{B}^I}(x), \forall x \in X$ .
3. Complementation:  $(\tilde{A}^I)^c = \{ \langle x, \nu_{\tilde{A}^I}(x), \mu_{\tilde{A}^I}(x) \rangle \mid x \in X \}$ .  
To represent the minimum and maximum operator (that means: min and max operator), we use the symbols “ $\wedge$ ” and “ $\vee$ ” respectively.
4. Intersection:  $\tilde{A}^I \cap \tilde{B}^I = \{ \langle x, \mu_{\tilde{A}^I}(x) \wedge \mu_{\tilde{B}^I}(x), \nu_{\tilde{A}^I}(x) \vee \nu_{\tilde{B}^I}(x) \rangle \mid x \in X \}$ .
5. Union:  $\tilde{A}^I \cup \tilde{B}^I = \{ \langle x, \mu_{\tilde{A}^I}(x) \vee \mu_{\tilde{B}^I}(x), \nu_{\tilde{A}^I}(x) \wedge \nu_{\tilde{B}^I}(x) \rangle \mid x \in X \}$ .

$$\begin{aligned} \min \quad & f(\mathbf{x}) = (f_1(\mathbf{x}), f_2(\mathbf{x}), f_3(\mathbf{x}), \dots, f_k(\mathbf{x}))^T \\ \text{Subject to:} \quad & \mathbf{x} \in S = \left\{ \mathbf{x} \in \mathbb{R}^n \mid \begin{array}{l} g_j(\mathbf{x}) (\leq, \geq, =) 0, \quad j = 1, 2, \dots, m \\ x_i \geq 0, \quad i = 1, 2, \dots, n. \end{array} \right\} \end{aligned} \quad (1)$$

**Definition 2.2.** (Li and Hu, 2009) Let a vector  $\mathbf{x}^* \in S$  be a feasible solution to MOPP (1). Then

- $\mathbf{x}^*$  is **weakly Pareto-optimal** solution to MOPP (1) if there doesn't exist a new vector  $\mathbf{x} \in S$  such that  $f_t(\mathbf{x}) < f_t(\mathbf{x}^*)$  for all  $t = 1, 2, \dots, k$ .
- $\mathbf{x}^*$  is **Pareto-optimal (efficient)** solution to MOPP (1) if there doesn't exist a new vector  $\mathbf{x} \in S$  such that  $f_t(\mathbf{x}) \leq f_t(\mathbf{x}^*)$  for all  $t = 1, 2, \dots, k$ , and  $f_t(\mathbf{x}) < f_t(\mathbf{x}^*)$  for some  $t$ .

Any Pareto-optimal solution is weakly Pareto-optimal but the converse is hold for convex optimization problem. Assume that

$$\max (\min) \tilde{f}_t^I(\mathbf{x}) = \mathbf{C}\mathbf{x} + \mathbf{d}, \quad t = 1, 2, \dots, k \quad (2)$$

$$\text{Subject to: } \mathbf{x} \in \tilde{S}^I = \{ \mathbf{x} \in \mathbb{R}^n : \tilde{g}_i^I(\mathbf{x}) (\tilde{\leq}, \tilde{\geq}, \tilde{=}) b_i, \mathbf{x} \geq 0 \},$$

where  $\mathbf{C} \in \mathbb{R}^{k \times n}$ ,  $\mathbf{d}^T \in \mathbb{R}^k$  are deterministic parameters and the right-hand quantity is  $b_i \in \mathbb{R}$ ,  $i = 1, 2, \dots, m$ . The IF-version of classical inequality  $\leq, \geq$  and equality  $=$  in the model (1) are given as  $\tilde{\leq}, \tilde{\geq}$  and  $\tilde{=}$ , respectively. The function  $\tilde{f}_t^I(\mathbf{x})$  and  $\tilde{g}_i^I(\mathbf{x})$  are IF linear objective and constraints, respectively due to they have IF aspiration levels set by decision-makers (DMs).  $\tilde{S}^I$  is IF feasible con-

## 2.2. Multi-objective programming problem

Assume that a vector-valued objective function  $f : \mathbb{R}^n \rightarrow \mathbb{R}^k (f(\mathbf{x}) = (f_1(\mathbf{x}), f_2(\mathbf{x}), f_3(\mathbf{x}), \dots, f_k(\mathbf{x})))$ , and constraint functions  $g : \mathbb{R}^n \rightarrow \mathbb{R}^m (g(\mathbf{x}) = (g_1(\mathbf{x}), g_2(\mathbf{x}), g_3(\mathbf{x}), \dots, g_m(\mathbf{x})))$  are continuously differentiable for all decision vector  $\mathbf{x} = (x_1, x_2, x_3, \dots, x_n) \in S$  is formulated in the following way: (Tsegaye et.al., 2021; Razmi et.al, 2016)

the feasible set  $S \neq \emptyset$  (or  $Z = f(S) \neq \emptyset$ ) is compact and  $f_t(\mathbf{x}), \forall t$ , is continuous to ensure the Pareto-optimal is exist for MOPP (1).

## 3. MATHEMATICAL FORMULATION OF PROBLEM

### 3.1. Intuitionistic Fuzzy Multi-objective Linear Decision-Making Problem

Consider mathematical formulation of Intuitionistic Fuzzy Multi-objective Linear Decision-Making Problem (IF-MOLDMP) can be represented as: (Rukmani and Porchelvi, 2018a; Basumatary and Mitra, 2022; Garai et.al., 2015)

### 3.2. Intuitionistic Fuzzy Goal Model of IF-MOLDMP

In many real-life applications, the decision-maker is allowed to specify an imprecise aspiration-level for each of the constraint and objectives function in IF-MOLDMP (2). A goal with an imprecise

aspiration-level for an IF objective and constraints can be treated as an intuitionistic fuzzy goal (IFG) in the IFDE. Let  $\tilde{D}^I = \{\tilde{f}_1^I(\mathbf{x}), \tilde{f}_2^I(\mathbf{x}), \dots, \tilde{f}_k^I(\mathbf{x}), \tilde{g}_1^I(\mathbf{x}), \tilde{g}_2^I(\mathbf{x}), \dots, \tilde{g}_m^I(\mathbf{x}) | \mathbf{x} \in S\}$  be a set of IFGs, having maximization ( $M_1$ ) with aspiration-level  $\bar{f}_t$  for  $t \in M_1$ ,  $\bar{g}_i$  for  $i \in N_1$  and minimization ( $M_2$ ) with

$$\begin{aligned} & \text{Determine: } \mathbf{x} \in \tilde{S}^I \\ \text{Subject to: } & \begin{cases} f_t(\mathbf{x}) \geq \bar{f}_t, g_i(\mathbf{x}) \geq \bar{g}_i \text{ for } t \in M_1, i \in N_1 \\ f_t(\mathbf{x}) \leq \underline{f}_t, g_i(\mathbf{x}) \leq \underline{g}_i \text{ for } t \in M_2, i \in N_2 \end{cases} \end{aligned} \quad (3)$$

In order to find a P areto-optimal solution for IF-MOLDMP (2) in the IFDE, we need to determine a solution that simultaneously maximizes the level of satisfaction/ membership  $\mu_t(f_t(\mathbf{x})), \mu_i(g_i(\mathbf{x}))$  and minimizes the level of dissatisfaction/ non-membership  $\nu_t(f_t(\mathbf{x})), \nu_i(g_i(\mathbf{x}))$  of the IFGs under the given feasible region,  $\mathbf{x} \in S$ , ac-

aspiration-level  $\underline{f}_t$  for  $t \in M_2$ ,  $\underline{g}_i$  for  $i \in N_2$  for type of IFGs. Hence, to determine the crisp/ deterministic optimal solution, we need to formulate the IFG model of IF-MOLDMP (2) as: (Moges et al., 2023a; Razmi et.al, 2016)

cording to Angelov (1995) stated. Based on this idea, the Pareto-optimal and MN Pareto-optimal solution of IF-MOLDMP (2) are defined as follows:

**Definition 3.1.** (Razmi et.al, 2016; Tsegaye et.al., 2021) A solution vector  $\mathbf{x}^* \in \tilde{S}^I$  is said to be a Pareto-optimal to IF-MOLDMP (2) if there is no new-vector  $\mathbf{x} \in \tilde{S}^I$  such that

$$\begin{aligned} & \tilde{f}_t^I(\mathbf{x}) \leq \tilde{f}_t^I(\mathbf{x}^*) \wedge \mu_i(g_i(\mathbf{x})) \geq \mu_i(g_i(\mathbf{x}^*)) \wedge \nu_i(g_i(\mathbf{x})) \leq \nu_i(g_i(\mathbf{x}^*)), \forall t = 1, 2, \dots, k, \forall i = 1, 2, \dots, m, \\ & \tilde{f}_t^I(\mathbf{x}) < \tilde{f}_t^I(\mathbf{x}^*) \vee \mu_i(g_i(\mathbf{x})) > \mu_i(g_i(\mathbf{x}^*)) \vee \nu_i(g_i(\mathbf{x})) < \nu_i(g_i(\mathbf{x}^*)), \text{ for some } t \in \{1, 2, \dots, k\}, i \in \{1, 2, \dots, m\}. \end{aligned}$$

**Definition 3.2.** (Jafarian et.al., 2018; Razmi et.al, 2016) A solution vector  $\mathbf{x}^* \in \tilde{S}^I$  is said to be a MN Pareto-optimal solution to IF-MOLDMP (2) if there doesn't exists another vector  $\mathbf{x} \in \tilde{S}^I$  such that  $\mu_t(f_t(\mathbf{x})) \geq \mu_t(f_t(\mathbf{x}^*)) \wedge \nu_t(f_t(\mathbf{x})) \leq \nu_t(f_t(\mathbf{x}^*)) \wedge \mu_i(g_i(\mathbf{x})) \geq \mu_i(g_i(\mathbf{x}^*)) \wedge \nu_i(g_i(\mathbf{x})) \leq \nu_i(g_i(\mathbf{x}^*)), \forall t = 1, 2, \dots, k, \forall i = 1, 2, \dots, m$ , and strictly inequality holds for some  $t$  or  $i$ .

## 4. PROPOSED SOLUTION METHOD

### 4.1. Extended Yager-membership function in the IFDE

In the IFDE, the nadir and ideal points are useful for estimating the range of degrees of satisfying (membership) and rejection (non-membership) for the objective function in the IF-MOLDMP (2). To determine

nadir and ideal points, we need to find the optimal solution for each objective function  $f_t(\mathbf{x})$  subject to the given set of constraints. That means solving the following problem independently:

$$\begin{aligned} & \min f_t(\mathbf{x}) \quad \text{Subject to } \mathbf{x} \in S \\ & \quad \text{for } t = 1, 2, 3, \dots, k \end{aligned} \quad (4)$$

The solution obtained from model (4) we call as  $\mathbf{x}_t^B$  is best solution,  $\underline{Z}_t^B = f_t(\mathbf{x}_t^B)$  is objective value or aspiration-level for each  $t$ .  $Z^{id} = (\underline{Z}_1^B, \underline{Z}_2^B, \dots, \underline{Z}_k^B)$  is an ideal point and  $Z^{nad} = (\bar{Z}_1, \bar{Z}_2, \dots, \bar{Z}_k)$  is nadir point of IF-MOLDMP (2) where,  $\bar{Z}_t = \max_{\mathbf{x} \in P^*} f_t(\mathbf{x})$ ,  $P^*$  is Pareto-optimal set. Since  $P^* \subset S$ , we have  $\max_{\mathbf{x} \in S} f_t(\mathbf{x}) \geq \bar{Z}_t, \forall t = 1, 2, 3, \dots, k$ .

Due to the difficulties in finding the nadir point, some scholars suggested a heuristic approach called "Payoff matrix", but the re-

sult obtained by this approach may be an underestimation or overestimation of the nadir point, [Isermann and Steuer \(1997\)](#). The best solution  $\bar{x}_t^B$  is used to construct the payoff matrix as follows:

$$\begin{bmatrix} & f_1(\mathbf{x}) & f_2(\mathbf{x}) & \dots & f_k(\mathbf{x}) \\ \mathbf{x}_1^B & f_1(\mathbf{x}_1^B) & f_2(\mathbf{x}_1^B) & \dots & f_k(\mathbf{x}_1^B) \\ \mathbf{x}_2^B & f_1(\mathbf{x}_2^B) & f_2(\mathbf{x}_2^B) & \dots & f_k(\mathbf{x}_2^B) \\ \vdots & \vdots & \vdots & \ddots & \vdots \\ \mathbf{x}_k^B & f_1(\mathbf{x}_k^B) & f_2(\mathbf{x}_k^B) & \dots & f_k(\mathbf{x}_k^B) \end{bmatrix} \quad (5)$$

If the best solutions  $\mathbf{x}_t^B$  are unique for all  $t = 1, 2, 3, \dots, k$ , then the payoff matrix approach will never overestimate the nadir point  $Z^{nad}$ , ([Isermann and Steuer, 1997](#)). However, if  $\mathbf{x}_t^B$  not unique for at least one  $t$ ,  $\max\{f_t(\mathbf{x}_1^B), f_t(\mathbf{x}_2^B), \dots, f_t(\mathbf{x}_k^B)\}$  may overestimate the nadir point. When a component of the nadir point for an optimization problem is underestimated or overestimated in an IFDE, it may result in unnecessary information about the Pareto-optimal solution, and decision-makers use a wide-range.

If the model (4) produces more than one best solution for any  $s \in \{1, 2, \dots, k\}$ , then underestimated or overestimated solutions of nadir point exist. To estimate the correct nadir point, we use two-steps in the proposed method. In step one, we solve the following optimization problem for each  $s$ , using  $\sigma = \frac{1}{k} > 0$ .

$$\min \frac{f_s(\mathbf{x})}{\underline{Z}_s^B} + \sigma \sum_{t \neq s}^k \frac{f_t(\mathbf{x}_t)}{\underline{Z}_t^B} \quad (6)$$

Subject to:  $\mathbf{x} \in S$

Let  $\mathbf{x}_s^{BB}$  be a solution obtained from the model (6), and construct the Payoff-matrix (5) using this solution instead of  $\mathbf{x}_s^B$ . Using this two-step approach, we find upper and lower-bounds for the membership and non-membership functions of the objective function, which are used as degrees of rejection and acceptance of each IFGs.

In the case of minimization problem,  $U_t^\mu = \max\{f_t(\mathbf{x}_1^B), f_t(\mathbf{x}_2^B), \dots, f_t(\mathbf{x}_k^B)\}$  and  $L_t^\mu = \min\{f_t(\mathbf{x}_1^B), f_t(\mathbf{x}_2^B), \dots, f_t(\mathbf{x}_k^B)\}$  considered as upper and lower-bound of membership functions, respectively. Similarly,  $U_t^\nu = U_t^\mu$  and  $L_t^\nu = L_t^\mu + \epsilon_t(U_t^\mu - L_t^\mu)$  where,  $0 < \epsilon_t < 1$  for each  $t$  are upper and lower-bound of non-membership functions, respectively ([Bharati and Singh, 2014](#); [Moges et.al., 2023b](#)).

**Lemma 4.1.** The solution obtained from the model (6) never generates an overestimation of  $Z^{nad}$ , ([Ehrgott, 2000](#); [Isermann and Steuer, 1997](#)).

For minimization problem, membership ( $\mu_t(f_t(\mathbf{x}))$ ) and non-membership ( $\nu_t(f_t(\mathbf{x}))$ ) functions can be defined according to Eqs. 7 and Eqs. 8 respectively.

$$\mu_t(f_t(\mathbf{x})) = \begin{cases} 1 & \text{if } f_t(\mathbf{x}) \leq L_t^\mu \\ \frac{U_t^\mu - f_t(\mathbf{x})}{U_t^\mu - L_t^\mu} & \text{if } L_t^\mu < f_t(\mathbf{x}) \leq U_t^\mu \\ 0 & \text{if } f_t(\mathbf{x}) > U_t^\mu \end{cases} \quad (7)$$

$$\nu_t(f_t(\mathbf{x})) = \begin{cases} 0 & \text{if } f_t(\mathbf{x}) < L_t^\nu \\ \frac{f_t(\mathbf{x}) - L_t^\nu}{U_t^\nu - L_t^\nu} & \text{if } L_t^\nu \leq f_t(\mathbf{x}) \leq U_t^\nu \\ 1 & \text{if } f_t(\mathbf{x}) > U_t^\nu \end{cases} \quad (8)$$

Now, to overcome the limitation of the [Angelov \(1995\)](#) model, we first resolve the indeterminacy factors independently for each IFG using the [Yager \(2009\)](#) approach. Therefore, using the membership function  $\mu_t(f_t(\mathbf{x}))$  defined in Eqs.7 and the non-membership function  $\nu_t(f_t(\mathbf{x}))$  defined in Eqs.8, the new extended Yager-membership function is defined as follows: for any  $\lambda \in [0, 1]$ .

$$I_t^\lambda(f_t(\mathbf{x})) = (1 - \lambda)\mu_t(f_t(\mathbf{x})) + \lambda(1 - \nu_t(f_t(\mathbf{x}))) \quad (9)$$

for each  $t = 1, 2, \dots, k$ .

Without knowing any other details regarding the DM's attitude during this study, we arrived at  $\lambda = \frac{1}{2}$  in our discussion that follows. The piece-wise linear Yager-membership function for the minimization



problem shown in Figure 1(a): and defined as:

$$I_t^\lambda(f_t(\mathbf{x})) = \begin{cases} 1 & \text{if } f_t(\mathbf{x}) \leq L_t^\mu \\ 1 - \frac{1}{2}\epsilon_t \left( \frac{f_t(\mathbf{x}) - L_t^\mu}{L_t^\nu - L_t^\mu} \right) & \text{if } L_t^\mu \leq f_t(\mathbf{x}) < L_t^\nu \\ \frac{1}{2}(2 - \epsilon_t) \frac{U_t^\mu - f_t(\mathbf{x})}{U_t^\mu - L_t^\nu} & \text{if } L_t^\nu \leq f_t(\mathbf{x}) < U_t^\mu \\ 0 & \text{if } f_t(\mathbf{x}) \geq U_t^\mu \end{cases} \quad (10)$$

Now, we need to expand the range of function  $I_t^\lambda(f_t(\mathbf{x})) = 1$ , for  $f_t(\mathbf{x}) \leq L_t^\mu$  to  $I_t^\lambda(f_t(\mathbf{x})) > 1$ , for  $f_t(\mathbf{x}) < L_t^\mu$  to overcome the limitation of Dubey et.al. (2012) model.

$$\eta_t(f_t(\mathbf{x})) = \begin{cases} \frac{b_1(L_t^\mu - f_t(\mathbf{x}))}{L_t^\mu - L_t^{\min}} + 1 & \text{if } L_t^{\min} < f_t(\mathbf{x}) < L_t^\mu \\ 1 - \frac{1}{2}\epsilon_t \left( \frac{f_t(\mathbf{x}) - L_t^\mu}{L_t^\nu - L_t^\mu} \right) & \text{if } L_t^\mu \leq f_t(\mathbf{x}) < L_t^\nu \\ \frac{1}{2}(2 - \epsilon_t) \frac{U_t^\mu - f_t(\mathbf{x})}{U_t^\mu - L_t^\nu} & \text{if } L_t^\nu \leq f_t(\mathbf{x}) < U_t^\mu \\ \frac{b_2(f_t(\mathbf{x}) - U_t^\mu)}{U_t^\mu - U_t^{\max}} & \text{if } U_t^\mu \leq f_t(\mathbf{x}) \leq U_t^{\max} \end{cases} \quad (11)$$

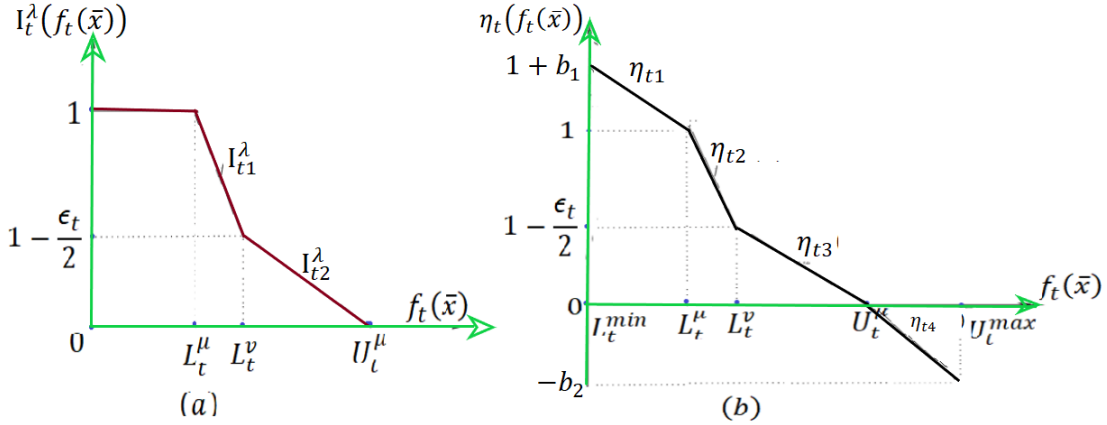


Figure 1: Yager-membership function  $I_t^\lambda(f_t(\mathbf{x}))$ , (Aggarwal et.al., 2019) and Extended Yager-membership function  $\eta_t(f_t(\mathbf{x}))$ , (Garai et.al., 2016) for the minimization problem

The piecewise linear extended Yager-membership function Eqs. (11) has the following properties:

- Over the interval containing all possible values of the objective function, it is a strictly monotonic function.
- It permits alternate point orderings with Yager-membership function values outside of  $[0, 1]$ .
- It is equivalent to the Yager-membership function  $I_t^\lambda(f_t(\mathbf{x}))$  Eqs. (10) on  $[L_t^\mu, U_t^\mu]$  for each  $t$ .
- If  $f_t(\mathbf{x}) < L_t^\mu$ , then  $\eta_t(f_t(\mathbf{x})) \geq 1$ , and if  $f_t(\mathbf{x}) > U_t^\mu$ , then  $\eta_t(f_t(\mathbf{x})) \leq 0$ .
- It shows the level of satisfaction of the decision-maker for every objective function.

Additionally, we modified these piecewise

linear extended Yager-membership functions  $\eta_t(f_t(\mathbf{x}))$  as follows: based on the method suggested by Wu and Guu (2001) to solve MOPP

$$\eta_t(f_t(\mathbf{x})) = \eta_t(a_t^1) + s_t^1(f_t(\mathbf{x}) - a_t^1) + \sum_{l=2}^{m-1} \frac{(s_t^l - s_t^{l-1})}{2} (|f_t(\mathbf{x}) - a_t^l| + f_t(\mathbf{x}) - a_t^l) \quad (12)$$

where,  $a_t^l$ ,  $l = 1, 2, 3, \dots, m$  are the breaking/ jumping points of  $\eta_t(f_t(\mathbf{x}))$ ,  $t = 1, \dots, k$ , the slope of line segment between  $a_t^l$  and  $a_t^{l+1}$  is given by  $s_t^l = \frac{\eta_t(a_t^{l+1}) - \eta_t(a_t^l)}{a_t^{l+1} - a_t^l}$  for  $l = 1, \dots, m-1$ ;  $t = 1, 2, \dots, k$ .

#### 4.2. Develop a new intuitionistic fuzzy (IF) aggregation operator

A number of logical operators are available in the IFDE, enabling the combination of numerous objectives into a single objective. We employed the convex combination of the arithmetic mean-operator and the max-min operator on the extended Yager-membership functions  $\eta_t(f_t(\mathbf{x}))$  Eqs. (11) in order to create a novel operator in the IFDE. Therefore, the new IF aggregation operator is formulated as:

$$\eta_{\bar{D}I}(\mathbf{x}) = \delta \min_{t=1}^k \eta_t(f_t(\mathbf{x})) + (1-\delta) \frac{1}{k} \sum_{t=1}^k \eta_t(f_t(\mathbf{x})), \quad (13)$$

#### Model I:

$$\begin{aligned} & \max \delta \alpha_0 + (1-\delta) \sum_{t=1}^k \alpha_t \\ \text{Subject to: } & \left\{ \begin{array}{l} \alpha_0 + \alpha_t \leq \eta_t(f_t(\mathbf{x})) \quad \text{for } t = 1, 2, \dots, k. \\ \eta_t(f_t(\mathbf{x})) = \eta_t(a_t^1) + s_t^1(f_t(\mathbf{x}) - a_t^1) + \dots + (s_t^{m-1} - s_t^{m-2})(f_t(\mathbf{x}) - a_t^{m-1} + q_t^{m-2}) \\ f_t(\mathbf{x}) + q_t^{l-2} \geq a_t^{l-1} \quad \text{for } l = 3, 4, \dots, m \\ \alpha_0, \alpha_t, q_t^{l-2} \geq 0 \quad \text{for } t = 1, 2, \dots, k; l = 3, 4, \dots, m. \\ \mathbf{x} \in S \end{array} \right\} \end{aligned} \quad (15)$$

#### 4.3. The intuitionistic fuzzy goal programming method

The higher-value of  $\eta_t(f_t(\mathbf{x}))$  is regarded as the best acceptable value for DMs in the IFDE. As a result, DMs must minimize

(1) under an IFDE without introducing extra binary variables.

where  $0 < \delta < 1$  represent the degree of preference of DMs. Using this novel IF aggregation operator and decision-makers' preference value  $\delta \in [0, 1]$ , the IF-MOLDMP (2) is transformed into a crisp single-objective optimization problem to determine the Pareto-optimal solution based on Eqs.(14).

$$\max_{\mathbf{x} \in S} \eta_{\bar{D}I}(\mathbf{x}) \quad (14)$$

Therefore, using a non-negative variable  $q_t^l$ , the extended Yager-membership function defined in Eqs.(12), and the IF aggregation operator defined in (13), the equivalent deterministic single-objective optimization problem of model (14) is formulated as follows:

the under-achievement (negative-deviational) variable  $d_t^-$  by assigning weight  $w_t^-$  to each objective function  $t$  in the goal programming approach  $\eta_t(f_t(\mathbf{x})) + d_t^- \geq 1$ . Therefore, the intuitionistic fuzzy goal programming (IFGP)

model of IF-MOLDMP (2) is formulated as follows:

**Model II:**

$$\begin{aligned} & \min \sum_{t=1}^k w_t^- d_t^- \\ \text{Subject to: } & \begin{cases} \eta_t(f_t(\mathbf{x})) + d_t^- \geq 1 \text{ for } t = 1, 2, 3, \dots, k \\ \mathbf{x} \in S \\ d_t^- \geq 0, \sum_{t=1}^k w_t^- = 1, w_t^- > 0 \end{cases} \end{aligned} \quad (16)$$

#### 4.4. Interactive Penalty Function Method (IPFM)

In an intuitionistic fuzzy decision environment (IFDE), the interactive approach is very effective at solving IF-MOLDMP (2). In this process, the algorithm generates an initial solution before consulting the DM and obtaining a new solution(s) if the DM is dissatisfied with the current one. Let  $\mathbf{x}^*$  be the optimal solution of model I (15) or model II (16). Assume that the existing solution  $\mathbf{x}^*$  does not satisfy the DMs.

To discuss how the penalty function

method is applied in the interactive method once DMs update the problem for some objective functions, we considered the following Figure 2 that shows the level of satisfaction and dissatisfaction by DMs. Furthermore, the Figure 2 demonstrates how to determine a solution from a large space by relaxing the constraint set. The green region in the Figure 2 represents DMs who are completely satisfied with the current solution, while the red region represents DMs who are dissatisfied, and the row depicts how the algorithm generates the best solution from a large space.

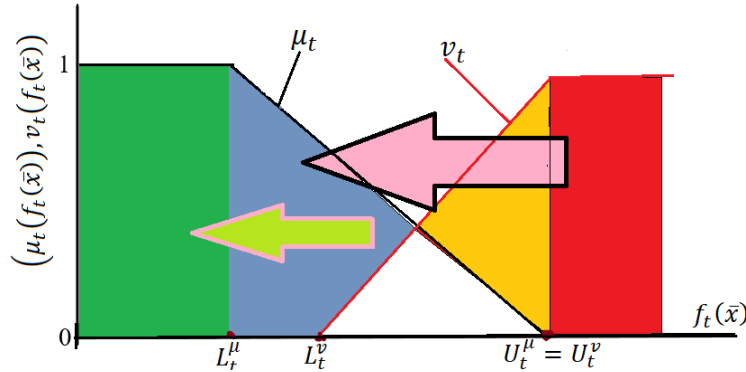


Figure 2: How penalty function method applied on minimization type problem

**Definition 4.1.** A vector  $\mathbf{x} \in S$  is DM-feasible solution if  $\forall t \in 1, 2, \dots, k, \eta_{\tilde{D}^I}^\lambda(f_t(\mathbf{x})) - \eta_{\tilde{D}^I}^\lambda(f_t(\mathbf{x}^*)) \geq \gamma_t$ , for nonnegative variable  $\gamma_t$ . Where,  $\mathbf{x}^*$  is optimal solution to either model I (15) or model II (16).

Let the set of DM-feasible solution be denoted by  $S^{DM}$  and defined as  $S^{DM} = \{\mathbf{x} \in S | \eta_{\tilde{D}^I}^\lambda(f_t(\mathbf{x})) - \eta_{\tilde{D}^I}^\lambda(f_t(\mathbf{x}^*)) \geq \gamma_t, \forall t\}$ .

To find a preferable Pareto-optimal solution based on  $\mathbf{x}^*$  to IF-MOLDMP (2), we



solve the following optimization problem:

$$\max_{\mathbf{x} \in S^{DM}, \gamma_t \geq 0} \sum_{t=1}^j \gamma_t \quad (17)$$

Now choose  $\mathbf{x} \in S$  such that  $\eta_t^\lambda(f_t(\mathbf{x})) - \eta_t^\lambda(f_t(\mathbf{x}^*)) < \gamma_t^2$  (i.e.,  $\mathbf{x} \notin S^{DM}$ ). The non-linear penalty function is defined as  $P(\mathbf{x}) = \sum_{t=1}^j [\max\{0, \eta_{D_I}^\lambda(f_t(\mathbf{x}^*)) - \eta_{D_I}^\lambda(f_t(\mathbf{x})) + \gamma_t^2\}]^2$  Meng et.al. (2011); Jameel and Radhi (2014) and satisfies:

$$P(\mathbf{x}) = \begin{cases} 0 & \text{if } \mathbf{x} \in S^{DM} \\ > 0 & \text{if } \mathbf{x} \notin S^{DM} \end{cases} \quad (18)$$

Now, using the penalty function, we can transform it into unconstrained optimization, where the objective function is defined as:

$$F(\mathbf{x}, c_i) = \sum_{t=1}^j \gamma_t + c_i (\sum_{t=1}^j [\max\{0, \eta_t^\lambda(f_t(\mathbf{x}^*)) - \eta_t^\lambda(f_t(\mathbf{x})) + \gamma_t^2\}]^2)$$

Based on the penalty parameter  $c_i > 0$ , we formulate the penalty optimization problem as follows:

$$\begin{aligned} (P_{\lambda, c_i}) \quad & \max F(\mathbf{x}, c_i) \\ \text{Subject to} \quad & \mathbf{x} \in R^n, \end{aligned} \quad (19)$$

The main benefit of this model is that, instead of starting from scratch, it will use a wide domain to improve the existing solution and attempt to discover a solution that satisfies DMs by ignoring the non-update membership and non-membership functions.

#### IPFM Algorithm:

Initial Step:

- Using current solution  $\mathbf{x}^*$  and  $\gamma_{t_i} = \eta_{D_I}^\lambda(\frac{U_t^\mu - L_t^\mu}{2})$ , choose initial solution  $\mathbf{x}_1 \in S$  such that  $\eta_t^\lambda(f_t(\mathbf{x}_1)) - \eta_t^\lambda(f_t(\mathbf{x}^*)) < \gamma_{t_i}^2$ . That means:  $\mathbf{x}_1 \notin S^{DM}$ .
- Choose  $\lambda = \frac{1}{2}, c_1 > 0, \beta > 1$  and set  $i=1$

Main Step:

Step I. Using  $\mathbf{x}_i$  and  $\gamma_{t_i}$  solve the problem  $\max F(\mathbf{x}, c_i)$  Subject to  $\mathbf{x} \in R^n$  and let call  $\mathbf{x}_{i+1}$  be an optimal solution.

Step II. If  $\mathbf{x}_{i+1}$  be DM feasible solution, then stop  $\hat{x} = \mathbf{x}_{i+1}$  and the corresponding decision vector  $\hat{\gamma}$  are optimal solutions to model (17). Otherwise, put  $c_{i+1} = \beta c_i$ ,  $i = i + 1$  and go to step I.

**Theorem 4.1 (Optimality test).** Let  $\hat{x}$  and  $\hat{\gamma}$  are optimal solutions to model (17). Then

- If  $\gamma_t = 0, \forall t = 1, \dots, k$ , then the Pareto optimal solution to IF-MOLDMP (2) in an IFDE is  $\mathbf{x}^*$ .
- In an IFDE,  $\mathbf{x}^*$  is not Pareto's optimal solution to IF-MOLDMP (2) if at least one  $\gamma_t > 0$ . Instead of  $\mathbf{x}^*$ , Pareto's optimal solution to IF-MOLDMP (2) is  $\hat{x}$ .

(Analogous theorem proofs can be found in literature for instance see Garai et.al. (2015, 2016))

## 5. ALGORITHM FOR PENALIZED IFGP METHOD

Based on the idea discussed above, we proposed a general framework or algorithm for finding Pareto-optimal solutions for IF-MOLDMP (2) in an IFDE. The proposed algorithm's steps are as follows:

**Step 1:** Solve each objective function independently under the constraint set. That means: solve model (4).

**Step 2:** If the solution  $\mathbf{x}_t^B$  of model (4) is unique for each  $t$ , then go to step 3. Otherwise, solve model (6) and use its solution  $\mathbf{x}_t^{BB}$  instead of  $\mathbf{x}_t^B$ , then go to step 3.

**Step 3:** Construct the payoff matrix (see Eqs. 5) and find the upper and lower-tolerances of membership and non-membership functions.

**Step 4:** Formulate the extended Yager-membership function in an intuitionistic fuzzy decision environment. See Eqs. (11).

**Step 5:** Solve either model I (15) or model II (16).

If the decision-maker is satisfied with the current solution  $\mathbf{x}^*$ , then stop, and the current solution  $\mathbf{x}^*$  is the Pareto optimal solution to IF-MOLDMP (2). Otherwise, go to step 6.

**Step 6:** Ask the decision-maker to change the membership and nonmembership functions for  $j \leq k$  objective functions, then go to step 7.

**Step 7:** Solve model 17 with the above-mentioned algorithm for interactive penalty function method to get solutions  $\hat{x}$  and  $\gamma_t$ . Then there are the fol-

lowing scenarios:

Case-I If  $\gamma_t = 0, \forall t = 1, \dots, k$ , decision-makers must adjust either  $\delta$  for model I and weight of objective function for model II or  $\lambda$ , then go to step 5.

Case-II In an IFDE, if at least one  $\gamma_t > 0$ , then Pareto's optimal solution to IF-MOLDMP (2) is  $\hat{x}$ .

## 6. NUMERICAL EXAMPLE

Consider the following intuitionistic fuzzy multi-objective linear decision-making problem (IF-MOLDMP) that is given in an intuitionistic fuzzy decision environment:

$$\begin{aligned} \tilde{max} f_1(\mathbf{x}) &= -x_1 + 2x_2 \\ \tilde{max} f_2(\mathbf{x}) &= 2x_1 + x_2 \\ \text{Subject to: } \mathbf{x} \in S &= \left\{ \mathbf{x} \in R^2 \left| \begin{array}{l} -x_1 + 3x_2 \leq 21, 4x_1 + 3x_2 \leq 45, \\ x_1 + 3x_2 \leq 27, 3x_1 + x_2 \leq 30, \\ x_1, x_2 \geq 0. \end{array} \right. \right\} \end{aligned} \quad (20)$$

Following the proposed solution method discussed so far, we solve the given IF-MOLDMP (20) step by steps:

- Individual Solution:  $\mathbf{x}_1^B = (0, 7), \mathbf{x}_2^B = (9, 3)$ , and Ideal point:  $(Z_1^B, Z_2^B) = (14, 21)$
- Using Payoff matrix the upper and lower bounds are:  $U_1^\mu = 14, L_1^\mu = -3, L_1^{min} = -6, U_1^{max} = 27$  and  $U_2^\mu = 21, L_2^\mu = 7, L_2^{min} = -10, U_2^{max} = 32$  using a tolerances  $\epsilon_1 = 0.4, \epsilon_2 = 0.3$ .
- The brake points are:  $a_1^1 = -6, a_1^2 = -3, a_1^3 = 7, a_1^4 = 14, a_1^5 = 27$  and its corresponding values are  $\eta_1(a_1^1) = -b_2, \eta_1(a_1^2) = 0, \eta_1(a_1^3) = 0.8, \eta_1(a_1^4) = 1, \eta_1(a_1^5) = 1 + b_1$  for ob-

jective function  $f_1(\mathbf{x})$ .

$a_2^1 = -10, a_2^2 = 7, a_2^3 = 17, a_2^4 = 21, a_2^5 = 32$  and its corresponding values are  $\eta_2(a_2^1) = -b_2, \eta_2(a_2^2) = 0, \eta_2(a_2^3) = 0.85, \eta_2(a_2^4) = 1, \eta_2(a_2^5) = 1 + b_1$  for objective function  $f_2(\mathbf{x})$ .

- The extended Yager-membership functions are:
 
$$\begin{aligned} \eta_1(f_1(\mathbf{x})) &= -0.0286x_1 + 0.057x_2 - 0.59q_1^1 \\ &\quad - 0.0514q_1^2 + 0.61 \text{ and} \\ \eta_2(f_2(\mathbf{x})) &= 0.074x_1 + 0.037x_2 - 0.033q_2^1 \\ &\quad - 0.048q_2^2 + 0.227 \end{aligned}$$
- Based on the proposed model (15), we formulated IF-MOLDMP (20) as single-objective optimization model:

**Model I:** Assign the value of  $\delta \in [0, 1]$

$$\begin{aligned} & \max \delta \alpha_0 + (1 - \delta) \alpha_1 + (1 - \delta) \alpha_2 \\ \text{Subject to } & \left\{ \begin{array}{l} \alpha_0 + \alpha_1 + 0.0286x_1 - 0.057x_2 + 0.59q_1^1 + 0.0514q_1^2 \leq 0.61 \\ \alpha_0 + \alpha_2 - 0.074x_1 - 0.037x_2 + 0.033q_2^1 + 0.048q_2^2 \leq 0.227 \\ x_1 - 2x_2 - q_1^1 \leq 3, x_1 - 2x_2 - q_1^2 \leq -7 \\ -2x_1 - x_2 - q_2^1 \leq -7, -2x_1 - x_2 - q_2^2 \leq -17 \\ -x_1 + 3x_2 \leq 21, 4x_1 + 3x_2 \leq 45, x_1 + 3x_2 \leq 27, 3x_1 + x_2 \leq 30 \\ x_1, x_2, \alpha_0, \alpha_1, \alpha_2, q_1^1, q_1^2, q_2^1, q_2^2 \geq 0. \end{array} \right. \end{aligned} \quad (21)$$

- In a similar way, using the proposed model (16), we converted the given IF-MOLDMP (20) into the following single-objective optimization model:

**Model II:** Assign the relative important of each objective function  $w_t^-$

$$\begin{aligned} & \min w_1^- d_1^- + w_2^- d_2^- \\ \text{Subject to: } & \left\{ \begin{array}{l} 0.0286x_1 - 0.057x_2 + 0.59q_1^1 + 0.0514q_1^2 - d_1^- \leq -0.39 \\ -0.074x_1 - 0.037x_2 + 0.033q_2^1 + 0.048q_2^2 - d_2^- \leq -0.773 \\ x_1 - 2x_2 - q_1^1 \leq 3, x_1 - 2x_2 - q_1^2 \leq -7 \\ -2x_1 - x_2 - q_2^1 \leq -7, -2x_1 - x_2 - q_2^2 \leq -17 \\ -x_1 + 3x_2 \leq 21, 4x_1 + 3x_2 \leq 45, x_1 + 3x_2 \leq 27, 3x_1 + x_2 \leq 30 \\ x_1, x_2, d_1^-, d_2^-, q_1^1, q_1^2, q_2^1, q_2^2 \geq 0. \end{array} \right. \end{aligned} \quad (22)$$

Now, using MATLAB-R2023 software to solve model I (21) and model II (22), we obtained the Pareto-optimal solution  $\mathbf{x}_1 = 6, \mathbf{x}_2 = 7, \mathbf{f}_{\text{val}} = 1.1311$ ,  $\mathbf{f}_1(\mathbf{x}^*) = 8$ , and  $\mathbf{f}_2(\mathbf{x}^*) = 19$  for the given IF-MOLDMP (20) and shown in Table 1.

Table 1: Results for model I (21) and model II (22) in different cases

	$\delta, w_t^-$	Optimal Solution	Optimal Value
Model I	$\delta = 0.36$	$\alpha_0 = 0, \alpha_1 = 0.83739, \alpha_2 = 0.929$ , $\mathbf{x}_1 = 6, \mathbf{x}_2 = 7, \mathbf{f}_{\text{val}} = 1.1311$	$\mathbf{f}_1(\mathbf{x}^*) = 8$ , $\mathbf{f}_2(\mathbf{x}^*) = 19$
	$\delta = 0.5$	$\alpha_0 = 0, \alpha_1 = 0.8374, \alpha_2 = 0.93$ , $x_1 = 5.991, x_2 = 7, f_{\text{val}} = 0.8837$	$f_1(\mathbf{x}^*) = 8.009$ , $f_2(\mathbf{x}^*) = 18.982$
	$\delta = 0.8$	$\alpha_0 = 0.8777, \alpha_1 = 0, \alpha_2 = 0$ , $x_1 = 5.152, x_2 = 7.282, f_{\text{val}} = 0.7022$	$f_1(\mathbf{x}^*) = 9.412$ , $f_2(\mathbf{x}^*) = 17.586$
Model II	$w_1^- = 0.6, w_2^- = 0.4$	$d_1^- = 0.10548, d_2^- = 0.144$ , $x_1 = 4.800, x_2 = 7.399, f_{\text{val}} = 0.12089$	$f_1(\mathbf{x}^*) = 9.998$ , $f_2(\mathbf{x}^*) = 16.882$
	$w_1^- = 0.5, w_2^- = 0.5$	$d_1^- = 0.1626, d_2^- = 0.0700$ , $x_1 = 6.00, x_2 = 6.999, f_{\text{val}} = 0.1163$	$f_1(\mathbf{x}^*) = 7.998$ , $f_2(\mathbf{x}^*) = 18.999$
	$w_1^- = 0.3, w_2^- = 0.7$	$d_1^- = 0.1626, d_2^- = 0.0700$ , $\mathbf{x}_1 = 6, \mathbf{x}_2 = 7.00, \mathbf{f}_{\text{val}} = 0.0978$	$\mathbf{f}_1(\mathbf{x}^*) = 8$ , $\mathbf{f}_2(\mathbf{x}^*) = 19$

## 7. RESULTS AND DISCUSSION

For different values of  $\delta \in (0.35, 0.85)$  and  $w_1^-, w_2^- \geq 0$  with  $w_1^- + w_2^- = 1$ , the comparative work of the resulted efficient solution is given in Table 1. Let the optimal or objective value of model I (21) and model II (22) be presented by  $f_{val}$ . As shown in Table 1, when the value of  $w_2^-$  (relative-weight of  $f_2(\mathbf{x})$ ) increases and the value of  $\delta$  (de-

gree of compensation),  $w_1^-$  (relative-weight of  $f_1(x)$ ) decreases, the preferable optimal value  $f_{val}$  is obtained. Thus, the optimal solution of both model I (21) and model II (22) is identical, i.e.,  $\mathbf{x}_1 = \mathbf{6}, \mathbf{x}_2 = \mathbf{7}, \mathbf{f}_{val} = \mathbf{1.1311}$ , which is the candidate Pareto-optimal solution of IF-MOLDMP (20). Now to test the Pareto-optimality, we need to formulate the following single-objective problem (23) based on Eqs. (17) and solve it:

$$\begin{aligned} & \max \quad \gamma_1 + \gamma_2 \\ \text{Subject to: } & \left\{ \begin{array}{l} -0.0286x_1 + 0.057x_2 - 0.59q_1^1 - 0.0514q_1^2 - \gamma_1 \geq 0.2274 \\ 0.074x_1 + 0.037x_2 - 0.033q_2^1 - 0.048q_2^2 - \gamma_2 \geq 0.703 \\ x_1 - 2x_2 - q_1^1 \leq 3, x_1 - 2x_2 - q_1^2 \leq -7 \\ -2x_1 - x_2 - q_2^1 \leq -7, -2x_1 - x_2 - q_2^2 \leq -17 \\ -x_1 + 3x_2 \leq 21, 4x_1 + 3x_2 \leq 45, x_1 + 3x_2 \leq 27, 3x_1 + x_2 \leq 30 \\ x_1, x_2, \gamma_1, \gamma_2 \geq 0 \end{array} \right\} \end{aligned} \quad (23)$$

When the model above (23) is solved using the MATLAB-R2023 program,  $\gamma_1 = \gamma_2 = 0$  is the outcome. This suggests that the Pareto-optimal solution to IF-MOLDMP (20) is provided by the found solutions  $\mathbf{x}_1 = \mathbf{6}, \mathbf{x}_2 = \mathbf{7}$ . The suggested method, however, allows decision-makers to select the goal that must be accomplished first in order of importance. For instance, as  $\delta \nearrow$  (increases), the value of  $f_1(\mathbf{x}) \nearrow$  and the value of  $f_2(\mathbf{x}) \searrow$  (decreases), etc.

## 8. CONCLUSION

In this paper, the penalized intuitionistic fuzzy goal programming strategy has been proposed for finding Pareto-optimal solutions to the IF-MOLDMP in an intuitionistic fuzzy decision environment. When applied to optimization problems in an imprecise environment, the IFO methodology is among the most effective methods available, yielding more satisfactory outcomes than fuzzy and classical optimizations. The significant contribution of the proposed method is

the development of an extended intuitionistic fuzzy interactive technique to determine the most preferred Pareto-optimal for IF-MOLDMP in an intuitionistic fuzzy environment. This technique combines the penalty function method with an appropriate intuitionistic fuzzy aggregation operator. When compared to the existing IFO method, the proposed method can choose from a set of compromise solutions that are both efficient and meet the DM's preference for IF-MOLDMP. Furthermore, the advantages of the proposed method are that there is no need to add an extra zero-one variable, it eliminates the limitation of overestimation or underestimation of the nadir point when establishing a reference point for decision-makers, and it guarantees that the existing solution  $\mathbf{x}^*$  satisfies the Pareto-optimally condition.

A future study could focus on applying the proposed solution method to different real-world application problems, such as water resource allocation and inventory control problems, and comparing the outcomes to existing optimization methods.

## Acknowledgments

All authors are grateful to the editor-in-chief and anonymous reviewers for providing in depth comments and suggestions that enhanced the clarity and readability of the manuscript.

## Conflict of Interest

On behalf of all authors, the corresponding author state there is no conflict of interest.

## Funding

The authors did not receive any funding for this research.

## References

- Aggarwal A., Mehra A., Chandra S., Khan I. 2019. Solving Atanassov's I-fuzzy Linear Programming Problems Using Hurwicz's Criterion, *Fuzzy Information and Engineering*, 10 (3), 339–361.
- Angelov P. 1995. Intuitionistic Fuzzy Optimization, *Center of Biomedical Engineering-Bulgarian Academy of Sciences*.
- Atanassov K. T. 1986. Intuitionistic Fuzzy Sets, *Fuzzy Sets and Systems*, 20 ,87-96.
- Basumatary U.R., Miltra D.K. 2022. Application of Intuitionistic Fuzzy Optimization Techniques to Study Multi-objective Linear Programming in Agricultural Production Planning in Baksa District, Assam, India, *Advances and Applications in Mathematical Sciences*, 21 (6) , 3011-3028.
- Bellman R. E., Zadeh L. A. 1970. Decision Making in Fuzzy Environment, *national aeronautics and space administration, Washington, D. C.*.
- Bharati S. K., Singh S. R. 2014. Intuitionistic Fuzzy Optimization Technique in Agricultural Production Planning: A Small Farm Holder Perspective, *International Journal of Computer Applications*, Volume 89, No.6..
- Bharati, Nishad, Singh, 2014. Solution of Multi-Objective Linear Programming Problems in Intuitionistic Fuzzy Environment, *Advances in Intelligent Systems and Computing* 236.
- Cheng H., Huang W., Zhou Q., Cai J. 2013. Solving fuzzy multi-objective linear programming problems using deviation degree measures and weighted max–min method, *Applied Mathematical Modelling* 37 6855–6869.
- Dey S., Roy T.K. 2015. Intuitionistic Fuzzy Goal Programming Technique for Solving Non-Linear Multi-objective Structural Problem, *Journal of Fuzzy Set Valued Analysis*, 3, 00243, 1-15.
- Dubey D., Chandra S., Mehra A. 2012. Fuzzy linear programming under interval uncertainty based on IFS representation, *Fuzzy Sets and Systems* 188 68 – 87.
- Dubois, D., Fortemps, P. 1999. Computing improved optimal solutions to max–min flexible constraint satisfaction problems, *European Journal of Operational Research*, 118 , 95-126.
- Ehrgott M. 2000. Approximation Algorithms for Combinatorial Multicriteria Optimization problems, *International Transactions in Operational Research*, 51 7, 1-11.
- Fathy E., Ammar E, Helmy M.A. 2023. Fully intuitionistic fuzzy multi-level linear fractional programming problem, *Alexandria Engineering Journal* 77 684-694.
- Fuller R. 1998. Fuzzy Reasoning and Fuzzy Optimization, *Turku Centre for Computer Science*.
- Garai A., Mandal P., Roy T.K. 2015. Intuitionistic fuzzy T-sets based solution

- technique for multiple objective linear programming problems under imprecise environment, *Notes on Intuitionistic Fuzzy Sets, Mersin, Turkey*, 14–18.
- Garai, A., Mandal, P., Roy, T.K. 2016 Interactive intuitionistic fuzzy technique in multi-objective optimisation, *Int. J. Fuzzy Computation and Modelling*, 2(1), 14 -26.
- Ghosh P., Kumar T. 2014. Intuitionistic fuzzy goal geometric programming problem, *Notes on Intuitionistic Fuzzy Sets*, 20 (1), 63–78.
- Husain S., Ahmad Y., Alam M.A. 2012. A study on the Role of Intuitionistic Fuzzy Set in Decision making problems, *International Journal of Computer Applications*, 48 (19), 1-7.
- Hanine, Y., Lamrani Alaoui, Y., Tkiouat, M., Lahrichi, Y. 2021. Socially Responsible Portfolio Selection: An Interactive Intuitionistic Fuzzy Approach. *Mathematics*, 9, 3023.
- Isermann H., Steuer R.E. 1987. Computational experience concerning payoff tables and minimum criterion values over efficient set. *European Journal of Operational Research*, 33 , 91-97.
- Jameel A.F., Radhi A.Z. 2014. Penalty Function Method For Solving Fuzzy Non-linear Programming Problem, *International Journal of Recent Research in Mathematics Computer Science and Information Technology*, 1 (1), 1-13.
- Jafarian E., Razmi J., Baki M. F. 2018. A flexible programming approach based on intuitionistic fuzzy optimization and geometric programming for solving multi-objective nonlinear programming problems, *Expert Systems with Applications* 93, 245-256.
- Jiménez M., Bilbao A. 2009. Pareto-optimal solutions in fuzzy multi-objective linear programming, *Fuzzy Sets and Systems* 160, 2714 – 2721.
- Kahraman C., Öztayşi B., Çevik S. 2016. A Comprehensive Literature Review of 50 Years of Fuzzy Set Theory, *International Journal of Computational Intelligence Systems*.
- Kassa S.M., Tsegaye T.H. 2018. An iterative method for tri-level quadratic fractional programming problems using fuzzy goal programming approach, *J. Ind. Eng. Int.* 14, 255–264.
- Khan M.F., Haq A., Ahmed A., Ali I., 2021. Multiobjective Multi-Product Production Planning Problem Using Intuitionistic and Neutrosophic Fuzzy Programming, *IEEEs Access multidisciplinary*.
- Kumar P. S. 2020. Algorithms for solving the optimization problems using fuzzy and intuitionistic fuzzy set, *International Journal of System Assurance Engineering and Management* 11, 189–222.
- Li D.F. 2020, Decision and Game Theory in Management with Intuitionistic Fuzzy Sets, *Studies in Fuzziness and Soft Computing*, 308, 2941-2955.
- Li S., Hu C. 2009. Satisfying optimization method based on goal programming for fuzzy multiple objective optimization problem, *European Journal of Operational Research* 197, 675–684.
- Lu S., Su L., Xiao L., Zhu L.2015. Application of Two-Phase Fuzzy Optimization Approach to Multiproduct Multistage Integrated Production Planning with Linguistic Preference under Uncertainty, *Mathematical Problems in Engineering*, 780830, 1-20.
- Meng Z., Shen R., Jiang M. 2011. An Objective Penalty Functions Algorithm for Multiobjective Optimization Problem, *American Journal of Operations Research*, 1, 229-235.
- Moges D.M., Mushi A.R., Wordofa B.G. 2023. A New Method for Intuitionis-



- tic Fuzzy Multi- Objective Linear Fractional Optimization Problem and its Application in Agricultural Land allocation Problem, *Information Sciences* 625, 457-475.
- Moges D.M., Wordofa B.G. 2024. An efficient algorithm for solving multilevel multi-objective linear fractional optimization problem with neutrosophic parameters, *Expert Systems With Applications* 257, 125122.
- Moges D.M., Wordofa B.G., Mushi A.R. 2023. Solving multi-objective linear fractional decentralized bi-level decision-making problems through compensatory intuitionistic fuzzy mathematical method, *Journal of Computational Science* 71, 102075.
- Mollalign D., Mushi A., Guta B. 2022. Solving Multi-Objective Multilevel Programming problems using two-phase Intuitionistic Fuzzy Goal Programming method, *Journal of Computational Science* 63, 101786.
- Razmi J., Jafarian E., Amin S.H. 2016. An intuitionistic fuzzy goal programming approach for finding pareto-optimal solutions to multi-objective programming problems, *Expert Systems With Applications* 65, 181-193.
- Rukmani S., Porchelvi R.S. 1018. Goal Programming Approach in Multi-objective Intuitionistic Fuzzy Linear Fractional Programming Problem, *International Journal of Pure and Applied Mathematics*, 118 ( 6), 541-549.
- Rukmani S., Porchelvi R.S., 2018. Goal Programming Approach to Solve Multi-Objective Intuitionistic Fuzzy Non- Linear Programming Models, *International Journal of Mathematics Trends and Technology (IJMTT)*, 53 (7), 1-11.
- Sharma D.K., Jana R. K., Gaur A. 2007. Fuzzy Goal Programming for Agricultural Land Allocation Problems in Yugoslavia, *Journal of Operations Research* 17 (1), 31-42.
- Sharma K., Singh V.P., Ebrahimnejad A., Chakraborty D. 2023. Solving a multi-objective chance constrained hierarchical optimization problem under intuitionistic fuzzy environment with its application, *Expert Systems with Applications* ,217,119595.
- Singh S.K., Yadav S.P. 2015. Modeling and optimization of multi objective non-linear programming problem in intuitionistic fuzzy environment. *Applied Mathematical Modelling* 39, 4617-4629.
- Stanojević M., Stanojević B. 2009. Penalty Method for Fuzzy linear Programming with Trapezoidal Numbers, *Yugoslav Journal of Operations Research*, 19 (1), 149-156.
- Tadesse A., Acharya S., Belay B. 2023. Fuzzy Programming Approach to Solve Multi-Objective Fully Fuzzy Transportation Problem, *East Afr. J. Biophys. Comput. Sci.*, Vol. 4, Issue. 2, 43-53.
- Tsegaye H., Thillaigovindan N., Alemayehu G. 2021. An Efficient Method for Solving Intuitionistic Fuzzy Multi-objective Optimization Problems, *Punjab University Journal of Mathematics*,53(9), 631-664.
- Werners B.M. 1998. Aggregation Models in Mathematical Programming: Mathematical Models for decision Supports, *Springer Berlin Heldelberg*, 295-305.
- Wu Y.K., Guu S.M. 2001. A compromise model for solving fuzzy multi objective linear programming problems, *Journal of the Chinese Institute of Industrial Engineers*, Vol. 18, No. 5, pp. 87-93.
- Yager R.R. 2009. Intuitionistic fuzzy sets, Fuzzy optimization and Decision making, 8 (1), 67-90.
- Zimmermann H.J. 2001. Fuzzy Set Theory and Its Applications, *Springer Science and Business Media*, New York.

## A Mathematical Model for the Transmission Dynamics of COVID-19 Pandemic Considering Protected and Hospitalized with Optimal Control

Tinaw Tilahun Asmamaw<sup>1</sup>, Kiros Gebrearegawi Kebedow<sup>2,\*</sup>

<sup>1</sup>Department of Mathematics, Mezan Tepi University, Ethiopia

<sup>2</sup>Department of Mathematics, Hawassa University, Ethiopia

### KEYWORDS

COVID-19;  
Protection;  
Stability analysis;  
Forward  
bifurcation;  
Sensitivity  
analysis;  
Optimal control

### ABSTRACT

In this paper, we propose a mathematical model to investigate coronavirus diseases (COVID-19) transmission in the presence of protected and hospitalized classes. We establish that the solution of the dynamical system remains positive and bounded. We compute the disease free equilibrium point and analyze the stability behavior of the steady state solutions. We determine the basic reproduction number ( $R_0$ ) and demonstrate that the disease fades away when  $R_0 < 1$  but persists in the population when  $R_0 > 1$ . The center manifold theory is used to assess the local stability of the endemic equilibrium. The model demonstrates a forward bifurcation, and a sensitivity analysis is conducted. The sensitivity analysis reveals that  $R_0$  is highly influenced by the protection rate, highlighting the necessity of maintaining a high level of protection along with hospitalization to effectively control the disease. We develop optimal strategies for protection and hospitalization. The characterization of the optimal control is derived using Pontryagin's Maximum Principle. Numerical results for the dynamics of the COVID-19 outbreak and its optimal control show that a combination of protection and hospitalization is the most effective strategy for reducing the spread of COVID-19 within the population..

### Research article

### 1. INTRODUCTION

Coronavirus disease 2019 (COVID-19) is an infectious disease caused by a newly discovered coronavirus [Gurmu et al. \(2020\)](#). The new virus was first appeared late December 2019 in the Chinese city of Wuhan and eventually invaded the world due to fast modern air trans-

portation [Lemecha Obsu and Feyissa Balcha \(2020\)](#). The novel coronavirus- now referred to as COVID-19 is caused by severe acute respiratory syndrome (SARS-CoV-2) and consists of single-stranded ribonucleic acid (RNA) structure [Sohrabi et al. \(2020\)](#).

The novel coronavirus is mainly spread

Corresponding author

Email address: [kirosg@hu.edu.et](mailto:kirosg@hu.edu.et) +251926528484

<https://dx.doi.org/10.4314/eajbcs.v5i2.55>



from person to person, through respiratory droplets, the spread is more likely when people are within 6 feet of each other [Toquero \(2020\)](#). There is no known curing medicine to combat the COVID-19 pandemic. Standard recommendations by the WHO to prevent the spread of COVID-19 include frequent cleaning of hands using soap or alcohol-based sanitizer, covering the nose and mouth with a flexed elbow or disposable tissue when coughing and sneezing and avoiding close contact with anyone that has a fever and cough [Toquero \(2020\)](#).

Mathematical modeling in epidemiology helps to understand the fundamental mechanisms that drive the spread of disease, while also offering insights into potential control strategies. The model formulation process clarifies the assumptions, variables, and parameters involved. Furthermore, models offer conceptual insights such as thresholds, basic reproduction numbers, contact numbers, and replacement numbers. Mathematical models and computer simulations are useful experimental tools for building and testing theories, assessing quantitative conjectures, answering specific questions, determining sensitivities to changes in parameter values, and estimating parameters from data [Brauer et al. \(2019\)](#).

The first mathematical model was developed by Daniel Bernoulli [Allen et al. \(2008\)](#) on pandemic of smallpox by introducing two systems of ordinary differential equations. He assumed that recovery from infection confers immunity (no re-infection). He also assumed that the probability that infected individuals for the first time die does not depend on those who survive from the infection. He showed that inoculation was advantageous if the associated risk of dying was less than 11%.

A number of compartmental models have been proposed and analyzed for the COVID-19 outbreak in different countries. In particular, Yang and Wang [Yang and Wang \(2020\)](#) proposed a mathematical model for COVID-19 incorporating multiple transmission pathways, including both human-to-

human and environment-to-human transmission routes. Global stability was analysed using Lyapunov function. The authors employed a bilinear incidence rate based on the law of mass action and fitted the model with the data of Wuhan city of China and estimated the reproduction number.

In 2020, Haileyesus and Getachew [Alemneh and Telahun \(2020\)](#) proposed a conceptual SEIR model to study the pandemic COVID-19 transmission in Ethiopia. Global stability was analysed using Lyapunov function. Additionally, they incorporated time-dependent controls into the basic model and extended it to an optimal control framework for the disease. An optimal control problem was formulated and analyzed using Pontryagin's Maximum Principle. However, none of the authors cited here are considering protected and hospital-ized classes with optimal controls. Thus we are improved the existed model, by including the protected and hospitalized classes with optimal controls.

The remainder of the paper is organized as follows. In Section 2 we provided the description of the problems and its mathematical model formulation. Section 3 gives details the qualitative analysis of the model. The numerical analysis of our model is presented in Section 4, furthermore we present the extensions of the model to optimal controls and its numerical simulations 5 and 6. Finally, Section 7 concludes the paper.

## 2. MATHEMATICAL MODEL FORMULATION

### 2.1. The modified mathematical model

In this subsection, we modify the existing SEIR model to study the transmission dynamics of COVID-19 infection in a population. The model is a modification of what is presented in [Alemneh and Telahun \(2020\)](#). In the present model we extended SEIR model by including protected and hospitalized classes

## 2.2. Model formulation

We formulate a mathematical model to investigate coronavirus diseases (COVID-19) transmission in the presence of protected and hospitalized classes. The model divides the total population into six sub-classes according to their disease status. Susceptible (S), protected (P), exposed (E), infected (I), hospitalized (H) and recovered (R).

The following assumptions have been used in the formulation of the model:

1. The population under study is heterogeneous and varying with time.
2. All recruited human population is susceptible.
3. Susceptible individuals who keeping social distancing, using an alcohol-based hand sanitizer and wearing face masks progress into protected class.
4. Protected individuals cannot acquire infection of COVID-19 disease due to proper use of an alcohol-based hand sanitizer, wearing face masks and keeping social distancing.
5. The latently infected individuals (exposed) could infect other people with a

higher probability than people in the infected class. Since exposed individuals show no symptoms and can easily spread the infection to other people with close contact, often in an unconscious manner.

6. Transmission through human-to-human route is alone considered. Other means of transmission are ignored.
7. We assume that individuals have no permanent immunity after recovery from the disease, that is the recovered individuals have a chance to be susceptible again.
8. The natural mortality rates are assumed to be the same for all the compartments.
9. All parameters in the model being non-negative.

We consider the force of infection  $\lambda$  which is given by

$$\lambda = \beta(\sigma_1 I + \sigma_2 E + \sigma_3 H), \quad (1)$$

where  $\beta$  is the effective contact rate, while  $\sigma_1$ ,  $\sigma_2$  and  $\sigma_3$  are the relative infectiousness parameters associated with the infected, exposed and hospitalized classes respectively.

Table 1: The state variables and their descriptions.

Variables	Description of the state variables
S	Susceptible individuals
P	Protected individuals, who keeping social distancing, using an alcohol-based hand sanitizer and wearing face masks properly to protect themselves from the virus
E	Latently infected individuals, who have no symptoms of COVID-19 virus disease but are capable of infecting others
I	Infected individuals, who have active COVID-19 virus disease and can infect other people
H	Hospitalized individuals, who are admitted to health care facility or isolated in their home due to virus infection active cases
R	Recovered individuals

The flow chart of the modified model is illustrated in Figure (1).

Table 2: Parameters of the modified model and their descriptions.

Parameter	Description of the parameter
$\Pi$	Recruitment rate of susceptible
$\theta$	Protection rate of susceptible individuals
$\nu$	Waning rate of protected individuals to susceptible class
$\beta$	Effective contact rate
$\sigma_1$	Modification parameter for relative infectiousness of infected individuals
$\sigma_2$	Modification parameter for relative infectiousness of exposed individuals
$\sigma_3$	Modification parameter for relative infectiousness of hospitalized individuals
$\delta$	The exposed progression rate
$\tau$	Proportion of exposed individuals who join infected class
$1 - \tau$	The progression from exposed individuals to recovered class
$\alpha$	Hospitalization rate of infected individuals
$\mu$	Natural death rate
$\rho$	Disease-induced death rate of infected individuals
$\xi$	Disease-induced death rate of hospitalized individuals
$\varepsilon$	Rate of recovery of the individuals from infected class
$\gamma$	Recovery rate of hospitalized patients
$\omega$	Waning immunity rate
$\eta$	The proportion of recovered individuals that become susceptible
$1 - \eta$	The progression from recovered individuals to protected class

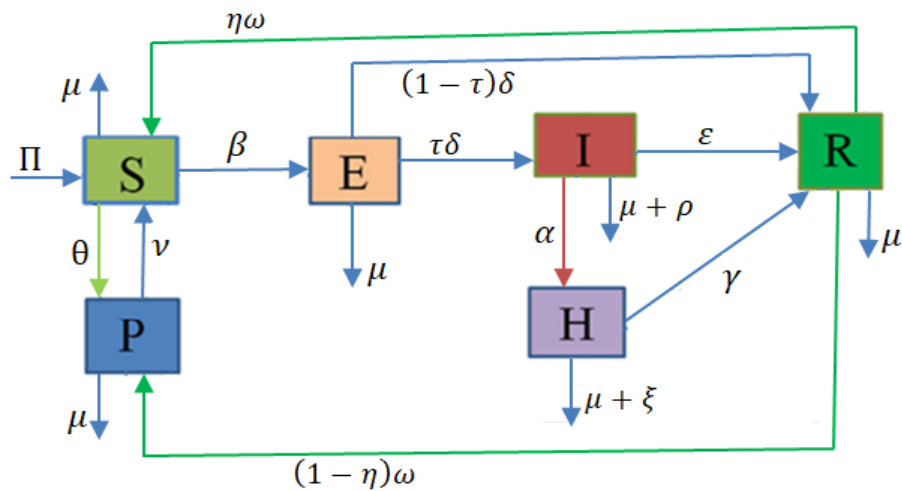


Figure 1: The flow chart for the modified model of COVID-19 pandemic.

Based on our assumptions and the flow chart (1), the modified model for the transmission dynamics of COVID-19 is given by the following deterministic system of non-linear differential equations:

$$\frac{dS}{dt} = \Pi + \eta\omega R + \nu P - \beta(\sigma_1 I + \sigma_2 E + \sigma_3 H)S - (\theta + \mu)S, \quad (2a)$$

$$\frac{dP}{dt} = \theta S + (1 - \eta)\omega R - (\nu + \mu)P, \quad (2b)$$

$$\frac{dE}{dt} = \beta(\sigma_1 I + \sigma_2 E + \sigma_3 H)S - (\delta + \mu)E, \quad (2c)$$

$$\frac{dI}{dt} = \tau\delta E - (\alpha + \varepsilon + \mu + \rho)I, \quad (2d)$$

$$\frac{dH}{dt} = \alpha I - (\gamma + \mu + \xi)H, \quad (2e)$$

$$\frac{dR}{dt} = (1 - \tau)\delta E + \varepsilon I + \gamma H - (\omega + \mu)R, \quad (2f)$$

with non-negative initial conditions  $S(0) = S_0 > 0$ ,  $P(0) = P_0 \geq 0$ ,  $E(0) = E_0 \geq 0$ ,  $I(0) = I_0 \geq 0$ ,  $H(0) = H_0 \geq 0$  and  $R(0) = R_0 \geq 0$ .

### 3. QUALITATIVE ANALYSIS OF THE MODIFIED MODEL

In this section, we present some basic qualitative properties of the modified model. These analysis include finding the set inside which the model can be sufficiently studied (i.e., the invariant region); local and global stability of equilibrium points of the model (2).

#### 3.1. Well-posedness

Since all the functions on the right hand side of the system (2) are continuously differentiable. Thus, the existence and uniqueness of the solutions is established by the Picard's theorem Valcher (2002). Now, we show the positivity and boundedness of solutions.

##### Theorem 3.1. (Positivity)

If  $S(0) > 0$ ,  $P(0) \geq 0$ ,  $E(0) \geq 0$ ,  $I(0) \geq 0$ ,  $H(0) \geq 0$  and  $R(0) \geq 0$ , then the solution  $(S(t), P(t), E(t), I(t), H(t), R(t))$  of the dynamical system (2) is non-negative for all time  $t \geq 0$ .

*Proof.* To show the positivity of the solution of the dynamical system (2), we will perform the proof by using contradiction. We assume that

$S(t) \leq 0$  for some  $t \geq 0$ , that is there exists small  $t_0 > 0$  such that  $S(t_0) = 0$ ,  $S'(t_0) \leq 0$  and  $S(t) > 0$  for  $t \in [0, t_0)$ . Then  $P(t) \geq 0$ ,  $E(t) \geq 0$  and  $I(t) \geq 0$  for  $t \in [0, t_0]$ . If this be not the case, there exists

**Option-I:**  $t_1 \in [0, t_0]$  such that  $P(t_1) = 0$ ,  $P'(t_1) < 0$  and  $P(t) > 0$  for  $t \in [0, t_1)$ . Then  $E(t) \geq 0$  and  $I(t) \geq 0$  for  $t \in [0, t_1]$ .

**Option-II:**  $t_2 \in [0, t_1]$  such that  $E(t_2) = 0$ ,  $E'(t_2) < 0$  and  $E(t) > 0$  for  $t \in [0, t_2)$ . Then  $P(t) \geq 0$  and  $I(t) \geq 0$  for  $t \in [0, t_2]$ .

**Option-III:**  $t_3 \in [0, t_2]$  such that  $I(t_3) = 0$ ,  $I'(t_3) < 0$  and  $I(t) > 0$  for  $t \in [0, t_3)$ . Then  $P(t) \geq 0$  and  $E(t) \geq 0$  for  $t \in [0, t_3]$ .

It follows from equation (2d) that we have

$$I'(t_3) = \tau\delta E(t_3) - (\alpha + \varepsilon + \mu + \rho)I(t_3).$$

This implies that  $I'(t_3) = \tau\delta E(t_3) \geq 0$ . This is a contradiction. Integration of equation (2e) leads to

$$H(t) = e^{-(\gamma+\mu+\xi)t} \left( H(0) + \alpha \int_0^t I(s)e^{(\gamma+\mu+\xi)s} ds \right) \geq 0, \quad \text{for } t \in [0, t_2].$$

Then  $E'(t_2) = \beta(\sigma_1 I(t_2) + \sigma_3 H(t_2))S(t_2) \geq 0$ . This is a contradiction. Hence  $H(t) \geq 0$  for every  $t \in [0, t_1]$ . Integration of equation (2f) leads to

$$R(t) = e^{-(\omega+\mu)t} \left( R(0) + \int_0^t ((1-\tau)\delta E(s) + \varepsilon I(s) + \gamma H(s)) e^{(\omega+\mu)s} ds \right) \geq 0, \\ \text{for } t \in [0, t_1].$$

Then  $P'(t_1) = \theta S(t_1) + (1-\eta)\omega R(t_1) \geq 0$ . This is a contradiction. Hence  $R(t) \geq 0$  for every  $t \in [0, t_0]$ . Thus  $S'(t_0) = \Pi + \eta\omega R(t_0) + \nu P(t_0) > 0$ , but this leads to a contradiction to the assumption that  $S'(t_0) \leq 0$ . Therefore, the solutions  $S(t), P(t), E(t), I(t), H(t), R(t)$  in the system (2) remain positive for all  $t > 0$ . This completes the proof.  $\square$

### Theorem 3.2. (Boundedness)

There exists a positively invariant region  $\Omega$  in which the solution  $(S(t), P(t), E(t), I(t), H(t), R(t))$  of the dynamical system (2) is bounded.

*Proof.* The positivity has already been established by Theorem (3.1). For this model the total population is  $N(t) = S(t) + P(t) + E(t) + I(t) + H(t) + R(t)$ . Then, we obtain:

$$\frac{dN}{dt} = \Pi - \mu N - (\rho I + \xi H).$$

This implies that

$$\frac{dN}{dt} \leq \Pi - \mu N,$$

Since the solution  $I(t)$  and  $H(t)$  are positive. Solving the differential inequality we get the relation,

$$N(t) \leq \frac{\Pi}{\mu} + \left( N(0) - \frac{\Pi}{\mu} \right) e^{-\mu t},$$

$$e_0 = (S^0, P^0, E^0, I^0, H^0, R^0) = \left( \frac{\Pi(\nu + \mu)}{\mu(\theta + \nu + \mu)}, \frac{\Pi\theta}{\mu(\theta + \nu + \mu)}, 0, 0, 0, 0 \right).$$

The existence of the endemic equilibrium point depends on the basic reproduction number  $R_0$  and will be presented later.

If  $N(0) \leq \frac{\Pi}{\mu}$ , then we obtain  $0 \leq N(t) \leq \frac{\Pi}{\mu}$ , for all  $t \geq 0$ . If  $N(0) \geq \frac{\Pi}{\mu}$ , then we have  $0 \leq N(t) \leq N(0)$ , for all  $t \geq 0$ . Thus, the feasible solution set of the system (2) remain in the region

$$\Omega = \left\{ (S, P, E, I, H, R) \in \mathbb{R}_+^6 : 0 \leq N(t) \leq \max \left( N(0), \frac{\Pi}{\mu} \right) \right\}.$$

If we start with initial data  $N(0) \in \Omega$ , then the solution  $N(t) \in \Omega$ , for every  $t > 0$ . This shows the positively invariance of  $\Omega$ . Thus, the solution of the dynamical system (2) is bounded.  $\square$

### 3.2. Steady state

The steady states of the system (2) are solutions of the following equations:

$$\begin{aligned} 0 &= \Pi + \eta\omega R + \nu P - \beta(\sigma_1 I + \sigma_2 E + \sigma_3 H)S - (\theta + \mu)S \\ 0 &= \theta S + (1-\eta)\omega R - (\nu + \mu)P \\ 0 &= \beta(\sigma_1 I + \sigma_2 E + \sigma_3 H)S - (\delta + \mu)E \\ 0 &= \tau\delta E - (\alpha + \varepsilon + \mu + \rho)I \\ 0 &= \alpha I - (\gamma + \mu + \xi)H \\ 0 &= (1-\tau)\delta E + \varepsilon I + \gamma H - (\omega + \mu)R. \end{aligned}$$

There are at most two steady states for the system (2): the disease free equilibrium  $e_0$  and endemic equilibrium  $e_1$ . The disease-free equilibrium point of our model is obtained by setting the disease state variables  $E = 0$ ,  $I = 0$  and  $H = 0$ . Thus, the disease free equilibrium point is given by

### 3.3. Basic reproduction number

The basic reproduction number, which is denoted by  $R_0$ , and defined as the average number of secondary infections produced by a single infected individual in a completely sus-

ceptible population. Using the next generation matrix method [Diekmann et al. \(2010\)](#), the basic reproduction number  $R_0$  can be calculated from the relation  $R_0 = \rho(FV^{-1})$ . Let

$$\mathcal{F}(x) = \begin{bmatrix} \beta(\sigma_1 I + \sigma_2 E + \sigma_3 H)S \\ 0 \\ 0 \end{bmatrix} \quad \text{and} \quad \mathcal{V}(x) = \begin{bmatrix} (\delta + \mu)E \\ (\alpha + \varepsilon + \mu + \rho)I - \tau\delta E \\ (\gamma + \mu + \xi)H - \alpha I \end{bmatrix}.$$

The Jacobian matrix to  $\mathcal{F}$  and  $\mathcal{V}$  are

$$F = \left[ \frac{\partial \mathcal{F}_i(e_0)}{\partial x_j} \right] = \begin{bmatrix} \beta\sigma_2 S^0 & \beta\sigma_1 S^0 & \beta\sigma_3 S^0 \\ 0 & 0 & 0 \\ 0 & 0 & 0 \end{bmatrix},$$

$$V = \left[ \frac{\partial \mathcal{V}_i(e_0)}{\partial x_j} \right] = \begin{bmatrix} \delta + \mu & 0 & 0 \\ -\tau\delta & k_1 & 0 \\ 0 & -\alpha & k_2 \end{bmatrix},$$

where  $k_1 = \alpha + \varepsilon + \mu + \rho$  and  $k_2 = \gamma + \mu + \xi$ . The next-generation matrix  $FV^{-1}$  is given by

$$FV^{-1} = \begin{bmatrix} R_1 + R_2 + R_3 & \frac{\beta S^0(\sigma_1 k_2 + \sigma_3 \alpha)}{k_1 k_2} & \frac{\beta \sigma_3 S^0}{k_2} \\ 0 & 0 & 0 \\ 0 & 0 & 0 \end{bmatrix},$$

where

$$R_1 = \frac{\beta\sigma_2 S^0}{\delta + \mu}, \quad R_2 = \frac{\beta\sigma_1 S^0 \tau \delta}{k_1(\delta + \mu)} \quad \text{and} \quad R_3 = \frac{\beta\sigma_3 S^0 \tau \delta \alpha}{k_1 k_2(\delta + \mu)}. \quad (3)$$

$\mathcal{F}$  be the vector for the newly infected and  $\mathcal{V}$  be the vector for the transfer of individuals into and out of the infected compartments. Let  $x = (E, I, H)$ , then we obtain:

We find the eigenvalues of  $FV^{-1}$  by solving the characteristic equation  $|FV^{-1} - \lambda I| = 0$  as  $\lambda_1 = R_1 + R_2 + R_3$ ,  $\lambda_2 = 0$  and  $\lambda_3 = 0$ . The basic reproduction number  $R_0$  is the spectral radius (the largest eigenvalues in modulus) of  $FV^{-1}$  which is given by

$$R_0 = \rho(FV^{-1}) = R_1 + R_2 + R_3.$$

The parts  $R_1$ ,  $R_2$  and  $R_3$  represent the contributions from the human-to-human transmission routes (exposed-to-susceptible, infected-to-susceptible and hospitalized-to-susceptible individuals, respectively). We can rewrite the basic reproduction number as follows:

$$R_0 = \frac{\Pi\beta(\nu + \mu)}{\mu(\theta + \nu + \mu)(\delta + \mu)} \left( \sigma_2 + \frac{\sigma_1 \tau \delta}{\alpha + \varepsilon + \mu + \rho} + \frac{\sigma_3 \tau \delta \alpha}{(\alpha + \varepsilon + \mu + \rho)(\gamma + \mu + \xi)} \right). \quad (4)$$

### 3.4. Local stability of disease free equilibrium

**Theorem 3.3.** The disease free equilibrium point  $e_0$  of the system (2) is locally asymptotically stable if  $R_0 < 1$  and unstable if  $R_0 > 1$ .

*Proof.* The Jacobian matrix of the system (2) at the disease-free equilibrium  $e_0$  is given by

$$J(e_0) = \left[ \begin{array}{cc|cccc} -(\theta + \mu) & \nu & -\beta\sigma_2 S^0 & -\beta\sigma_1 S^0 & -\beta\sigma_3 S^0 & \eta\omega \\ \theta & -(\nu + \mu) & 0 & 0 & 0 & (1 - \eta)\omega \\ \hline 0 & 0 & \beta\sigma_2 S^0 - (\delta + \mu) & \beta\sigma_1 S^0 & \beta\sigma_3 S^0 & 0 \\ 0 & 0 & \tau\delta & -k_1 & 0 & 0 \\ 0 & 0 & 0 & \alpha & -k_2 & 0 \\ 0 & 0 & (1 - \tau)\delta & \varepsilon & \gamma & -(\omega + \mu) \end{array} \right].$$

The matrix  $J(e_0)$  is an upper triangular block matrix. Its eigenvalues are  $\lambda_1, \lambda_2, \lambda_3, \lambda_4, \lambda_5$  and  $\lambda_6$ . Where  $\lambda_1, \lambda_2$  are eigenvalues of the first block matrix of  $J(e_0)$

and  $\lambda_3, \lambda_4, \lambda_5, \lambda_6$  are eigenvalues of the fourth block matrix of  $J(e_0)$ . The first block matrix of  $J(e_0)$  given by

$$J_1(e_0) = \begin{bmatrix} -(\theta + \mu) & \nu \\ \theta & -(\nu + \mu) \end{bmatrix}.$$

We find the eigenvalues of  $J_1(e_0)$  by solving the characteristic equation  $|J_1(e_0) - \lambda I| = 0$  as

$$\lambda_1 = -\mu \text{ and } \lambda_2 = -(\theta + \nu + \mu).$$

The fourth block matrix of  $J(e_0)$  is given by

$$J_4(e_0) = \begin{bmatrix} \beta\sigma_2 S^0 - (\delta + \mu) & \beta\sigma_1 S^0 & \beta\sigma_3 S^0 & 0 \\ \tau\delta & -k_1 & 0 & 0 \\ 0 & \alpha & -k_2 & 0 \\ (1 - \tau)\delta & \varepsilon & \gamma & -(\omega + \mu) \end{bmatrix}.$$

Thus the eigenvalues  $\lambda_3, \lambda_4, \lambda_5, \lambda_6$  are obtained from the characteristic equation of  $J_4(e_0)$ :

$$\begin{aligned} &(-(\omega + \mu) - \lambda)[\lambda^3 + ((\delta + \mu)(1 - R_1) + k_1 + k_2)\lambda^2 + [k_1(\delta + \mu)(1 - (R_1 + R_2)) \\ &+ k_2(\delta + \mu)(1 - R_1) + k_1 k_2]\lambda + k_1 k_2(\delta + \mu)(1 - R_0)] = 0. \end{aligned}$$

From this equation, we obtain the values for  $\lambda$  to be  $\lambda_3 = -(\omega + \mu)$  and the eigenvalues  $\lambda_4, \lambda_5, \lambda_6$  are the roots of the cubic polynomial:

$$p(\lambda) = a_0 \lambda^3 + a_1 \lambda^2 + a_2 \lambda + a_3 = 0,$$

where

$$\begin{aligned} a_0 &= 1, \\ a_1 &= (\delta + \mu)(1 - R_1) + k_1 + k_2, \\ a_2 &= k_1(\delta + \mu)(1 - (R_1 + R_2)) + k_2(\delta + \mu)(1 - R_1) + k_1 k_2, \\ a_3 &= k_1 k_2(\delta + \mu)(1 - R_0). \end{aligned}$$

Furthermore,

$$\begin{aligned} a_1 a_2 - a_3 &= k_1(\delta + \mu)^2(1 - R_1)(1 - (R_1 + R_2)) + k_2(\delta + \mu)^2(1 - R_1)^2 + k_1 k_2(\delta + \mu)(1 - R_1) \\ &+ k_1^2(\delta + \mu)(1 - R_0) + k_1(k_1 + k_2)[k_1(\delta + \mu)R_3 + k_2(\delta + \mu)(1 - R_1) + k_1 k_2]. \end{aligned}$$

If  $R_0 < 1$ , then  $R_1, R_2, R_3$  and  $R_1 + R_2$  are strictly less than one. Since  $R_0 = R_1 + R_2 + R_3$ . The coefficients  $a_1, a_2$  and  $a_3$  are positive and  $a_1 a_2 > a_3$  if  $R_0 < 1$ . Thus, all the eigenvalues of  $J(e_0)$  are negative. It follows by

Routh-Hurwitz criteria that the disease free equilibrium  $e_0$  is locally asymptotically stable for  $R_0 < 1$ . If  $R_0 > 1$ , then  $a_3$  is negative and the Routh-Hurwitz criterion tells that the disease free equilibrium  $e_0$  is unstable.

□

### 3.5. Global stability of disease free equilibrium

**Theorem 3.4.** For  $R_0 < 1$ , the disease free equilibrium  $e_0$  of the system (2) is globally asymptotically stable if  $S^0 \geq S$ .

*Proof.* Let us rewrite our model system (2) as

$$\begin{aligned}\frac{dZ_1}{dt} &= F(Z_1, Z_2), \\ \frac{dZ_2}{dt} &= G(Z_1, Z_2), \quad G(Z_1, 0) = 0.\end{aligned}$$

Where  $Z_1 = (S, P, R) \in \mathbb{R}_+^3$  represents the class of uninfected individuals and  $Z_2 = (E, I, H) \in \mathbb{R}_+^3$  represents the class of infected individuals. The disease free equilibrium point of the model is denoted by  $U_0 = (Z_1^*, 0)$ , where

$Z_1^* = \left( \frac{\Pi(\nu+\mu)}{\mu(\theta+\nu+\mu)}, \frac{\Pi\theta}{\mu(\theta+\nu+\mu)}, 0 \right)$ . Since the disease free equilibrium point is locally asymptotically stable (see theorem (3.3)), to prove global stability, we will apply the Castillo-Chavez theorem Castillo-Chavez et al. (2002). From system (2), we have

$$\begin{aligned}\frac{dZ_1}{dt} = F(Z_1, Z_2) &= \begin{bmatrix} \Pi + \eta\omega R + \nu P - \beta(\sigma_1 I + \sigma_2 E + \sigma_3 H)S - (\theta + \mu)S \\ \theta S + (1 - \eta)\omega R - (\nu + \mu)P \\ (1 - \tau)\delta E + \varepsilon I + \gamma H - (\omega + \mu)R \end{bmatrix}, \\ \frac{dZ_2}{dt} = G(Z_1, Z_2) &= \begin{bmatrix} \beta(\sigma_1 I + \sigma_2 E + \sigma_3 H)S - (\delta + \mu)E \\ \tau\delta E - (\alpha + \varepsilon + \mu + \rho)I \\ \alpha I - (\gamma + \mu + \xi)H \end{bmatrix}.\end{aligned}$$

- I. To show  $Z_1^*$  is globally asymptotically stable for the system  $\frac{dZ_1}{dt} = F(Z_1, 0)$ , let us consider the reduced system

$$\frac{dZ_1}{dt} = F(Z_1, 0) = \begin{bmatrix} \Pi + \eta\omega R + \nu P - (\theta + \mu)S \\ \theta S + (1 - \eta)\omega R - (\nu + \mu)P \\ -(\omega + \mu)R \end{bmatrix}. \quad (5)$$

We can rewrite the system (5) as:

$$\frac{dS}{dt} = -(\theta + \mu)S + \nu P + \eta\omega R + \Pi, \quad (61)$$

$$\frac{dP}{dt} = \theta S - (\nu + \mu)P + (1 - \eta)\omega R, \quad (62)$$

$$\frac{dR}{dt} = -(\omega + \mu)R, \quad (63)$$



and admits as solutions

$$\begin{aligned}
 S(t) &= \frac{\Pi(\nu + \mu)}{\mu(\theta + \nu + \mu)} + \frac{1}{\theta + \nu} \left[ \left( \nu(S(0) + P(0) + R(0)) - \frac{\Pi\nu}{\mu} \right) e^{-\mu t} \right. \\
 &\quad \left. + \left( \theta S(0) - \nu P(0) + \frac{\omega(\nu - \eta(\theta + \nu))}{\theta + \nu - \omega} R(0) - \frac{\Pi\theta}{\theta + \nu + \mu} \right) e^{-(\theta + \nu + \mu)t} \right] \\
 &\quad - \frac{(\nu - \eta\omega)}{\theta + \nu - \omega} R(0) e^{-(\omega + \mu)t}, \\
 P(t) &= \frac{\Pi\theta}{\mu(\theta + \nu + \mu)} + \frac{1}{\theta + \nu} \left[ \left( \theta(S(0) + P(0) + R(0)) - \frac{\Pi\theta}{\mu} \right) e^{-\mu t} \right. \\
 &\quad \left. - \left( \theta S(0) - \nu P(0) + \frac{\omega(\nu - \eta(\theta + \nu))}{\theta + \nu - \omega} R(0) - \frac{\Pi\theta}{\theta + \nu + \mu} \right) e^{-(\theta + \nu + \mu)t} \right] \\
 &\quad - \frac{(\theta - (1 - \eta)\omega)}{\theta + \nu - \omega} R(0) e^{-(\omega + \mu)t}, \\
 R(t) &= R(0) e^{-(\omega + \mu)t}.
 \end{aligned}$$

Taking the limit as  $t$  goes to  $\infty$ , we obtain

$$(S(t), P(t), R(t)) \rightarrow \left( \frac{\Pi(\nu + \mu)}{\mu(\theta + \nu + \mu)}, \frac{\Pi\theta}{\mu(\theta + \nu + \mu)}, 0 \right) = Z_1^*.$$

Therefore,  $Z_1^*$  is globally asymptotically stable for the system  $\frac{dZ_1}{dt} = F(Z_1, 0)$ .

II. We will show that  $G(Z_1, Z_2) = AZ_2 - \hat{G}(Z_1, Z_2)$ ,  $\hat{G}(Z_1, Z_2) \geq 0$  for  $(Z_1, Z_2) \in \Omega$  where  $A = \frac{\partial G}{\partial Z_2}(Z_1^*, 0)$  is a Metzler matrix (the off diagonal elements of  $A$  are non-negative) and  $\Omega$  is the region where the model makes biological sense. Consider a matrix

$$A = \frac{\partial G}{\partial Z_2}(Z_1^*, 0) = \begin{bmatrix} \beta\sigma_2 S^0 - (\delta + \mu) & \beta\sigma_1 S^0 & \beta\sigma_3 S^0 \\ \tau\delta & -(\alpha + \varepsilon + \mu + \rho) & 0 \\ 0 & \alpha & -(\gamma + \mu + \xi) \end{bmatrix}.$$

Hence,  $A$  is a Metzler matrix (off diagonal elements are non-negative). Here,

$$\hat{G}(Z_1, Z_2) = AZ_2 - G(Z_1, Z_2).$$

After some simplification, we obtain

$$\begin{aligned}
 \hat{G}(Z_1, Z_2) &= \begin{bmatrix} \beta\sigma_2 E(S^0 - S) + \beta\sigma_1 I(S^0 - S) + \beta\sigma_3 H(S^0 - S) \\ 0 \\ 0 \end{bmatrix}, \\
 \hat{G}(Z_1, Z_2) &= (S^0 - S) \begin{pmatrix} \beta(\sigma_2 E + \sigma_1 I + \sigma_3 H) \\ 0 \\ 0 \end{pmatrix} \geq 0.
 \end{aligned}$$

Therefore by Castillo-Chavez theorem [Castillo-Chavez et al. \(2002\)](#), the disease free equilibrium point  $e_0$  of the system (2) is globally asymptotically stable for  $R_0 < 1$ .  $\square$

### 3.6. Endemic equilibrium point

Endemic equilibrium point is a steady state solution where the disease persists in the population. In the presence of disease in the population, there exist an equilibrium point

called endemic equilibrium point denoted by  $e_1 = (S^*, P^*, E^*, I^*, H^*, R^*)$ . It can be obtained by setting each equation of the system (2) equal to zero. Then we obtained

$$\begin{aligned} S^* &= \frac{S^0}{R_0}, \\ P^* &= \frac{\theta S^0 K + (1 - \eta)\omega\mu\delta(\theta + \nu + \mu)[(1 - \tau)k_1k_2 + \varepsilon\tau k_2 + \gamma\alpha\tau]S^0(R_0 - 1)}{(\nu + \mu)KR_0}, \\ E^* &= \frac{k_1k_2\mu(\omega + \mu)(\theta + \nu + \mu)S^0(R_0 - 1)}{KR_0}, \\ I^* &= \frac{k_2\delta\mu\tau(\omega + \mu)(\theta + \nu + \mu)S^0(R_0 - 1)}{KR_0}, \\ H^* &= \frac{\alpha\delta\mu\tau(\omega + \mu)(\theta + \nu + \mu)S^0(R_0 - 1)}{KR_0}, \\ R^* &= \frac{\delta\mu(\theta + \nu + \mu)[(1 - \tau)k_1k_2 + \varepsilon\tau k_2 + \gamma\alpha\tau]S^0(R_0 - 1)}{KR_0}, \end{aligned}$$

where

$$K = k_1k_2[\mu(\nu + \mu)(\omega + \delta + \mu) + \delta\mu(1 - \eta)\omega] + \omega\delta\tau(\eta\mu + \nu)[\alpha(\mu + \xi) + k_2(\mu + \rho)],$$

provided that  $R_0 > 1$ . From this we see that for the endemic equilibrium to exist  $R_0 > 1$ .

Moreover, the force of infection can be updated as

$$\lambda^* = \beta(\sigma_1 I^* + \sigma_2 E^* + \sigma_3 H^*). \quad (7)$$

When we substitute the expression for  $E^*, I^*$  and  $H^*$  into the force of infection  $\lambda^*$ , we obtain

$$\lambda^* = \frac{\mu k_1 k_2 (\delta + \mu)(\omega + \mu)(\theta + \nu + \mu)(R_0 - 1)}{K}, \quad (8)$$

provided that  $R_0 > 1$ . From this, we see that, there is no endemic equilibrium of the system (2) if  $R_0 < 1$ . Therefore, this condition shows that it is not possible for backward bifurcation in this model. Hence we have established the following result.

### 3.7. Local stability of endemic equilibrium

**Theorem 3.6.** The endemic equilibrium  $e_1$  of the system (2) is locally asymptotically stable

**Theorem 3.5.** A unique endemic equilibrium point  $e_1 = (S^*, P^*, E^*, I^*, H^*, R^*)$  exists and is positive if  $R_0 > 1$ .

When we plot the force of infection  $\lambda^*$  over  $R_0$  by using the expression for  $\lambda^*$  we got a forward bifurcation in Figure (2).

if  $R_0 > 1$ .

*Proof.* To determine the local stability of endemic equilibrium, we used the center manifold theory [Castillo-Chavez and Song \(2004\)](#), by taking  $\beta$  as a bifurcation parameter. We make the following change of variables on the system (2). Let  $S = x_1, P = x_2, E = x_3, I = x_4, H =$

$x_5$  and  $R = x_6$ . Moreover, by using vector notation  $x = (x_1, x_2, x_3, x_4, x_5, x_6)^T$ , the system (2) can be written in the form  $\frac{dx}{dt} = F(x)$ , with  $F = (f_1, f_2, f_3, f_4, f_5, f_6)^T$ .

We choose  $\beta = \beta^*$  as a bifurcation parameter. Solving for  $\beta^*$  from  $R_0 = 1$ , we obtain

$$\beta^* = \frac{\mu(\theta + \nu + \mu)(\delta + \mu)(\alpha + \varepsilon + \mu + \rho)(\gamma + \mu + \xi)}{\Pi(\nu + \mu)[\sigma_2(\alpha + \varepsilon + \mu + \rho)(\gamma + \mu + \xi) + \sigma_1\tau\delta(\gamma + \mu + \xi) + \sigma_3\tau\delta\alpha]}.$$

The Jacobian matrix of the system (2) evaluated at the disease free equilibrium  $e_0$  with  $\beta = \beta^*$  is given by

$$J^* = \begin{bmatrix} -(\theta + \mu) & \nu & -\beta^*\sigma_2S^0 & -\beta^*\sigma_1S^0 & -\beta^*\sigma_3S^0 & \eta\omega \\ \theta & -(\nu + \mu) & 0 & 0 & 0 & (1 - \eta)\omega \\ 0 & 0 & \beta^*\sigma_2S^0 - (\delta + \mu) & \beta^*\sigma_1S^0 & \beta^*\sigma_3S^0 & 0 \\ 0 & 0 & \tau\delta & -k_1 & 0 & 0 \\ 0 & 0 & 0 & \alpha & -k_2 & 0 \\ 0 & 0 & (1 - \tau)\delta & \varepsilon & \gamma & -(\omega + \mu) \end{bmatrix},$$

where  $k_1 = \alpha + \varepsilon + \mu + \rho$ ,  $k_2 = \gamma + \mu + \xi$ .

The Jacobian matrix  $J^*$  of the linearized system has a simple zero eigenvalue with all other eigenvalues having negative real part, hence the center manifold theory will be used to analyse the dynamics of the sys-

tem near  $\beta = \beta^*$ . Thus,  $e_0$  is a non-hyperbolic equilibrium, when  $\beta = \beta^*$ . Now, the components of the right eigenvector  $w = (w_1, w_2, w_3, w_4, w_5, w_6)^T$  of  $J^*$  associated with the zero eigenvalue are given by

$$\begin{aligned} w_1 &= -\frac{k_1k_2[\mu(\nu + \mu)(\omega + \delta + \mu) + \delta\mu(1 - \eta)\omega] + \omega\delta\tau(\eta\mu + \nu)[\alpha(\mu + \xi) + k_2(\mu + \rho)]}{\tau\delta\mu k_2(\theta + \nu + \mu)(\omega + \mu)}w_4, \\ w_2 &= -\frac{\omega\delta\mu[\tau(k_2(\mu + \rho) + \alpha(\mu + \xi))(2 - \eta) - (1 - \eta)] + \theta\mu(\delta + \omega + \mu)}{\tau\delta\mu k_2(\theta + \nu + \mu)(\omega + \mu)}w_4, \\ w_3 &= \frac{\alpha + \varepsilon + \mu + \rho}{\tau\delta}w_4, \quad w_4 = w_4 > 0, \quad w_5 = \frac{\alpha}{\gamma + \mu + \xi}w_4, \\ w_6 &= \frac{(1 - \tau)(\alpha + \varepsilon + \mu + \rho)(\gamma + \mu + \xi) + \varepsilon\tau(\gamma + \mu + \xi) + \gamma\alpha\tau}{\tau(\omega + \mu)(\gamma + \mu + \xi)}w_4. \end{aligned}$$

Similarly, the components of the left eigenvector  $v = (v_1, v_2, v_3, v_4, v_5, v_6)^T$  of  $J^*$  associ-

ated with the zero eigenvalue are given by

$$v_1 = v_2 = v_6 = 0, \quad v_3 = v_3 > 0, \quad v_4 = \frac{\beta^*S^0(\sigma_1(\gamma + \mu + \xi) + \alpha\sigma_3)}{(\alpha + \varepsilon + \mu + \rho)(\gamma + \mu + \xi)}v_3, \quad v_5 = \frac{\beta^*S^0\sigma_3}{\gamma + \mu + \xi}v_3.$$

Since the first, second and six component of  $v$  are zero, we don't need the partial derivatives of  $f_1, f_2$  and  $f_6$ . From the partial derivatives

of  $f_3, f_4$  and  $f_5$  at the disease free equilibrium point, the only ones that are nonzero are the following:

$$\begin{aligned} \frac{\partial^2 f_3}{\partial x_3 \partial x_1} &= \frac{\partial^2 f_3}{\partial x_1 \partial x_3} = \beta^* \sigma_2, & \frac{\partial^2 f_3}{\partial x_4 \partial x_1} &= \frac{\partial^2 f_3}{\partial x_1 \partial x_4} = \beta^* \sigma_1, & \frac{\partial^2 f_3}{\partial x_5 \partial x_1} &= \frac{\partial^2 f_3}{\partial x_1 \partial x_5} = \beta^* \sigma_3, \\ \frac{\partial^2 f_3}{\partial x_3 \partial \beta} &= \sigma_2 S^0, & \frac{\partial^2 f_3}{\partial x_4 \partial \beta} &= \sigma_1 S^0, & \frac{\partial^2 f_3}{\partial x_5 \partial \beta} &= \sigma_3 S^0. \end{aligned}$$

The direction of the bifurcation at  $R_0 = 1$  is determined by the signs of the bifurcation coefficients  $a$  and  $b$ . Hence,

$$\begin{aligned} a &= v_3 \sum_{i,j=1}^6 w_i w_j \frac{\partial^2 f_3}{\partial x_i \partial x_j} (S^0, P^0, 0, 0, 0, 0) = 2v_3 w_1 (w_3 \beta^* \sigma_2 + w_4 \beta^* \sigma_1 + w_5 \beta^* \sigma_3) \\ &= 2\beta^* w_1 \left( \frac{\sigma_2 k_1}{\tau \delta} + \sigma_1 + \frac{\alpha \sigma_3}{k_2} \right) v_3 w_4 \\ &= - \frac{2(\delta + \mu)}{(\tau \delta)^2 k_2 \Pi(\nu + \mu)(\omega + \mu)} [k_1^2 k_2 (\mu(\nu + \mu)(\omega + \delta + \mu) + \delta \mu(1 - \eta)\omega) \\ &\quad + \omega \delta \tau k_1 (\eta \mu + \nu) (\alpha(\mu + \xi) + k_2(\mu + \rho))] v_3 w_4^2 < 0. \end{aligned}$$

and

$$\begin{aligned} b &= v_3 \sum_{i=1}^6 w_i \frac{\partial^2 f_3}{\partial x_i \partial \beta} (S^0, P^0, 0, 0, 0, 0) = v_3 \left( \frac{k_1 w_4 \sigma_2 S^0}{\tau \delta} + w_4 \sigma_1 S^0 + \frac{\alpha w_4 \sigma_3 S^0}{k_2} \right) \\ &= \frac{(\delta + \mu)(\alpha + \varepsilon + \mu + \rho)}{\beta^* \tau \delta} v_3 w_4 > 0. \end{aligned}$$

Since  $a < 0$  and  $b > 0$  at  $\beta = \beta^*$ . Based on the Theorem 4.1 stated in [Castillo-Chavez and Song \(2004\)](#), the system (2) undergoes a for-

ward bifurcation at  $R_0 = 1$  and the unique endemic equilibrium  $e_1$  is locally asymptotically stable for  $R_0 > 1$ .

□

### 3.8. Bifurcation analysis

We investigate the nature of the bifurcation by using the center manifold theory [Castillo-Chavez and Song \(2004\)](#). In short, the theory is summarized by Theorem 4.1 in [Castillo-Chavez and Song \(2004\)](#). In such a theorem, there are two important quantities: the coefficients, say  $a$  and  $b$ , of the normal form representing the dynamics of the system on the central manifold. These coefficients decide the bifurcation. In particular, if  $a < 0$  and  $b > 0$ ,

then the bifurcation is forward. In the proof of Theorem (3.6), we have already justified the system (2) undergoes a forward bifurcation at  $R_0 = 1$ . Thus the basic reproduction number  $R_0$  plays an important role in the disease spread. If  $R_0 < 1$ , then its easy to control the disease but if  $R_0 > 1$ , then the society will experience endemic disease spreading. The forward bifurcation diagram can be seen in Figure (2).

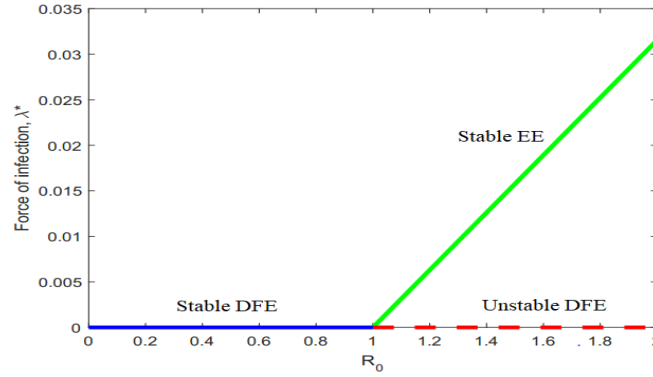


Figure 2: Forward bifurcation diagram for the COVID-19 model (2).

From Figure (2), it is clear that when  $R_0 < 1$ , the system (2) has no endemic equilibrium and the disease-free equilibrium is stable. When  $R_0 > 1$ , a stable endemic equilibrium appears and the disease free equilibrium becomes unstable, i.e. exchange of stability of the equilibrium's (forward bifurcation) occurs at the bifurcation point  $R_0^* = 1$ .

### 3.9. Sensitivity analysis

Sensitivity analysis is a useful tool in model building as well as in model evaluation by showing how the model behavior responds to changes in parameter values [Martcheva \(2015\)](#). The threshold parameter  $R_0$  which determines stability is a function of the parameters  $\Pi, \beta, \sigma_1, \sigma_2, \sigma_3, \nu, \mu, \theta, \delta, \gamma, \xi, \alpha, \varepsilon, \rho, \tau$ . We recall that the basic reproduction number  $R_0$  is given by

$$R_0 = \frac{\Pi\beta(\nu + \mu) [(\gamma + \mu + \xi) [\sigma_2(\alpha + \varepsilon + \mu + \rho) + \sigma_1\tau\delta] + \sigma_3\tau\delta\alpha]}{\mu(\theta + \nu + \mu)(\delta + \mu)(\alpha + \varepsilon + \mu + \rho)(\gamma + \mu + \xi)}.$$

Thus, in order to identify the most sensitive parameters for model (2), we compute the relative sensitivity of  $R_0$  with respect to the above parameters. Then using the parameter

values from Table (3), we display the sensitivity indices of  $R_0$  with respect to the parameters in Figure (3).

$$\begin{aligned}
\Delta_{\beta}^{R_0} &= \frac{\partial R_0}{\partial \beta} \times \frac{\beta}{R_0} = 1, \\
\Delta_{\Pi}^{R_0} &= \frac{\partial R_0}{\partial \Pi} \times \frac{\Pi}{R_0} = 1, \\
\Delta_{\sigma_1}^{R_0} &= \frac{\partial R_0}{\partial \sigma_1} \times \frac{\sigma_1}{R_0} = \frac{\sigma_1 \tau \delta (\gamma + \mu + \xi)}{(\gamma + \mu + \xi) [\sigma_2 (\alpha + \varepsilon + \mu + \rho) + \sigma_1 \tau \delta] + \sigma_3 \tau \delta \alpha}, \\
\Delta_{\sigma_2}^{R_0} &= \frac{\partial R_0}{\partial \sigma_2} \times \frac{\sigma_2}{R_0} = \frac{\sigma_2 (\alpha + \varepsilon + \mu + \rho) (\gamma + \mu + \xi)}{(\gamma + \mu + \xi) [\sigma_2 (\alpha + \varepsilon + \mu + \rho) + \sigma_1 \tau \delta] + \sigma_3 \tau \delta \alpha}, \\
\Delta_{\sigma_3}^{R_0} &= \frac{\partial R_0}{\partial \sigma_3} \times \frac{\sigma_3}{R_0} = \frac{\sigma_3 \tau \delta \alpha}{(\gamma + \mu + \xi) [\sigma_2 (\alpha + \varepsilon + \mu + \rho) + \sigma_1 \tau \delta] + \sigma_3 \tau \delta \alpha}, \\
\Delta_{\tau}^{R_0} &= \frac{\partial R_0}{\partial \tau} \times \frac{\tau}{R_0} = \frac{\tau \delta [\sigma_1 (\gamma + \mu + \xi) + \sigma_3 \alpha]}{(\gamma + \mu + \xi) [\sigma_2 (\alpha + \varepsilon + \mu + \rho) + \sigma_1 \tau \delta] + \sigma_3 \tau \delta \alpha}, \\
\Delta_{\nu}^{R_0} &= \frac{\partial R_0}{\partial \nu} \times \frac{\nu}{R_0} = \frac{\theta \nu}{(\theta + \nu + \mu) (\nu + \mu)}, \\
\Delta_{\alpha}^{R_0} &= \frac{\partial R_0}{\partial \alpha} \times \frac{\alpha}{R_0} = \frac{\alpha \tau \delta [\sigma_3 (\varepsilon + \mu + \rho) - \sigma_1 (\gamma + \mu + \xi)]}{(\alpha + \varepsilon + \mu + \rho) [(\gamma + \mu + \xi) [\sigma_2 (\alpha + \varepsilon + \mu + \rho) + \sigma_1 \tau \delta] + \sigma_3 \tau \delta \alpha]}, \\
\Delta_{\delta}^{R_0} &= \frac{\partial R_0}{\partial \delta} \times \frac{\delta}{R_0} = \frac{\delta [(\gamma + \mu + \xi) [\sigma_1 \tau \mu - \sigma_2 (\alpha + \varepsilon + \mu + \rho)] + \sigma_3 \tau \alpha \mu]}{(\delta + \mu) [(\gamma + \mu + \xi) [\sigma_2 (\alpha + \varepsilon + \mu + \rho) + \sigma_1 \tau \delta] + \sigma_3 \tau \delta \alpha]}, \\
\Delta_{\theta}^{R_0} &= \frac{\partial R_0}{\partial \theta} \times \frac{\theta}{R_0} = -\frac{\theta}{\theta + \nu + \mu}, \\
\Delta_{\varepsilon}^{R_0} &= \frac{\partial R_0}{\partial \varepsilon} \times \frac{\varepsilon}{R_0} = -\frac{\varepsilon \tau \delta [\sigma_1 (\gamma + \mu + \xi) + \sigma_3 \alpha]}{(\alpha + \varepsilon + \mu + \rho) [(\gamma + \mu + \xi) [\sigma_2 (\alpha + \varepsilon + \mu + \rho) + \sigma_1 \tau \delta] + \sigma_3 \tau \delta \alpha]}, \\
\Delta_{\rho}^{R_0} &= \frac{\partial R_0}{\partial \rho} \times \frac{\rho}{R_0} = -\frac{\rho \tau \delta [\sigma_1 (\gamma + \mu + \xi) + \sigma_3 \alpha]}{(\alpha + \varepsilon + \mu + \rho) [(\gamma + \mu + \xi) [\sigma_2 (\alpha + \varepsilon + \mu + \rho) + \sigma_1 \tau \delta] + \sigma_3 \tau \delta \alpha]}, \\
\Delta_{\gamma}^{R_0} &= \frac{\partial R_0}{\partial \gamma} \times \frac{\gamma}{R_0} = -\frac{\sigma_3 \tau \delta \alpha \gamma}{(\gamma + \mu + \xi) [(\gamma + \mu + \xi) [\sigma_2 (\alpha + \varepsilon + \mu + \rho) + \sigma_1 \tau \delta] + \sigma_3 \tau \delta \alpha]}, \\
\Delta_{\xi}^{R_0} &= \frac{\partial R_0}{\partial \xi} \times \frac{\xi}{R_0} = -\frac{\sigma_3 \tau \delta \alpha \xi}{(\gamma + \mu + \xi) [(\gamma + \mu + \xi) [\sigma_2 (\alpha + \varepsilon + \mu + \rho) + \sigma_1 \tau \delta] + \sigma_3 \tau \delta \alpha]}, \\
\Delta_{\mu}^{R_0} &= \frac{\partial R_0}{\partial \mu} \times \frac{\mu}{R_0} = \frac{1}{(\nu + \mu) D} [\mu D - [\sigma_2 A (\alpha + \varepsilon + \mu + \rho)^2 (\gamma + \mu + \xi)^2 (\nu + \mu) \\
&\quad + \sigma_1 \tau \delta [(\alpha + \varepsilon + \rho) A + B] (\gamma + \mu + \xi)^2 (\nu + \mu) + \sigma_3 \tau \delta \alpha [(\gamma + \xi) (A + B) \\
&\quad + (\alpha + \varepsilon + \rho) B + C] (\nu + \mu)],
\end{aligned}$$

where

$$\begin{aligned}
A &= \delta (\theta + \nu) + 2\mu (\delta + \theta + \nu) + 3\mu^2, \quad B = 2\mu \delta (\theta + \nu) + 3\mu^2 (\delta + \theta + \nu) + 4\mu^3, \\
C &= 3\mu^2 \delta (\theta + \nu) + 4\mu (\delta + \theta + \nu) + 5\mu^4, \\
D &= (\alpha + \varepsilon + \mu + \rho) (\gamma + \mu + \xi) (\delta + \mu) (\theta + \nu + \mu) [(\gamma + \mu + \xi) [\sigma_2 (\alpha + \varepsilon + \mu + \rho) + \sigma_1 \tau \delta] \\
&\quad + \sigma_3 \tau \delta \alpha].
\end{aligned}$$

Note that the sensitivity index may depend on several parameters of the system, but also can be constant, independent of any parameter. For example,  $\Delta_{\beta}^{R_0} = +1$  means that in-

creasing (decreasing)  $\beta$  by a given percentage increases (decreases) always  $R_0$  by that same percentage.

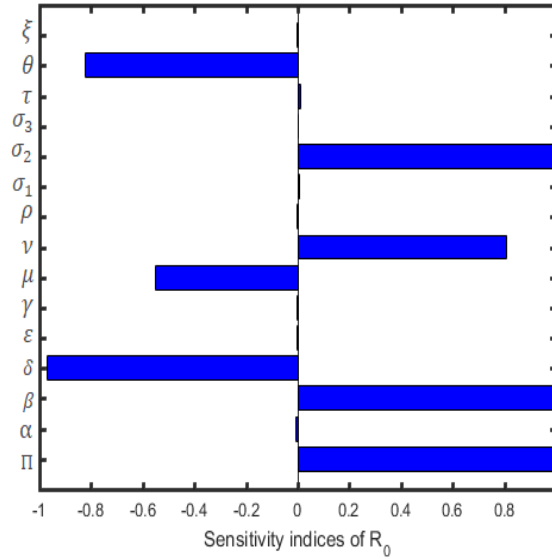


Figure 3: The sensitivity indices of  $R_0$  with respect to the parameters.

Figure (3) shows that the recruitment rate  $\Pi$ , the contact rate  $\beta$ , the modification parameter  $\sigma_2$ , the exposed progression rate  $\delta$ , the natural death rate  $\mu$ , the protection rate  $\theta$  and the waning rate of protected individuals to susceptible class  $\nu$  are the most sensitive parameters for  $R_0$ . The parameters  $\tau, \sigma_1, \sigma_2, \sigma_3, \nu, \beta$  and  $\Pi$  have positive correlation with  $R_0$ . This indicates that the spread of COVID-19 decreases with decrease of these parameters. The parameters  $\xi, \theta, \rho, \mu, \gamma, \varepsilon, \delta$  and  $\alpha$  have negative correlation with  $R_0$ . This implies that the spread of the virus decreases with an increase of these parameters.

#### 4. NUMERICAL SIMULATIONS AND DISCUSSION

In this section, we perform numerical simulation to support our analytical results. The

numerical simulations are carried out with help of the ode45 Matlab tool. Using the parameter values given in Table (3) and the initial conditions below in the model equations (2) simulation study is conducted. The parameter values have been taken based on the literature and the real characteristics of the virus. Furthermore, initial conditions are determined as follow. The total population of Ethiopia for the year 2021 is estimated about  $N(0) = 114,963,588$  people Kifle and Obsu (2022). On December 31, 2020 the total active cases (Infected individuals are 10,245 i.e  $I(0) = 10,245$ ), and the Hospitalized are  $H(0) = 5062$  and the total recovered by the date are  $R(0) = 81,144$  and we are assumed  $P(0) = 108076, E(0) = 15000$  and hence is  $S(0) = N(0) - (P(0) + E(0) + I(0) + H(0) + R(0)) = 114,744,061$ .

Table 3: The parameter values of the modified model (per day).

Parameter	Value	Source
$\Pi$	1300	Assumed
$\theta$	0.7	Assumed
$\nu$	0.15	Assumed
$\beta$	0.00000058	Assumed
$\sigma_1$	0.0001	<a href="#">Alemneh and Telahun (2020)</a>
$\sigma_2$	0.02	<a href="#">Alemneh and Telahun (2020)</a>
$\sigma_3$	0.00003	Assumed
$\delta$	1/14	<a href="#">Kifle and Obsu (2022)</a>
$\alpha$	0.04	Assumed
$\mu$	1/(64*12*30)	<a href="#">Kifle and Obsu (2022)</a>
$\rho$	0.0004	<a href="#">Alemneh and Telahun (2020)</a>
$\xi$	0.015	Assumed
$\tau$	0.7	<a href="#">Alemneh and Telahun (2020)</a>
$\varepsilon$	0.0476	Assumed
$\gamma$	0.033	Assumed
$\eta$	0.4	Assumed
$\omega$	0.011	Assumed



Figure (4) shows the predicted total confirmed cases and the real data total confirmed cases for Ethiopia from 31 December 2020 to 30 March 2022 (It the data has been taken [COVID-19 pandemic \(2022\)](#) ). There is some differences between the prediction and the real

data that should come due to the fact that there were no enough covid test kits during the early time not only in Ethiopia but also all over the world. After wards we continue to validate the local stability of DFE and EEP of model.

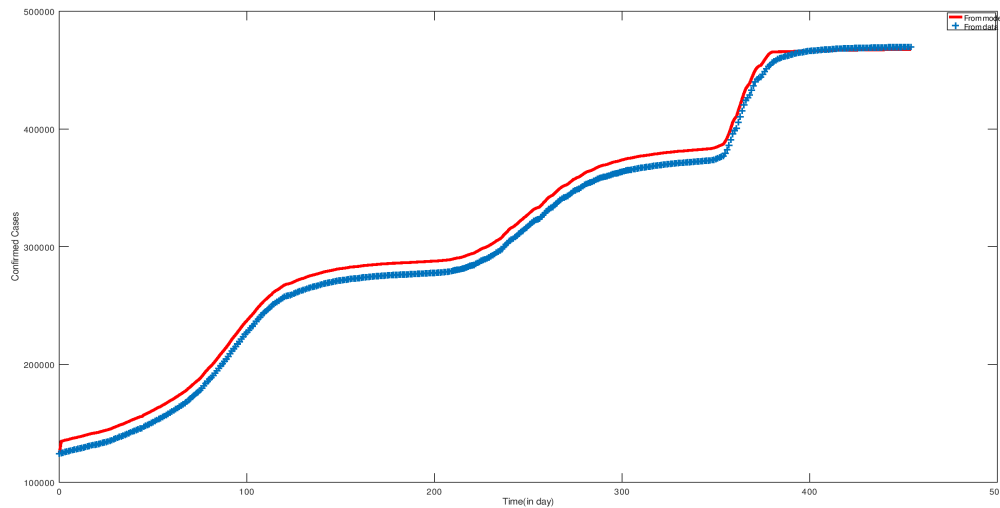


Figure 4: The prediction using model (2) and the real data of confirmed cases for Ethiopia from 31 December 2020 to 30 March 2022

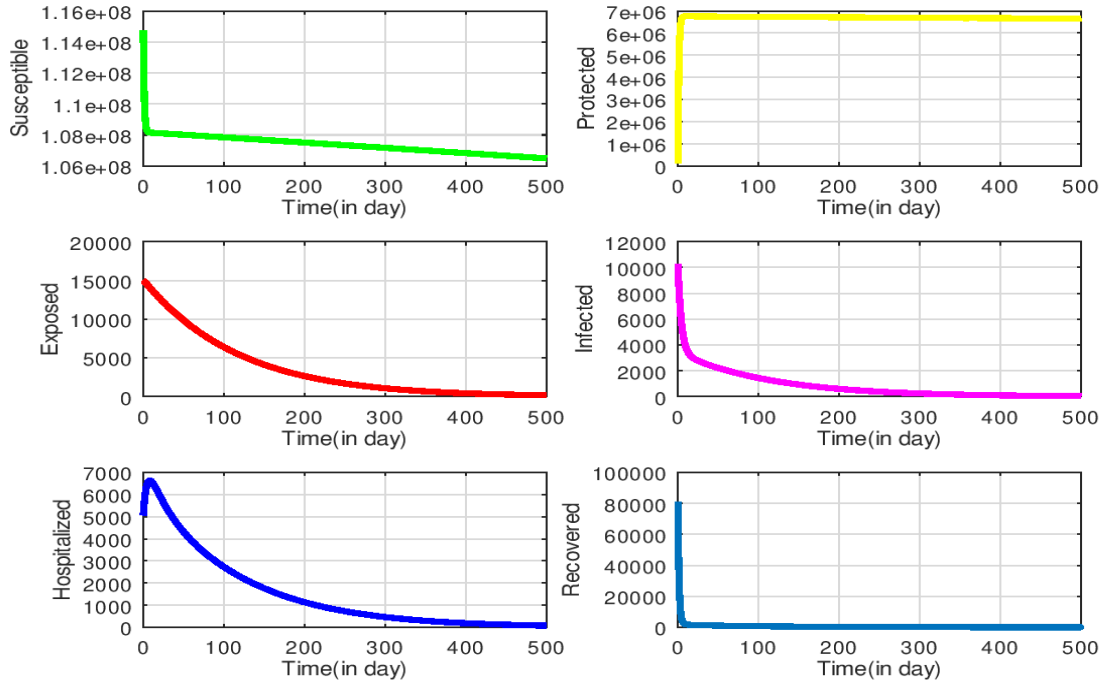
In Figure (5) with  $R_0 = 0.22950$ , we observe that for the basic reproduction number  $R_0 < 1$ , all solutions curve goes to the disease free equilibrium point. As a result, the disease goes to extinct or the disease dies out.

In Figure (6) with  $R_0 = 1.10791$ , we observe that for the basic reproduction number

$R_0 > 1$ , all solutions curve goes away from the disease free equilibrium point. These indicate that the disease-free equilibrium point is unstable for the values of  $R_0 > 1$ , and the solutions will go to the endemic equilibrium point. Consequently, the disease invade in a population.

In Figure (7), we observe as the protection rate  $\theta$  increases, all infected classes will significantly decrease over time. This confirmed the result from the fact that strict use of safety (protection) measures within the population plays a critical role in confine the spread of

the disease as in [Bachar et al. \(2021\)](#). It is predicted that the population will be disease-free. This is due to the case that when protection rate increases the basic reproduction number decreases.


 Figure 5: The time series plot of model (2) when  $R_0 = 0.22950$ 

In Figure (8), we observe that as the contact rate  $\beta$  decrease,  $R_0$  and also all infected classes are decreasing. Further this habitual the result obtained from the fact that a decrease in contact among the population plays a indispensable role in curtailing the spread of the disease as in [Ahmed et al. \(2021\)](#).

## 5. EXTENSION OF THE MODIFIED MODEL INTO AN OPTIMAL CONTROL

In this section, we will use optimal control theory to find protection (for susceptible) and hospitalization (for infected) strategies that would mitigate the spread of COVID-19 in the population.

### 5.1. Optimal protection and hospitalization using modified model

In this subsection, we study the optimal protection of susceptible population and hospitalization of infected individuals in order to minimize the outbreak of COVID-19 in the

population. Let us define our control set  $U$  to be

$$U = \{(\theta(t), \alpha(t)) : 0 \leq \theta(t), \alpha(t) \leq \epsilon_i, 0 \leq t \leq T, 0 < \epsilon_i \leq 1, i = 1, 2\} \quad (9)$$

where  $\theta(t)$  and  $\alpha(t)$  are Lebesgue measurable quantities bounded above by  $\epsilon_1$  and  $\epsilon_2$  respectively. We will minimize the objective functional

$$J[\theta(t), \alpha(t)] = \int_0^T \left( B_1 E(t) + B_2 I(t) + \frac{1}{2} (A_1 \theta^2(t) + A_2 \alpha^2(t)) \right) dt, \quad (10)$$

where constants  $B_1, B_2, A_1$  and  $A_2$  are positive. Here, we want to find the optimal values  $\theta(t)$  and  $\alpha(t)$  that minimizes the objective functional (10) subject to the state system (2).

The goal is to find the optimal control  $(\theta^*(t), \alpha^*(t))$  such that

$$J[\theta^*(t), \alpha^*(t)] = \min_{(\theta, \alpha) \in U} J[\theta(t), \alpha(t)]. \quad (11)$$

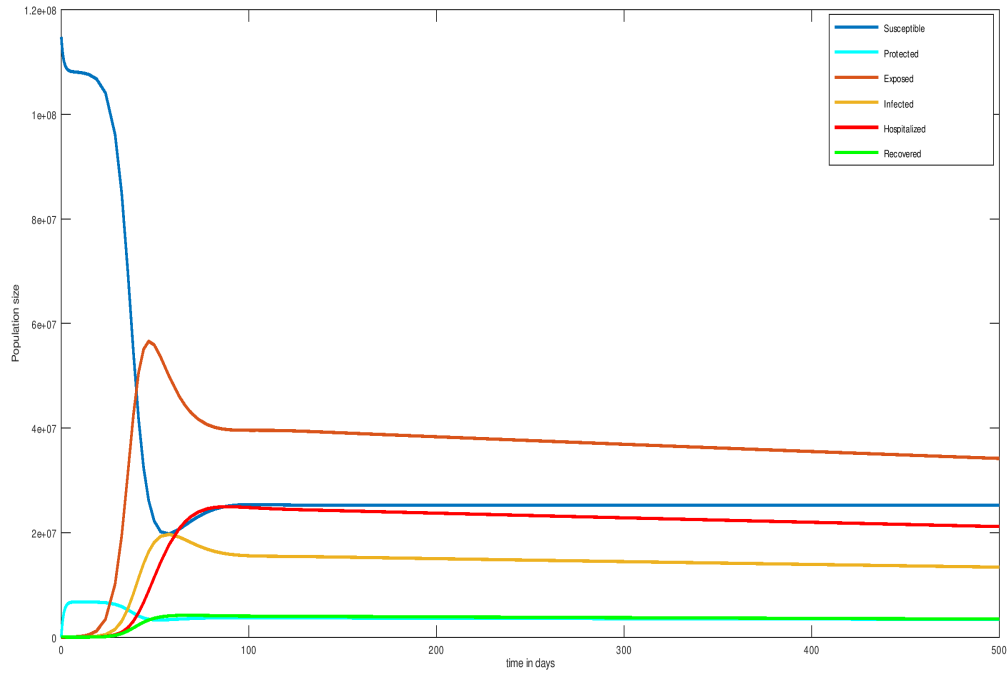


Figure 6: The time series plot of model (2) when  $\beta = 0.0000028$  with  $R_0 = 1.11073$

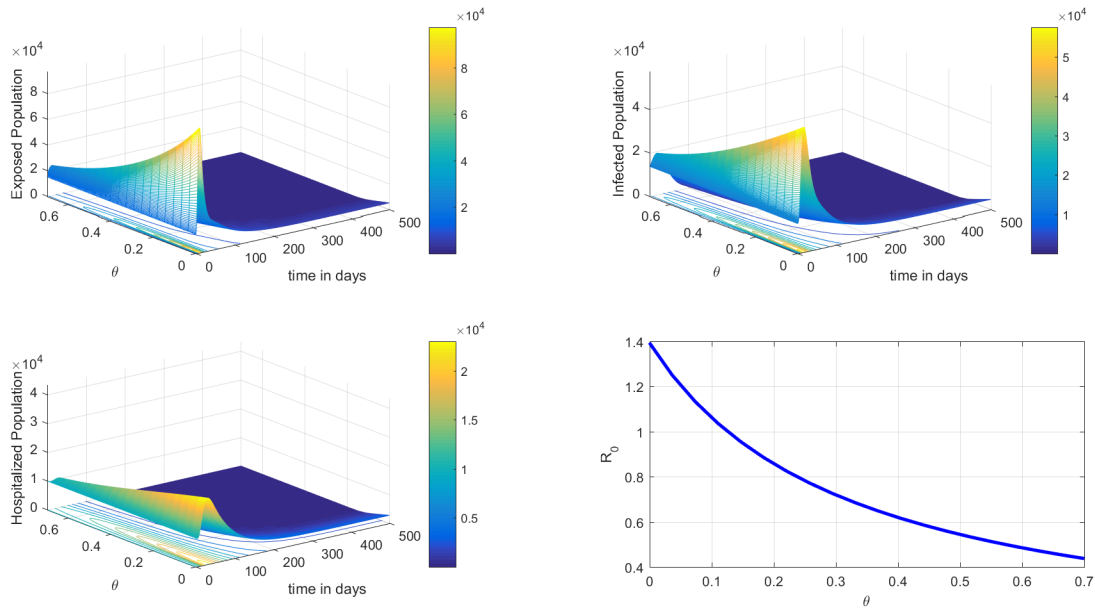
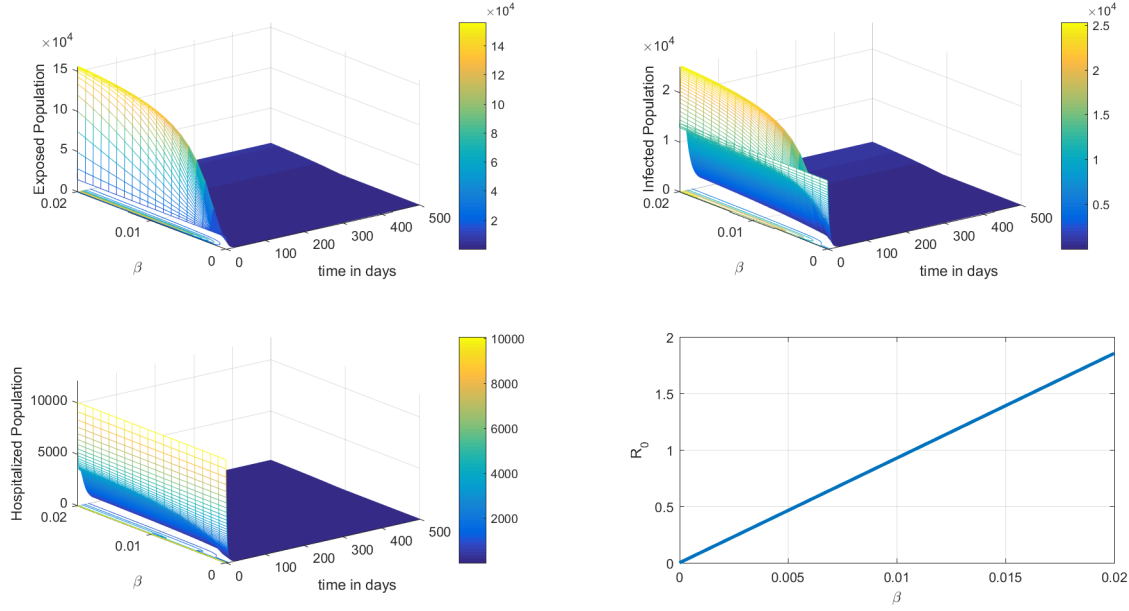


Figure 7: Impact of protection rate  $\theta$  on  $R_0$  and infected classes.

## 5.2. Existence of an optimal control

The existence of the optimal control can be showed by using an approach of Fleming and


 Figure 8: Impact of contact rate  $\beta$  on  $R_0$  and infected classes.

Rishel (2012).

**Theorem 5.1.** Given the objective functional  $J(\theta(t), \alpha(t))$  (10) with admissible control set  $U$ , subject to the state system (2), then there

*Proof.* To prove the existence of optimal control, we need to verify the following conditions.

- The set of solutions to the state system (2) and control parameters in (9) are non-empty.
- The set  $U$  is convex and closed.
- The right hand side of system (2) is bounded above by sum of bounded control and state and can be written as a linear function of the control variables with coefficients dependent on time and state variables.
- The integrand function  $L(E, I, \theta, \alpha, t)$  is convex on  $U$  and  $L(E, I, \theta, \alpha, t) \geq h(u)$ , where  $h(u)$  is continuous and  $\|u\|^{-1}h(u) \rightarrow \infty$  when  $\|u\| \rightarrow \infty$ . Here  $u = (\theta(t), \alpha(t))$ .

exist an optimal control double  $u^* = (\theta^*, \alpha^*)$  in  $U$  such that

$$J[\theta^*, \alpha^*] = \min_{(\theta, \alpha) \in U} J[\theta(t), \alpha(t)]. \quad (12)$$

In Theorem (3.2), we have already justified the boundedness of the solution of the state system (2). Since our solution for the model is bounded by  $N(t) \leq \max\left(N(0), \frac{\Pi}{\mu}\right)$  for all  $t \geq 0$ . This implies that the solutions of the state system are continuous and bounded for each admissible control functions in  $U$ . Moreover, the right hand side of the model equations (2) satisfies the Lipschitz condition with respect to state variables. Hence, the state system (2) has a unique solution corresponding to each admissible control function  $(\theta(t), \alpha(t)) \in U$ . Thus, condition (a) is achieved.

To verify condition (b), given that the control set  $U = \{u \in \mathbb{R}^2 : \|u\|_\infty \leq 1\}$ . Let  $\psi \in [0, 1]$  and  $v_1, v_2 \in U$  such that  $\|v_1\|_\infty \leq 1$  and  $\|v_2\|_\infty \leq 1$ , then

$$\|\psi v_1 + (1-\psi)v_2\|_\infty \leq \psi\|v_1\|_\infty + (1-\psi)\|v_2\|_\infty \leq 1.$$

Thus, the set  $U$  is convex and closed.

To verify condition (c), let  $u = (\theta(t), \alpha(t)) \in U$ ,  $X = (S, P, E, I, H, R)$  and the right hand side of the state system (2) is given by

$$f(t, X, u) = \begin{bmatrix} \Pi + \eta\omega R + \nu P - \beta(\sigma_1 I + \sigma_2 E + \sigma_3 H)S - (\theta(t) + \mu)S \\ \theta(t)S + (1 - \eta)\omega R - (\nu + \mu)P \\ \beta(\sigma_1 I + \sigma_2 E + \sigma_3 H)S - (\delta + \mu)E \\ \tau\delta E - (\alpha(t) + \varepsilon + \mu + \rho)I \\ \alpha(t)I - (\gamma + \mu + \xi)H \\ (1 - \tau)\delta E + \varepsilon I + \gamma H - (\omega + \mu)R \end{bmatrix}. \quad (13)$$

Then from (13) we get,  $f(t, X, u) = g(t, X) + h(t, X)u^T$ , where

$$g(t, X) = \begin{bmatrix} \Pi + \eta\omega R + \nu P - \beta(\sigma_1 I + \sigma_2 E + \sigma_3 H)S - \mu S \\ (1 - \eta)\omega R - (\nu + \mu)P \\ \beta(\sigma_1 I + \sigma_2 E + \sigma_3 H)S - (\delta + \mu)E \\ \tau\delta E - (\varepsilon + \mu + \rho)I \\ -(\gamma + \mu + \xi)H \\ (1 - \tau)\delta E + \varepsilon I + \gamma H - (\omega + \mu)R \end{bmatrix} \quad \text{and} \quad h(t, X) = \begin{bmatrix} -S & 0 \\ S & 0 \\ 0 & 0 \\ 0 & -I \\ 0 & I \\ 0 & 0 \end{bmatrix}.$$

Since, by using the properties of a norm of a matrix we have,

$$\|f(t, X, u)\| = \|g(t, X) + h(t, X)u^T\| \leq \|g(t, X)\| + \|h(t, X)\| \|u\|.$$

Thus, condition (c) is proved.

To verify condition (d), the integrand of the objective functional (10)

$$L(E, I, \theta, \alpha, t) = B_1 E(t) + B_2 I(t) + \frac{1}{2} (A_1 \theta^2(t) + A_2 \alpha^2(t)) \quad (14)$$

is the sum of convex function and hence convex with respect to control parameters  $\theta(t)$  and  $\alpha(t)$ . Moreover,

$$L(E, I, \theta, \alpha, t) = B_1 E(t) + B_2 I(t) + \frac{1}{2} (A_1 \theta^2(t) + A_2 \alpha^2(t)) \geq \frac{1}{2} (A_1 \theta^2(t) + A_2 \alpha^2(t)).$$

We define a continuous function  $h(u) = \phi \|u\|^2$ , where  $\phi = \min(\frac{A_1}{2}, \frac{A_2}{2}) > 0$  and  $u = (\theta(t), \alpha(t))$ . Then we have

$$L(E, I, \theta, \alpha, t) \geq \frac{1}{2} (A_1 \theta^2(t) + A_2 \alpha^2(t)) \geq \phi \|u\|^2, \quad (15)$$

since  $\phi = \min(\frac{A_1}{2}, \frac{A_2}{2}) > 0$ . This implies that  $L(E, I, \theta, \alpha, t) \geq h(u)$ . Consider,  $\|u\|^{-1} h(u) = \|u\|^{-1} \phi \|u\|^2 = \phi \|u\|$ . This gives that  $\|u\|^{-1} h(u) = \phi \|u\| \rightarrow \infty$  when  $\|u\| \rightarrow \infty$ . Thus, condition (d) is proved. Hence, all conditions (a)-(d) shows that there exists an optimal control  $u^* = (\theta^*, \alpha^*)$  that minimizes the cost functional  $J(\theta(t), \alpha(t))$  over  $U$ . Therefore, the existence of optimal control is established.

□

### 5.3. The Hamiltonian and optimality system

We used Pontryagin's Maximum Principle [Lenhart and Workman \(2007\)](#) to drive the necessary conditions that an optimal control

must satisfy. This principle converts the objective functional (10) subject to the state system (2) into a problem of minimizing point-wise a Hamiltonian ( $\mathcal{H}$ ), with respect to  $\theta(t)$  and  $\alpha(t)$  as:

$$\begin{aligned}
 \mathcal{H} = & B_1 E + B_2 I + \frac{1}{2} A_1 \theta^2 + \frac{1}{2} A_2 \alpha^2 \\
 & + \lambda_1 [\Pi + \eta \omega R + \nu P - \beta(\sigma_2 E + \sigma_1 I + \sigma_3 H)S - (\theta + \mu)S] \\
 & + \lambda_2 [\theta S + (1 - \eta)\omega R - (\nu + \mu)P] \\
 & + \lambda_3 [\beta(\sigma_2 E + \sigma_1 I + \sigma_3 H)S - (\delta + \mu)E] \\
 & + \lambda_4 [\tau \delta E - (\alpha + \varepsilon + \mu + \rho)I] + \lambda_5 [\alpha I - (\gamma + \mu + \xi)H] \\
 & + \lambda_6 [(1 - \tau)\delta E + \varepsilon I + \gamma H - (\omega + \mu)R],
 \end{aligned} \tag{16}$$

where  $\lambda_i, i = 1, 2, 3, 4, 5, 6$ , represent the adjoint variables associated with the state variables  $S, P, E, I, H$  and  $R$  to be determined suitably by applying Pontryagin's Maximal Principle [Lenhart and Workman \(2007\)](#).

**Theorem 5.2.** For an optimal control set  $\theta, \alpha$  that minimizes  $J$  over  $U$ , there are adjoint variables,  $\lambda_1, \dots, \lambda_6$  such that:

$$\begin{aligned}
 \frac{d\lambda_1}{dt} &= [\beta(\sigma_2 E + \sigma_1 I + \sigma_3 H) + \theta + \mu]\lambda_1 - \theta\lambda_2 - \beta(\sigma_2 E + \sigma_1 I + \sigma_3 H)\lambda_3, \\
 \frac{d\lambda_2}{dt} &= -\nu\lambda_1 + (\nu + \mu)\lambda_2, \\
 \frac{d\lambda_3}{dt} &= -B_1 + \beta\sigma_2 S\lambda_1 - [\beta\sigma_2 S - (\delta + \mu)]\lambda_3 - \tau\delta\lambda_4 - (1 - \tau)\delta\lambda_6, \\
 \frac{d\lambda_4}{dt} &= -B_2 + \beta\sigma_1 S\lambda_1 - \beta\sigma_1 S\lambda_3 + (\alpha + \varepsilon + \mu + \rho)\lambda_4 - \alpha\lambda_5 - \varepsilon\lambda_6, \\
 \frac{d\lambda_5}{dt} &= \beta\sigma_3 S\lambda_1 - \beta\sigma_3 S\lambda_3 + (\gamma + \mu + \xi)\lambda_5 - \gamma\lambda_6, \\
 \frac{d\lambda_6}{dt} &= -\eta\omega\lambda_1 - (1 - \eta)\omega\lambda_2 + (\omega + \mu)\lambda_6.
 \end{aligned} \tag{17}$$

with transversality conditions

$$\lambda_i(T) = 0, i = 1, \dots, 6. \tag{18}$$

Moreover, we obtain the control set  $(\theta^*, \alpha^*)$  characterized by

$$\begin{aligned}
 \theta^*(t) &= \max \left\{ 0, \min \left( \epsilon_1, \frac{S(\lambda_1 - \lambda_2)}{A_1} \right) \right\}, \\
 \alpha^*(t) &= \max \left\{ 0, \min \left( \epsilon_2, \frac{I(\lambda_4 - \lambda_5)}{A_2} \right) \right\}.
 \end{aligned} \tag{19}$$

*Proof.* The form of the adjoint equations and transversality conditions are standard results from Pontryagin's Maximum Principle [Lenhart and Workman \(2007\)](#). We differentiate Hamiltonian  $(\mathcal{H})$  (16) with respect to the state variables  $S, P, E, I, H$  and  $R$ , respectively, and then the adjoint

system can be written as

$$\begin{aligned}
 \frac{d\lambda_1}{dt} &= -\frac{\partial \mathcal{H}}{\partial S} = [\beta(\sigma_2 E + \sigma_1 I + \sigma_3 H) + \theta + \mu]\lambda_1 - \theta\lambda_2 - \beta(\sigma_2 E + \sigma_1 I + \sigma_3 H)\lambda_3, \\
 \frac{d\lambda_2}{dt} &= -\frac{\partial \mathcal{H}}{\partial P} = -\nu\lambda_1 + (\nu + \mu)\lambda_2, \\
 \frac{d\lambda_3}{dt} &= -\frac{\partial \mathcal{H}}{\partial E} = -B_1 + \beta\sigma_2 S\lambda_1 - [\beta\sigma_2 S - (\delta + \mu)]\lambda_3 - \tau\delta\lambda_4 - (1 - \tau)\delta\lambda_6, \\
 \frac{d\lambda_4}{dt} &= -\frac{\partial \mathcal{H}}{\partial I} = -B_2 + \beta\sigma_1 S\lambda_1 - \beta\sigma_1 S\lambda_3 + (\alpha + \varepsilon + \mu + \rho)\lambda_4 - \alpha\lambda_5 - \varepsilon\lambda_6, \\
 \frac{d\lambda_5}{dt} &= -\frac{\partial \mathcal{H}}{\partial H} = \beta\sigma_3 S\lambda_1 - \beta\sigma_3 S\lambda_3 + (\gamma + \mu + \xi)\lambda_5 - \gamma\lambda_6, \\
 \frac{d\lambda_6}{dt} &= -\frac{\partial \mathcal{H}}{\partial R} = -\eta\omega\lambda_1 - (1 - \eta)\omega\lambda_2 + (\omega + \mu)\lambda_6.
 \end{aligned}$$

with transversality conditions

$$\lambda_i(T) = 0, i = 1, \dots, 6.$$

Similarly by following the approach of Pontryagin et al [Pontryagin \(2018\)](#), the characterization of optimal controls  $\theta^*(t)$ ,  $\alpha^*(t)$ , that is, the optimality equations are obtained based on the conditions:  $\frac{\partial \mathcal{H}}{\partial \theta} = 0$  and  $\frac{\partial \mathcal{H}}{\partial \alpha} = 0$ , which gives,

$$\theta = \frac{S(\lambda_1 - \lambda_2)}{A_1}, \quad \alpha = \frac{I(\lambda_4 - \lambda_5)}{A_2}.$$

Since  $\theta$  and  $\alpha$  are bounded in  $U$  by  $\epsilon_1$  and  $\epsilon_2$  respectively. Therefore, the optimal controls  $\theta^*(t)$  and  $\alpha^*(t)$  are given by

$$\begin{aligned}
 \theta^*(t) &= \max \left\{ 0, \min \left( \epsilon_1, \frac{S(\lambda_1 - \lambda_2)}{A_1} \right) \right\}, \\
 \alpha^*(t) &= \max \left\{ 0, \min \left( \epsilon_2, \frac{I(\lambda_4 - \lambda_5)}{A_2} \right) \right\}.
 \end{aligned}$$

This completes the proof. □

The optimality system is formed from the state system (2) and the adjoint variable system (17) by incorporating the characterized

control set and initial and transversal condition. Then we have the following optimality system:



$$\begin{aligned}
\frac{dS}{dt} &= \Pi + \eta\omega R + \nu P - \beta(\sigma_1 I + \sigma_2 E + \sigma_3 H)S - (\theta^* + \mu)S, \\
\frac{dP}{dt} &= \theta^* S + (1 - \eta)\omega R - (\nu + \mu)P, \\
\frac{dE}{dt} &= \beta(\sigma_1 I + \sigma_2 E + \sigma_3 H)S - (\delta + \mu)E, \\
\frac{dI}{dt} &= \tau\delta E - (\alpha^* + \varepsilon + \mu + \rho)I, \\
\frac{dH}{dt} &= \alpha^* I - (\gamma + \mu + \xi)H, \\
\frac{dR}{dt} &= (1 - \tau)\delta E + \varepsilon I + \gamma H - (\omega + \mu)R, \\
\frac{d\lambda_1}{dt} &= [\beta(\sigma_2 E + \sigma_1 I + \sigma_3 H) + \theta^* + \mu]\lambda_1 - \theta^* \lambda_2 - \beta(\sigma_2 E + \sigma_1 I + \sigma_3 H)\lambda_3, \\
\frac{d\lambda_2}{dt} &= -\nu\lambda_1 + (\nu + \mu)\lambda_2, \\
\frac{d\lambda_3}{dt} &= -B_1 + \beta\sigma_2 S\lambda_1 - [\beta\sigma_2 S - (\delta + \mu)]\lambda_3 - \tau\delta\lambda_4 - (1 - \tau)\delta\lambda_6, \\
\frac{d\lambda_4}{dt} &= -B_2 + \beta\sigma_1 S\lambda_1 - \beta\sigma_1 S\lambda_3 + (\alpha^* + \varepsilon + \mu + \rho)\lambda_4 - \alpha^* \lambda_5 - \varepsilon\lambda_6, \\
\frac{d\lambda_5}{dt} &= \beta\sigma_3 S\lambda_1 - \beta\sigma_3 S\lambda_3 + (\gamma + \mu + \xi)\lambda_5 - \gamma\lambda_6, \\
\frac{d\lambda_6}{dt} &= -\eta\omega\lambda_1 - (1 - \eta)\omega\lambda_2 + (\omega + \mu)\lambda_6, \\
\lambda_i(T) &= 0, i = 1, \dots, 6, (S(0), P(0), E(0), I(0), H(0), R(0)) = (S_0, P_0, E_0, I_0, H_0, R_0).
\end{aligned}$$

## 6. Numerical simulations of optimal control problem

In this section, we perform some numerical solutions on the modified model (2) and the resulting optimality system consisting of the state equations (2) and the adjoint system (17) with the characterizations (19). We make use of the parameter values given in Table (3) for the simulation.

An iterative scheme is used to find the optimal solution of the optimality system. Since the state system (2) has initial conditions and the adjoint systems (17) have final conditions, we solve the state system using a forward fourth-order Runge–Kutta method and solve the adjoint system using a backward fourth-order Runge–Kutta method ?. The solution iterative scheme involves making a guess of the

controls and using that guess to solve the state system. The initial guess of the control together with the solution of the state systems is used to solve the adjoint systems. The controls are then updated using a convex combination of the previous controls and the values obtained using the characterizations. The updated controls are then used to repeat the solution of the state and adjoint systems. This process is repeated until the values in the current iteration are close enough to the previous iteration values [Lenhart and Workman \(2007\)](#).

We used  $B_1 = B_2 = 1$ ,  $A_1 = 40$ ,  $A_2 = 80$  and final intervention time  $T = 350$  days for simulation of COVID-19 model with optimal control. Additionally, we used  $S(0) = 110079$ ,  $P(0) = 108076$ ,  $E(0) = 15000$ ,  $I(0) = 13813$ ,  $H(0) = 10050$ ,  $R(0) = 12156$  as initial values.

### 6.1. Optimal control comparisons and strategies

In this subsection, we compare the results of constant and optimal control as did in ?. We first compare the cost of infection for each strategies and then compare the exposed and infected population.

The optimal control cost for each parameter is less than the constant control at all times as depicted in Figures (91) and (101). It can be observed that for protection rate  $\theta$  the cost reduction is significant compared to the other parameters which is due to the high sensitivity of parameter over the system.

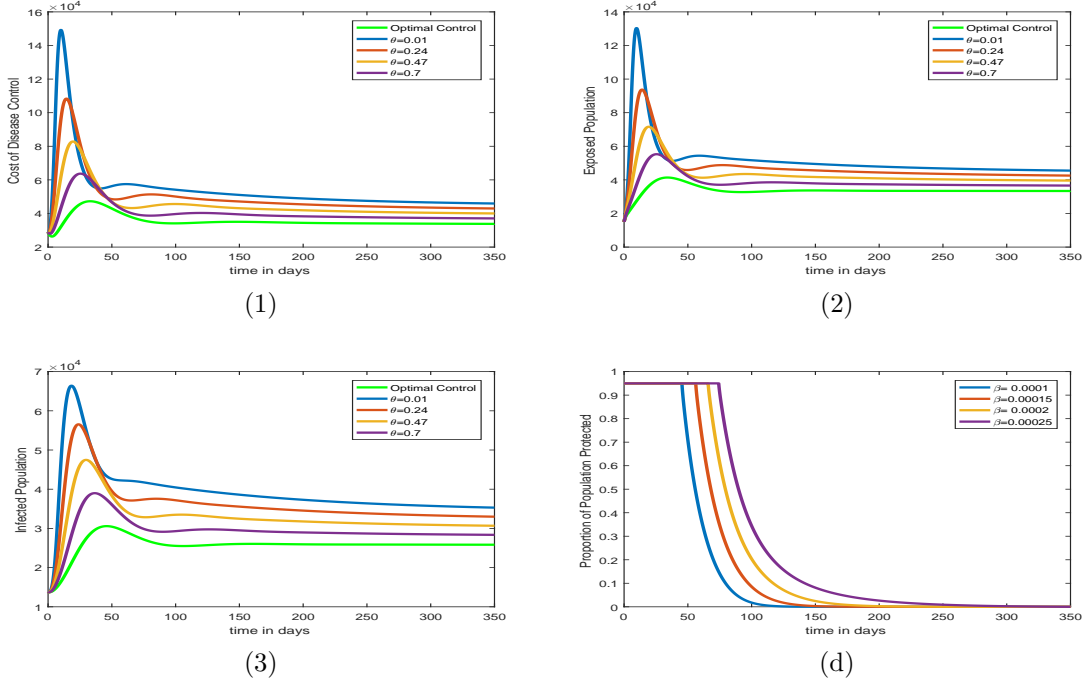


Figure 9: Optimal control for  $\theta$ . (a) Cost comparison for optimal and constant controls for  $\theta$ . (b) Exposed population comparison for optimal and constant controls for  $\theta$ . (c) Infected population comparison for optimal and constant controls for  $\theta$ . (d) Optimal strategies for  $\theta$  with different  $\beta$ .

Now we compare the exposed population using constant and optimal controls. In Figure (92), we observe that the optimal time dependent protection strategy,  $\theta$ , yields a significant drop in exposed population when compared to its constant counterparts, similarly using the optimal time dependent hospitalization strategy  $\alpha$  we see a significant drop in the exposed population as compared to constant rates of hospitalization over time as depicted in Figure (102).

We compare the infected population using

constant and optimal controls. In Figure (93), we observe that the optimal time dependent protection strategy,  $\theta$ , yields a significant drop in infected population when compared to its constant counterparts, similarly using the optimal time dependent hospitalization strategy  $\alpha$  we see a significant drop in the infected population as compared to constant rates of hospitalization over time as depicted in Figure (103).

As contact rate  $\beta$  increases, so does the time for which the maximum control should be applied. In Figures (9d) and (10d), we ob-

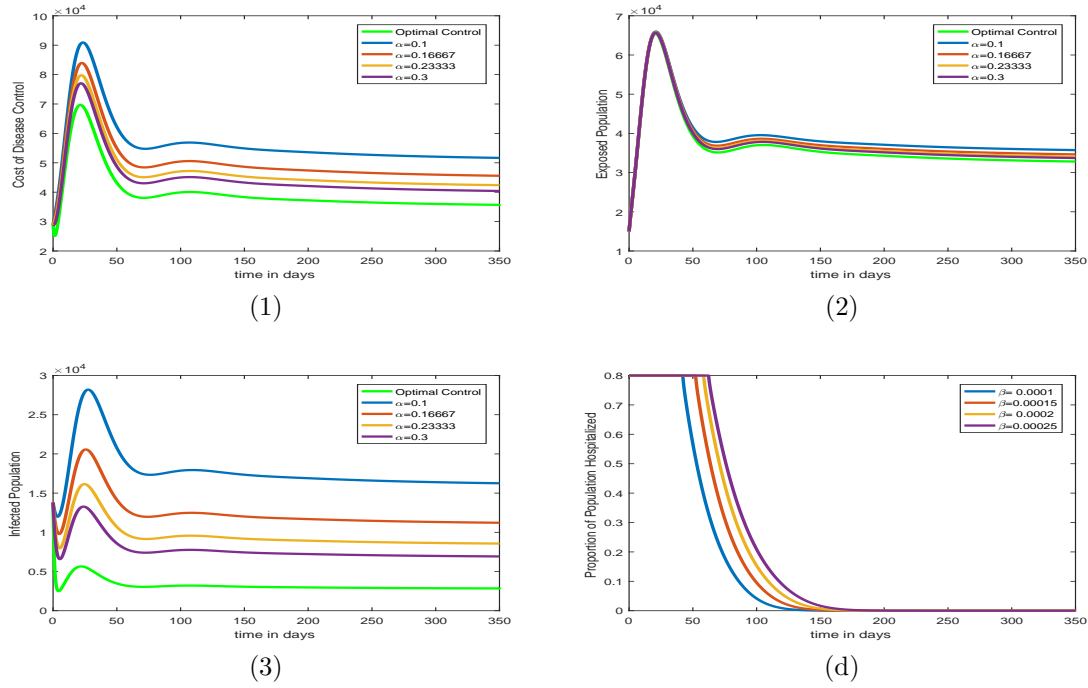


Figure 10: Optimal control for  $\alpha$ . (a) Cost comparison for optimal and constant controls for  $\alpha$ . (b) Exposed population comparison for optimal and constant controls for  $\alpha$ . (c) Infected population comparison for optimal and constant controls for  $\alpha$ . (d) Optimal strategies for  $\alpha$  with different  $\beta$ .

serve that for both protection and hospitalization the maximum possible protection and hospitalization rates should be maintained to the first few days of the disease which can then be reduced over time.

Finally, from Figures (112) and (113), one can easily conclude that the combination of the two controls is significantly more effective in reducing the spread of the virus than when each control is singly applied. Hence, the best choice is to apply two controls all together to mitigate the spread of COVID-19 in the population. From Figure (111), one can observe that the combined implementation of the two control measures is the most cost-effective when compared with the single implementation of each control measure.

## 7. CONCLUSION

In this paper, we proposed a deterministic compartmental model to study the transmis-

sion dynamics of COVID-19. The model was an extension of the existing SEIR model by including protected and hospitalized individuals. We established the well-posedness of the modified model by proving the existence, positivity, and boundedness of the solutions.

We computed the steady states and the basic reproduction number  $R_0$ . Based on the reproduction number  $R_0$ , it is revealed that whenever  $R_0 < 1$ , the system has only disease free equilibrium  $e_0$  which is locally as well as globally asymptotically stable. When  $R_0 > 1$ , the system has a unique endemic equilibrium  $e_1$  which is locally stable and the disease free equilibrium  $e_0$  becomes unstable. We have observed that the outbreak of the disease dies out if  $R_0 < 1$  and the disease is endemic if  $R_0 > 1$ . Using center manifold theory, bifurcation analysis of the modified model was proven and the model exhibits forward bifurcation at  $R_0 = 1$ .

In addition from sensitivity analysis of  $R_0$ , we observed that the recruitment rate  $\Pi$  and

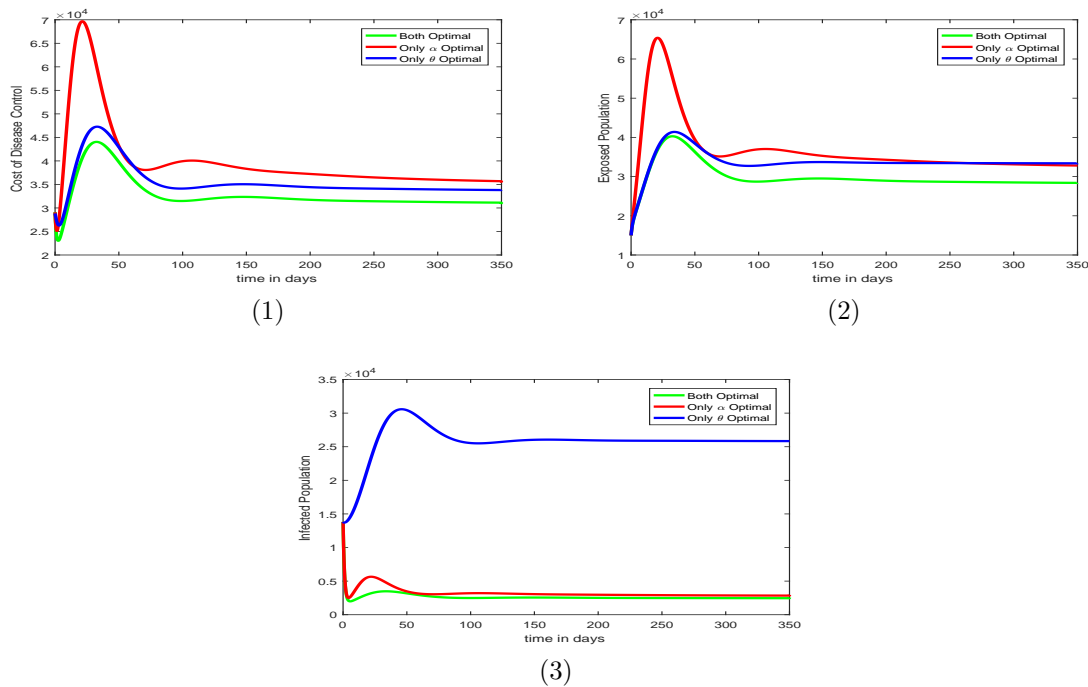


Figure 11: Optimal control for  $\theta, \alpha$  and both. (a) Cost comparison for optimal  $\theta, \alpha$  and both. (b) Exposed population comparison. (c) Infected population comparison.

contact rate  $\beta$  are most sensitive parameters to our model. Numerical results support the fact that decrease in the contact rate  $\beta$  causes the decrease in the value of  $R_0$  and after a certain level of  $\beta$ ,  $R_0$  become less than one.

If the protection rate increases, then all infected classes are decrease. It is predicted that the population will be disease-free.

Furthermore, using optimal control theory we suggest protection and hospitalization strategies. Pontryagin's Maximum Principle is used to establish the existence and characterization of optimal controls. The study demonstrates that the combined application of both controls is much more effective in reducing the spread of the virus than when each control is applied individually.

Finally, our analysis indicates that an optimal control is more preferable than maintaining a high constant control.

## References

- Ahmed I., Modu G. U., Yusuf A., Kummam P. and Yusuf I. (2021), 'A mathematical model of coronavirus disease (covid-19) containing asymptomatic and symptomatic classes', *Results in physics* **21**, 103776.
- Alemneh H. T. and Telahun G. T. (2020), 'Mathematical modeling and optimal control analysis of covid-19 in ethiopia', *medRxiv*.
- Allen L., Brauer F., van den Driessche P. and Wu, J. (2008), 'Mathematical epidemiology, volume 1945 of lecture notes in mathematics', *Springer, Berlin* **13**, 14.
- Bachar M., Khamsi M. A. and Bounkhel M. (2021), 'A mathematical model for the spread of covid-19 and control mechanisms in saudi arabia', *Advances in Difference Equations* **2021**(1), 1–18.
- Brauer F., Castillo-Chavez C. and Feng Z.

- (2019), *Mathematical models in epidemiology*, Vol. 32, Springer.
- Castillo-Chavez C. Blower, S. Van den Driessche P., Kirschner D. and Yakubu A.-A. (2002), *Mathematical approaches for emerging and reemerging infectious diseases: models, methods, and theory*, Vol. 126, Springer Science & Business Media.
- Castillo-Chavez C. and Song B. (2004), ‘Dynamical models of tuberculosis and their applications’, *Mathematical Biosciences & Engineering* **1**(2), 361.
- COVID-19 pandemic (2022), ‘Covid-19 pandemic in ethiopia — Wikipedia, the free encyclopedia’.
- Diekmann O., Heesterbeek J. and Roberts M. G. (2010), ‘The construction of next-generation matrices for compartmental epidemic models’, *Journal of the Royal Society Interface* **7**(47), 873–885.
- Fleming W. H. and Rishel R. W. (2012), *Deterministic and stochastic optimal control*, Vol. 1, Springer Science & Business Media.
- Gurmu E. D., Batu, G. B. and Wameko, M. S. (2020), ‘Mathematical model of novel covid-19 and its transmission dynamics’, *International Journal of Mathematical Modelling & Computations* **10**(2 (SPRING)), 141–159.
- Kifle Z. S. and Obsu, L. L. (2022), ‘Mathematical modeling for covid-19 transmission dynamics: A case study in ethiopia’, *Results in Physics* p. 105191.
- Lemecha Obsu L. and Feyissa Balcha S. (2020), ‘Optimal control strategies for the transmission risk of covid-19’, *Journal of biological dynamics* **14**(1), 590–607.
- Lenhart S. and Workman J. T. (2007), *Optimal control applied to biological models*, CRC press.
- Martcheva M. (2015), *An introduction to mathematical epidemiology*, Vol. 61, Springer.
- Pontryagin L. S. (2018), *Mathematical theory of optimal processes*, Routledge.
- Sohrabi C., Alsafi Z., O’Neill N., Khan, M., Kerwan A., Al-Jabir A., Iosifidis C. and Agha R. (2020), ‘World health organization declares global emergency: A review of the 2019 novel coronavirus (covid-19)’, *International journal of surgery* **76**, 71–76.
- Toquero C. M. (2020), ‘Challenges and opportunities for higher education amid the covid-19 pandemic: The philippine context.’, *Pedagogical Research* **5**(4).
- Valcher M. E. (2002), ‘Positive systems in the behavioral approach: main issues and recent results’, *Electronic proceedings of MTNS* **2002**.
- Yang C. and Wang J. (2020), ‘A mathematical model for the novel coronavirus epidemic in wuhan, china’, *Mathematical biosciences and engineering: MBE* **17**(3), 2708.

## Author's guideline of the Journal

### • Information for Authors

The East African Journal of Biophysical and Computational Sciences (EAJBCS) will provide sufficient information for all authors, including those invited to submit articles for publication (Appendix I). The information, as summarized hereunder, will cover the authorship policy, publication ethics and general requirement during the preparation of the manuscript.

All articles as well as the Editorials published in the East African Journal of Biophysical and Computational Sciences (EAJBCS) represent the opinion of the author(s) and do not necessarily reflect the official view of the Hawassa University and/or College of Natural and Computation Science, the Editorial Board or the institution within which the author(s) is/are affiliated unless this is clearly stated. Furthermore, the author(s) is/are fully responsible for the contents of the manuscript and for any claim or disclaim therein.

### • Plagiarism policy

Before submitting any manuscript, the authors should ensure that they have prepared entirely original works (i.e. not plagiarized from others or from their previous published works). If the work of others is used in any form (such as words, phrases, paragraphs or pictures), the original work should be acknowledged and appropriately cited or quoted. In general, the journal strongly condemn the act of plagiarism and apply different *Plagiarism Checking softwares* to reduce such fraud. If the plagiarism is detected at any stage of the publication process by our esteemed peer reviewers or editorial board members, the manuscript could be automatically rejected.

### • Authorship Policy

To qualify as an author on a research publication, an individual /the person included as a co-author must have made substantial contributions to at least one of the following categories:

- **Conceived of or designed the study:** *This includes conceiving the research question(s), developing the overall research plan, or designing the specific methodology. Just suggesting a general topic area does not qualify*
- **Performed research:** *This includes actively participating in the collection of data, conducting experiments, or implementing the research plan. This involves hands-on work beyond basic assistance. Routine data collection or performing technical tasks under direct supervision are not sufficient for authorship*
- **Analyzed data and interpretation:** *This refers to playing a crucial role in analyzing the collected data, interpreting results, and drawing meaningful conclusions. This includes applying statistical methods, creating visualizations, and explaining patterns*
- **Contributed new methods or models:** *This includes any significant contribution to the development or refinement of novel methods, models, or theoretical frameworks used in the research. It involves innovative contributions that go beyond standard techniques.*

- **Wrote the paper/ Manuscript drafting and revision:** *This includes making a substantial contribution to the writing process, including drafting significant sections of the manuscript, critically revising the content for intellectual input, and responding to reviewer feedback. Proofreading or minor editing (e.g. language) does not warrant authorship.*

It is the responsibility of the corresponding authors that the names, addresses, and affiliations of all authors are correct and in the right order, that institutional approvals have been obtained and that all authors have seen and agreed to a submission. This includes single authorship papers where appropriate. If at all in doubt, please double-check with e.g., Supervisors, line managers, department heads etc.

## • Publication ethics

The Journal requires an author or authors of a manuscript to sign a form of submission prepared for this purpose (Appendix II). The submission to the Journal means that the author(s) agree(s) to all of the contents of the form. The corresponding author for a co-authored manuscript is solely responsible for ensuring the agreement and managing all communications between the Journal and the co-author(s) before and after publication. Before submission, the corresponding author should ensure that the names of all authors of the manuscript are included on the author list, the order of the names of the authors should appear as agreed by all authors, and that all authors are aware that the paper was submitted. Any changes to the author's list after submissions, such as a change in the order of the author, or the deletion or addition of authors, needs to be approved by a signed letter from every author.

After acceptance, the proof is sent to the corresponding author to circulate it to all co-authors and deal with the Journal on their behalf. The Journal shall not necessarily correct errors after publication. The corresponding author is responsible for the accuracy of all contents in the proof, particularly including the correct spelling of the names of co-authors and their current addresses and affiliations.

After publication, the Journal regards the corresponding author as the point of contact for queries about the published manuscript and that it is his/her full responsibility to inform all co-authors about matters arising from the publication processes and that such matter is dealt with promptly. The corresponding author's role is to ensure that inquiries are answered promptly on behalf of all the co-authors. The names and email addresses of the author will be published in the paper. With prior permission of the Editorial Board, authors have the right to retract submitted manuscripts in case they decide to do so. Authors of a published material have the responsibility to inform the Journal promptly if they become aware of any part of their manuscript that requires correcting. The corrected part of the article will be mentioned in the next issue. In fact, any published correction requires the consent of all co-authors, so time is saved if requests for corrections are accompanied by a signed agreement by all authors (in the form of a scanned attachment to an email).



- **General requirements**

Upon submission of a manuscript, the author(s) is required to state that the paper has not been submitted for publication by any other journal or will not be submitted to any other journal by signing the manuscript submission and copyright transfer form (Appendix II).

Manuscripts should be written in English, with spelling according to recent editions of the Advanced Learner's Dictionary of Current English, Oxford University Press. The manuscript should include the following: **title**, **author's name(s)**, **Affiliation** (company or institute), **abstract** and **keywords**. The main parts of the manuscript should consist of **Introduction**, clear objective(s), **Materials and Methods**, **Results**, **Discussion** (or results and discussion merged), **Conclusion**, **Acknowledgement**, **References**, **Figures**, and **Tables** with captions and descriptions, in which detailed quantity, formatting, and unit are given under the following sub-heading.

### **General text formatting**

Manuscripts should be submitted as Microsoft Word documents (docx, doc, rtf) and /or Latex. The manuscript's font size for the text is 12-point, Times New Roman, 1.5 point line spacing with a minimum of 2.5 cm margins on all sides. All pages in the manuscript should be numbered by using the automatic page numbering function.

### **Permitted length of articles**

Original research articles and review articles should not exceed 6000 words in length, starting from the title page to the reference section. Generally, 3-4 tables and 5-6 figures are permitted. Short communications contain news of interest to researchers, including progress reports on ongoing research of unique nature, records of observations, short comments, corrections, and reinterpretation of articles previously published in EAJBCS *etc.* The maximum permissible length is 1500 words, including title, abstract, and references; they may contain no more than two figures and/or two tables. Book reviews with critical evaluation of recently published books in areas of Natural and Computational Sciences will be published under this column. The maximum permissible length of a book review is 1500 words, including any references.

### **Title Page**

The title page should include the title, author(s)' name and affiliation, email address of the corresponding author and a suggested running head (Maximum 50 characters).

### **Abstract**

An informative abstract shorter than 300 words is included. Informative abstracts include the purpose of the research, the main methods used, the most important results, and the most significant conclusions. The abstract should be in one paragraph and without any abbreviations.

### **Keywords**

Supply 3 to 7 keywords that describe the main content of the article, each separated with semicolon. Select words different than those in the title and list them alphabetically.

## **Text**

The text should be precise, clear, and concise. Avoid verbiage, excessive citations of the literature (especially to support well-known statements), discussions marginally relevant to the paper, and other information that adds length but little substance to the paper. All tables and figures should be relevant and necessary; do not present the same data in tables and figures, and do not use short tables for information that can be easily presented using text.

## **Introduction**

The introduction should give the pertinent background to the study and should explain why the work was done. The author(s) should clearly show the research gap, state the objectives of the work and avoid a detailed literature survey or a summary of the results.

## **Materials and Methods**

To ensure reproducibility, the methodology section should be detailed and transparent. The following information must be included: use precise and recognized scientific nomenclature for all materials and indicate their source; specify all equipment used, including the manufacturer's name, model number, and relevant technical specifications in parentheses (e.g., "centrifuge (Eppendorf, Model 5424)"); describe your procedures step-by-step, ensuring all experimental parameters are specified; provide a comprehensive description for any novel method, including rationale and limitations; reference the original source for established methods, clearly stating and justifying any deviations; and explicitly confirm that procedures involving human subjects or animals were conducted in adherence to ethical standards set by relevant national governing bodies, including providing approval details and measures taken to minimize harm.

The statistical analysis done and statistical significance of the findings, when appropriate, should be mentioned. Unless absolutely necessary for a clear understanding of the article, a detailed description of statistical treatment/analysis may be avoided. Articles based heavily on statistical considerations, however, need to give details particularly when new or uncommon methods are employed. Standard and routine statistical methods employed need to give only authentic references.

## **Results**

The purpose of your data presentation (i.e. the result section) is to support your discussion and conclusions. Therefore, only include data that is crucial to understand your key findings. Structure the data in a unified and logical sequence, allowing the reader to follow the remaining sections easily. Avoid unnecessary repetition: if data is presented in a table or figure, do not repeat it in the text. Instead, use the text to emphasize or summarize noteworthy findings. Choose either tables or figures to present the same data – avoid presenting it both ways. Critically

analyze and interpret the implications of your data within the discussion section, providing a thoughtful and comprehensive interpretation.

## **Discussion**

The discussion section should provide an insightful analysis or interpretation of your results, moving beyond a mere restatement of your findings. Interpret your results and explain their relevance to the wider scientific community, drawing clear connections to established knowledge and identifying new insights. Avoid directly repeating the results and rather analyze them with logical deductions and scientific justification. Acknowledge and discuss any study limitations or potential biases. The conclusions should answer your research questions, but avoid unsupported statements and refrain from claiming priority on ongoing work. Make sure hypotheses are clearly identified, and include recommendations only when they directly address your findings and are of critical importance.

## **Acknowledgment**

The acknowledgment section should be brief and reserved for recognizing specific and substantial scientific, technical, or financial contributions to the research. Avoid acknowledging routine departmental facilities, general encouragement, or assistance with manuscript preparation, such as typing or secretarial support. Focus only on acknowledging individuals and institutions that directly contributed to the intellectual or material aspects of the research.

## **Tables**

Tables should be prepared in MS Word's Table Editor, using (as far as possible) "Simple1" as the model:

(Table ... Insert ... Table ... Auto format ...Simple 1). Tables taken directly from Microsoft Excel are not generally acceptable for publication.

Use Arabic (1, 2, 3 ...), not Roman (I, II, III ...), numerals for tables. Footnotes in tables should be indicated by superscript letters beginning with "a" in each table. Descriptive material not designated as a footnote maybe placed under a table as a Note.

## **Illustrations**

Preparation: Similar figures should be arranged into plates whenever possible; leave very little space between adjoining illustrations or separate them with a thin white line. Line art should be scanned at 900 dpi, photographs (halftone or color) at 300 dpi, and figures with line art and halftones at 600 dpi. Crop the illustrations to remove non-printing borders. Make lines thick enough and text large enough to compensate for the reduction. Dimensions of the original artwork should not exceed 28 cm x 21.5 cm; the printed area of the journal page measures 20.3 x 14 cm. Submission: TIFF or JPG files of figures should be of high quality and readable in Adobe Photoshop. Do not embed figures in the manuscript document.

The figures will be evaluated during the Editorial reading of the article, and if necessary, instructions will be provided for the submission of adequate illustrations.

Insert ... Symbol ... Special characters

All data should be given in the metric system, using SI units of measurement.

Use “.” (point) as the decimal symbol. Thousands are shown spaced, thus: 1 000 000. Use a leading zero with all numbers <1, including probability values (*e.g.*  $p < 0.001$ ).

Numbers from one to nine should be written out in the text, except when used with units or in percentages (*e.g.* two occasions, 10 samples, Five seconds, 3.5%). At the beginning of a sentence, always spell out numbers (*e.g.* “Twenty-one trees were sampled...”).

Use the 24-hour time format, with a colon “:” as separator (*e.g.* 12:15 h). Use day/month/year as the full date format (*e.g.* 12 August 2001, or 12/08/01 for brevity in tables or figures). Give years in full (*e.g.* “1994–2001”, never “94–01”). Use the form “1990s”, not “1990’s” or “1990ies”.

Use the en-dash – for ranges, as in “1994–2001” (Insert ... Symbol ... Special characters En dash).

In stating temperatures, use the degree symbol “°”, thus “°C”, not a super script zero “0”. (Insert ... Symbol ... Normal text),

Define all symbols, abbreviations and acronyms the first time they are used, *e.g.* diameter at breast height (DBH), meters above sea-level (masl). In the text, use negative exponents, *e.g.*  $\text{g m}^{-2}$ ,  $\text{g m}^{-2} \text{ sec}^{-1}$ ,  $\text{m}^3 \text{ ha}^{-1}$  as appropriate. Use “h” for hours; do not abbreviate “day”.

If possible, format mathematical expressions in their final version (*e.g.* by means of Equation Editor in MS Word or its equivalent in Word Perfect or Open Office); otherwise, make them understandable enough to be formatted during typesetting (*e.g.* use underlining for fractions and type the numerator and denominator on different lines).

MS word equations can be used for all mathematical equations and formulae (Insert....Equations).

## References

All literatures referred to in the text should be cited as exemplified below.

Please inspect the examples below carefully, and adhere to the styles and punctuation shown.

Capitalize only proper names (“Miocene”, “Afar”, “The Netherlands”) and the initial letter of the title of papers and books, *e.g.* write “Principles and procedures of statistics”, not “Principles and Procedures of Statistics”.

Do not italicize Latin abbreviations: write “et al.”, not “*et al.*”

*References in the text should use the ‘author-year’ (Harvard) format:*

(Darwin and Morgan, 1993) or, if more than two authors, (Anderson et al., 1993). Arrange multiple citations chronologically (Hartman and Kester, 1975; Anderson et al., 1993; Darwin and Morgan, 1994).

*References in the list should be in alphabetical order, in the following formats:*

### **Journal article**

Kalb J.E. 1978. Miocene to Pleistocene deposits in the Afar depression, Ethiopia. *SINET: Ethiop. J. Sci.* 1: 87-98.

### **Books**

Whitmore T.C. 1996. An introduction to tropical rain forests. Clarendon Press, Oxford, 226 pp.

Steel R.G.D. and Torrie J.H. 1980. Principles and procedures of statistics. 2<sup>nd</sup> ed. McGraw-Hill Book Co., New York. 633 pp.

### **Book chapter**

Dubin H.J. and Grinkel M. 1991. The status of wheat disease and disease research in warmer areas. In: Lange L.O., Nose P.S. and Zeigler H. (Eds.) *Encyclopedia of plant physiology. Vol. 2 A Physiological plant ecology*. Springer-Verlag, Berlin. pp. 57-107.

### **Conference /workshop/seminar proceedings**

Demel Teketay. 2001. Ecological effects of eucalyptus: ground for making wise and informed decision. Proceedings of a national workshop on the Eucalyptus dilemma, 15 November 2000, Part II: 1-45, Addis Ababa.

Daniel L.E. and Stubbs R.W. 1992. Virulence of yellow rust races and types of resistance in wheat cultivars in Kenya. In: Tanner D.G. and Mwangi W. (eds.). *Seventh regional wheat workshop for eastern, central and southern Africa*. September 16-19, 1991. Nakuru, Kenya: CIMMYT. pp. 165-175.

### **Publications of organizations**

WHO (World Health Organization) 2005. Make every mother and child count: The 2005 World Health Report. WHO, Geneva, Switzerland.

CSA (Central Statistical Authority) 1991. *Agricultural Statistics*. 1991. Addis Ababa, CTA Publications. 250 pp.

**Dissertation or Thesis**

Roumen E.C.1991. Partial resistance to blast and how to select for it. Ph.D. Thesis. Agricultural University, Wageningen. The Netherlands.108 pp.

Gatluak Gatkuoth 2008. Agroforestry potentials of under-exploited multipurpose trees and shrubs (MPTS) in Lare district of Gambella region. MSc. Thesis, College of Agriculture, Hawassa University, Hawassa.92 pp.

**Publications from websites (URLs)**

FAO 2000.Crop and Food Supply Assessment Mission to Ethiopia. FAOIWFP. Rome. (<http://www.fao.org/GIEWS/>). (Accessed on 21 July 2000).

## *Scope and indexing*

**East African Journal of Biophysical and Computational Sciences (EAJBCS)** is a [double-blind peer-reviewed open-access journal](#) published by Hawassa University, College of Natural & Computational Sciences. This Journal is a multi and interdisciplinary journal that is devoted to attracting high-quality, latest, and valuable advancements in the fields of natural sciences. The Journal invites publications from different geographical contexts and disciplines to advance the depths of knowledge related to **physics, chemistry, geology, biology, & veterinary medicine**. The manuscript originated from other sciences such as **biotechnology, sport science, statistics, and mathematics** can also be accepted based on their adjunct nature. The Journal encourages publications of both scholarly and industrial papers on various themes with the aim of giving innovative solutions to natural sciences. It encourages the publishing of [open access academic journals](#) on a regular basis (presumably **biannual**). The Journal publishes original research articles, critical reviews, mini-reviews, short communications, case reports related to the specific theme & a variety of special issues **in English**. The Journal, published under the [Creative Commons](#) open access license ([CC BY-NC-ND](#)), **doesn't charge fees for publishing** an article and hence offers an opportunity to all social classes regardless of their economic statuses. This helps to promote academic research published by resource-poor researchers as a mechanism to give back to society.

*East Afr. J. Biophys. Comput. Sci.* is officially available online on the following sites

- ✓ <https://journals.hu.edu.et/hu-journals/index.php/eajbcs>
- ✓ <https://doaj.org/toc/2789-3618>
- ✓ <https://www.ajol.info/index.php/eajbcs>
- ✓ <https://www.cabidigitallibrary.org> (in short: <https://surl.li/yjffzm>)



The background of the page features a teal and white wavy pattern, resembling stylized waves or a modern abstract design, framing the central white area.

**ISSN (Online): 2789-3618**

**ISSN (Print): 2789-360X**